INHIBITION OF TUMOURIGENICITY AND METASTASIS OF PROSTATE CANCER BY SUPPRESSING THE EXPRESSION OF C-FABP GENE PLUS ANDROGEN DEPLETION

This thesis is submitted in accordance with the requirements of the University of Liverpool for the degree of Doctor in Philosophy

by

Elwin Alex Morgan

October 2005

ACKNOWLEDGEMENTS

I would like to thank my supervisor Professor Ke for his advice, support, guidance and enduring patience throughout the duration of this project. I would also like to thank Dr Janet Adamson for her continued support and guidance from the first day of this PhD study. I am very grateful for Professor Foster for his kind words of encouragement and his incredible enthusiasm for all work conducted within the department. I thank Professor Foster and Dr Shiva Forootan for their help in examining H/E stained slides. I would also like to thank Mrs Carol Beesley for contributing her time and energy to help me throughout my PhD study.

I would also like to thank Dr Bee, Dr Watson, Dr Rainbow, Dr Smith and Mrs Meacock for creating a friendly enjoyable working environment.

I would like to thank my brothers Eugene, Melvin and Alton for their inspiration at various stages of this study and finally, my parents, Dr Eugene Morgan and Mrs Miranda Morgan, and my grandmother Mrs Aba Fraser-Leigh for their continued support. I dedicate this work to your faith in me.

ABSTRACT

Prostate cancer is the most commonly occurring form of non-tobacco related cancers of man in the developed world. Our understanding of the molecular pathology of prostate cancer is currently very limited. At present, clinical therapy focuses on androgen blockage by physical or pharmaceutical castration. Previous work in our molecular pathology laboratory has led to the identification of several genes whose elevated expression may contribute to the malignant progression of the prostate cancer cells. One such gene is that coding for human cutaneous fatty acid binding protein (C-FABP). The work described in this thesis is aimed to study the specific role of C-FABP on the tumourigenicity of prostate cancer, to investigate whether the elevated expression of C-FABP is related to androgen sensitivity of the cancer cells, and to explore the therapeutic possibility of inhibiting the development and expansion of prostate cancer through suppressing the expression of C-FABP gene combined with the androgen depletion.

To investigate the biological significance of elevated expression of C-FABP in prostate cancer, C-FABP expression in highly malignant prostate cancer cells PC3M was suppressed by the transfection of a reverse transcript of CFABP. Two antisense transfectant cells, C-FABP-PC3M-1 and C-FABP-PCM-3 were produced with 3.8 fold and 6.9 fold reduction in normal C-FABP expression respectively. Exploration of tumourigenic potential of transfectant cells by invasion assay showed that 7% of antisense transfectant cells invaded the ECM, compared to 14% of control transfectant cells. Subcutaneous inoculation of antisense and control transfectant cells into immuno-compromised male nude mice demonstrated a significant reduction in tumour incidence and tumour volume in antisense transfectant cells compared to control transfectant tumours.

Previous work in our laboratory showed that C-FABP was over-expressed in androgen independent prostate cancer cells. To investigate whether elevated C-FABP expression is related to androgen sensitivity, C-FABP expression was reduced by 95% by RNA interference in highly malignant androgen independent prostate cancer cells PC3M to study the effect of suppressed C-FABP expression and androgen deprivation on prostate cancer cells. *In vitro* assays for cell proliferation and colony formation show significant differences in cell growth rate and number of colonies formed in androgen positive and negative conditions, however, comparisons between the two conditions suggest that C-FABP may not have some bearing on androgen sensitivity *in vitro*.

Subcutaneous inoculation of RNAi transfectant cells into male immuno-compromised nude mice produced a significant reduction in tumour incidence and mean tumour volume in RNAi transfectant group 75% (3/4 animals) and 176mm^3 compared to that of the parental PC-3M group which produced 100% (4/4 animals) tumour incidence and 1471mm^3 mean tumour volume respectively. However, castration of mice and orthotopic implantation of RNAi transfectant cells and parental PC-3M cells into the prostate gland of mice produced 100% (4/4 animals) tumour incidence compared to 0% (0/3 animals) observed in the RNAi transfectant group. At autopsy, mice were dissected and primary tumours, lungs, heart and liver were removed for haematoxylin and eosin staining. From these groups, only the castrated and orthotopically implanted parental PC-3M cell group produced secondary micro-metastasis in the lungs and liver of mice (4/4 animals).

This data suggest that suppressed CFABP activity may not restore androgen sensitivity in highly malignant androgen insensitive PC3M cells *in vitro*. However, *in vivo* studies suggest that the combination of suppressed CFABP and androgen depletion have a synergistic effect resulting in enhanced suppression of tumourigenicity and metastasis.

CONTENTS

LIST OF FIGURES

LIST OF TABLES

APPENDIX 1 - MATERIALS AND REAGENTS

CHAPTER - 1

INTRODUCTION

1.0: THE EPIDEMIOLGY OF PROSTATE CANCER

1.1.1 Incidence and mortality of prostate cancer

Prostate cancer is now the most common form of cancer diagnosed in men in England. In 2003, approximately 112,700 new cases of cancer were registered in England, and of that figure, prostate cancer accounted for 24 per cent of cases (Figure 1.1.1).

Figure 1.1.1 Incidence rates of cancers in England by gender, 2003

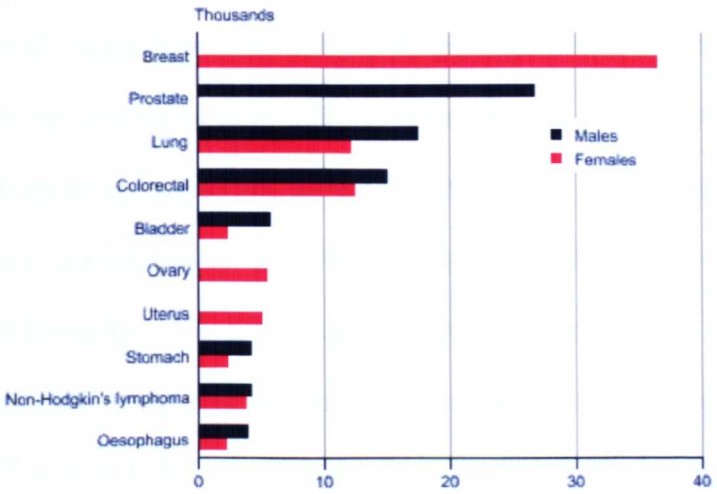

Taken with permission from National Statistics Office (www.**statistics**.gov.uk)

However, the last 20 years have seen a pronounced increase in prostate cancer incidence within the UK population at a rate of approximately 10-15% every 5 years. In 1997, levels of prostate cancer cases were approximated at being 18,300 in England and Wales; however,

the most recent data available from the office of national statistics places the yearly registration of new cases at approximately 27,000 cases in England.

Prostate cancer accounts for around 13% of male deaths and is the second most common form of cancer mortality after lung cancer. In 2003, the mortality rate of prostate cancer was reported as being 8, 582 deaths in England.

1.1.2 Age and ethnicity

Records from the National Office of Statistics show a relationship between increasing age, rising relative risk and incidence of prostate cancer. In 1997, approximately 900/100,000 males at 85 years or older were reported with this malignancy in England and Wales (Figure. 1.1.2a).

Data obtained from the National of Office Statistics shows that during the period of 1971-1997, there was a two hundred per cent increase in prostate cancer incidence from 30/100,000 males to 60/100,000 males (Figure 1.1.2b). Conversely, levels of prostate cancer death do not reflect this pattern (Figure 1.1.2c). In 1950, the mortality rate in 75-84 year olds was approximately 200/100,000 men. In 1999, this had increased to approximately 325/100,000. However, a greater level of mortality was observed in the 85 plus age group which demonstrated an approximate mortality rate of 250/100,000 in 1950, to approximately 775/100,000 in 1999. Clearly, these figures show a link between increasing age and prostate cancer incidence and mortality.

This up-surge in both incidence and mortality rates is replicated in other western nations. In the United States of America, prostate cancer accounts for 30% all diagnosed cancers in men. In 2002, 189,000 men for the USA were diagnosed with the disease, and in the same year, approximately 30,000 deaths were attributed to prostate cancer.

Prostate cancer incidence varies world-wide. The highest incidence rates are found in western developed nations such as United States and Canada, and the lowest incidence rates are found in countries such as China and Japan. Mortality levels follow a similar trend to incidence rates in that Caribbean and Western developed nations have a higher level of mortality than China and Japan (Crawford, 2003). This difference in prostate cancer incidence between western and eastern nations has been attributed to external factors such as diet. Shimuzu *et al*, (1991) demonstrated that Japanese male migrants developed comparable risks of developing prostate cancer as individuals who had lived in America all there lives.

Figure 1.1.2a Age specific incidence of prostate cancer in England and Wales, 1997

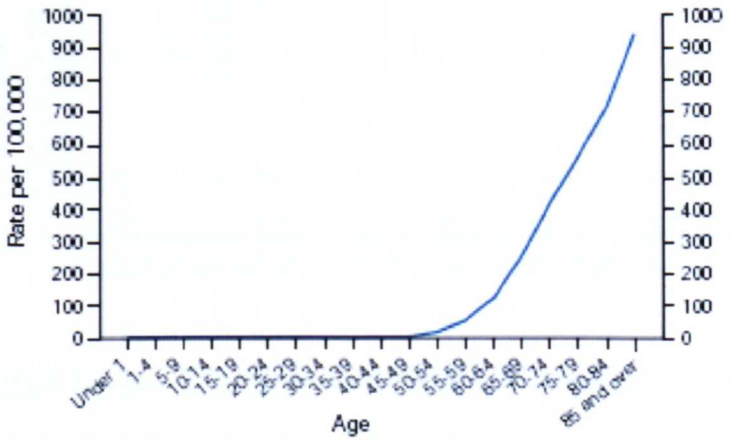

Figure 1.1.2a. Prostate cancer incidence is related to increasing age. This figure demonstrates that in 1997, prostate cancer incidence for men 85 years and older was registered at a higher rate per 100, 000 men, than for any other age group.

Figure 1.1.2b Prostate cancer incidence in England and Wales, 1971 -1997

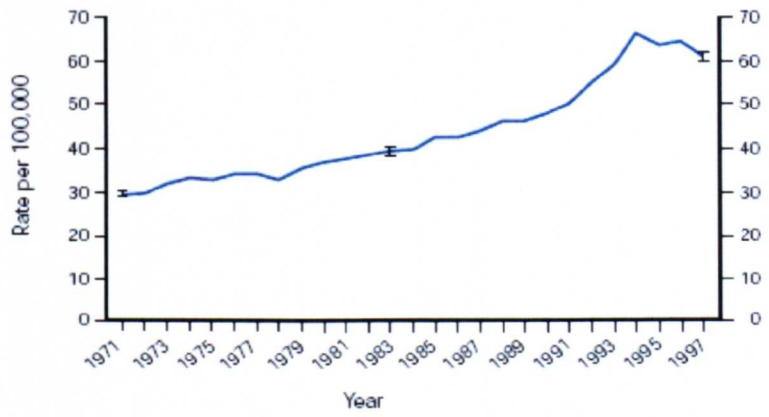

Figure 1.1.2b. The levels of prostate cancer incidence have increased dramatically from 1971 to 1997. In 1971, the rate of prostate cancer was 30/100, 000 men, whereas in 1997, this figure was placed at 60/100, 000 men. This up-surge in prostate cancer incidence has been attributed to an increase in PSA screening in men.

Figure 1.1.2c Age specific mortality, England and Wales, 1950 – 1999

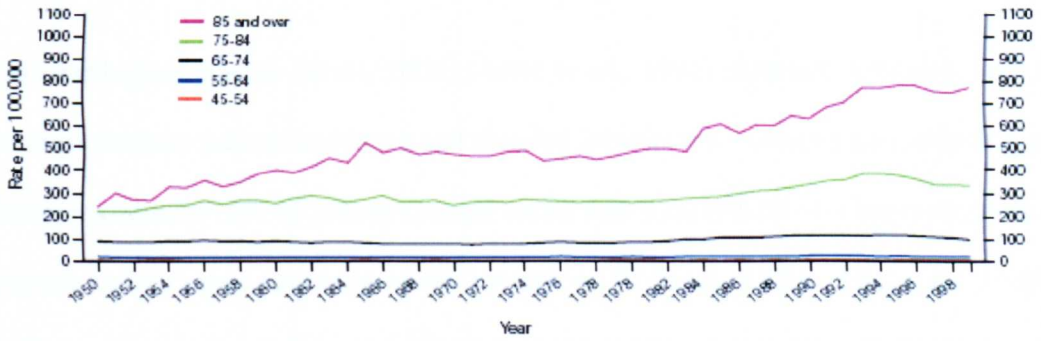

Figure 1.1.2c. This figure demonstrates the trend between age and mortality. The mortality rate for men between ages 65-74 remained constant from 1950 to 1999. In men aged 75-84, a rise is noticed from approximately 225/100, 000 men to 325/100, 000 men. However, the greatest increase in mortality rate is observed in men aged 85 and over. In this sub group, the approximate mortality rate rises from 350/100, 000 to 900/100, 000 men.

Taken with permission from National Statistics Office (www.**statistics**.gov.uk)

1.2 GENETIC SUSCEPTIBILITY

Epidemiological studies (Bratt, 2002; Carter *et al.*, 1992) reported a positive relationship between prostate cancer incidence and familial inheritance. Genetic susceptibility accounts for approximately 10% of prostate cancer cases, and is responsible for approximately 40% of prostate cancer cases occurring below the age of 55 (Bratt, 2002). Diagnosis of hereditary prostate cancer is dependent on fulfilment of one or more terms from the hereditary prostate cancer criteria set out by Carter *et al.*, (1993). This criterion included the inclusion of three or more relatives affected within a nuclear family, three successive generations or relatives affected in an individuals' paternal or maternal family, or having two relatives who are both affected by the disorder before their 56^{th} birthday. These criteria enabled identification of prostate cancer susceptible genes near known genetic markers to be located by linkage analysis.

1.2.1 Hereditary Prostate Cancer 1 (*HPC-1*)

Several potential genetic susceptibility regions have been identified using linkage analysis (Smith *et al.*, 1996; Xu *et al.*, 2001), however, only three candidate genes have been identified. The first identified candidate gene was the Hereditary Prostate Cancer 1 gene (*HPC-1*).

Using genome wide linkage analysis on 66 high risk prostate cancer families, Smith *et al.*, (1996) reported the existence of a dominant prostate cancer susceptibility locus at 1q24-q25. Additional analysis of 25 North American and Swedish families, and confirmation by Cher *et al*, (1996) demonstrated that the long arm of chromosome 1 regularly demonstrated increased

copy numbers in advanced prostate cancer specimens examined by comparative genomic hybridisation (CGH).

Positional cloning identified that the *RNASEL* gene, located in chromosomal region 1q25, demonstrated nonsense mutation and a frame-shift mutation in the initiation codon. Loss of *RNASEL* protein function mutations co-segregate to two *HPC-1* linked families (Carpten *et al.*, 2002), resulting in loss of control of cellular proliferation and apoptosis. A nonsense mutation produced a variant *RNASEL* gene with a 3-fold reduction in normal enzymatic function, but increased association to prostate cancer in its homozygous or heterozygous genotypes. A frame-shift mutation observed in the initiation codon of the *RNASEL* gene relating to increased risk to prostate cancer was identified in Ashkenazi Jewish populations (Dong, 2006). In the general population, inactivated *RNASEL* is expressed at a low frequency. However, infrequent linkage of this gene locus to large family groups suggests that it may only play a limited role in inherited prostate cancer incidence.

1.2.2 Hereditary Prostate Cancer 2 (*HPC-2*)

Another locus of interest was the hereditary prostate cancer 2 (*HPC-2*), and the *ELAC* gene identified to chromosomal region 17p11 (Tavtigian *et al.*, 2001). The *ELAC* gene is thought to code for an evolutionary conserved metal dependent hydrolase enzyme (Tavtigian *et al.*, 2001). Takaku *et al,* (2003) reported that the *ELAC* gene codes for a 3' processing endoribonuclease, an enzyme family responsible for degradation of RNA into constituent ribonucleotide subunits. This suggests a possible role in cell cycle control. Mutational cloning of this gene identified two common loss-of-function missense mutation regions that result in loss of enzymatic activity. These missense mutations occurring at ser217leu and Ala541thr are implicated in increased risk to prostate cancer. However, linkage analysis has

failed to produce results of such clarity. Xu *et al.*, (2001) found no such relationship among 169 families.

Other studies provided contradictory evidence by showing linkage among small family groups; however, this was offset by the limited linkage among different pedigrees. An inability to find a common locus in hereditary prostate cancer is one reason why it is believed to contribute approximately 2% of all prostate cancer cases presented. At present, studies are being conducted on common genetic polymorphic regions such as androgen receptor and 5-alpha reductase gene in order to determine if they may be involved in controlling genes involved in prostate cancer. However, more work is required in order to provide an understanding of its role in prostate cancer (Schaid, 2004).

1.2.3. Macrophage Scavenger Receptor 1 (MSR1)

The macrophage scavenger receptor gene is located on chromosome 8p22, and was identified as being a candidate gene for hereditary prostate cancer by linkage analysis and direct sequencing approach (Sun *et al.*, 2006).

Macrophage scavenger receptor 1 (MSR1) is a member of a family of membrane receptors that have the ability to bind to various types of molecules including bacteria and lipoproteins (Rennert *et al.*, 2005). MSR1 have been functionally implicated in biological processes including immune response, inflammation and apoptosis (Platt and Gordon, 2001).

The *MSR1* gene is located in a commonly deleted region of chromosome 8 in prostate cancer cases resulting in production of several mutant variants of the *MSR1* gene. Each of these variants was studied in order to assess the extent of their relationship with increased prostate cancer risk, however, many of the results provided from such studies lacked consistency with

other independent studies. Meta-analysis of independent studies into the effects of mutant MSR1 variants and prostate cancer was performed by Sun *et al.*, (2006).

Meta-analysis is an ideal manner of analysing a large body of independent studies in order to integrate their findings. Sun *et al.*, (2006) reported that the MSR1 gene does not present a major risk to prostate cancer, but may provide a moderate risk, especially in black men.

1.3 THE PATHOLOGY OF PROSTATE CARCINOMA

1.3.1 Anatomy of the prostate

The prostate gland is a small acorn-shaped gland located at the base of the bladder, surrounding the urethra (Figure 1.3.1). Its main function is secretion of an alkaline fluid which makes up the one of the components of semen. The gland is found in all male mammals, but does not appear to be critical for survival. One method of treating primary organ confined prostate cancer is by complete removal of the prostate gland. However, the prostate gland is important in reproduction as it provides an alkaline environment which buffers sperm against the acidic environment of the vagina. In humans, development of the prostate occurs during puberty, coinciding with a surge in circulating levels of androgens.

The human prostate consists of four morphological regions comprising of two peripheral zones, the transition zone, the central zone, and the fibromuscular zone. The peripheral zones (right and left) together consist of approximately 70% of the total tissue mass of the gland. It is very susceptible to inflammation, and it is within this zone that mature prostate tumour cells are commonly located (Abate-Shen and Shen, 2000). The central zone makes up 25% of the total tissue mass of the prostate gland, and is very resistant to inflammation and to prostatic carcinoma. In contrast, the transitional zone, making up 5% of the total prostate tissue mass is the most common site of Benign Prostatic Hyperplasia (BPH). The fibromuscular zone is responsible for secretion of prostatic fluids during ejaculation by initiating muscular contractions. (Abate-Shen and Shen, 2000)

Figure 1.3.1 Anatomy of the Prostate Gland

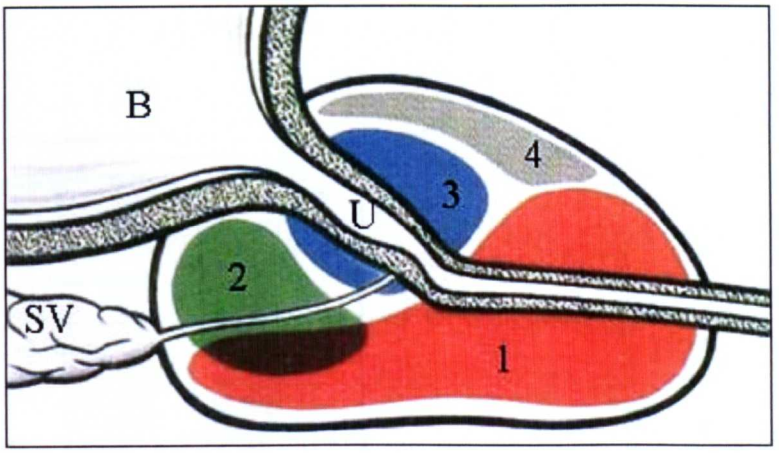

Figure 1.3.1 1= Peripheral Zone, 2= Central Zone, 3= Transitional Zone, 4= Anterior Fibromuscular Zone. B= Bladder, U= Urethra, SV= Seminal Vesicles

1.3.2 Prostatic epithelial cells and carcinogenesis

There are three main cell types within prostatic epithelium (Figure 1.3.2). The most common of these is the secretory luminal cell. These are androgen dependent cells that produce prostatic secretory proteins. They can be characterised by their expression of the androgen receptor and the filament high molecular weight proteins, cytokeratins 8 and 18, and the cell surface marker CD57 (Liu *et al.*, 1997).

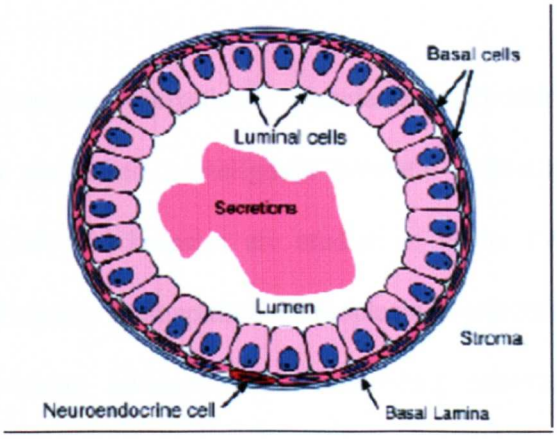

Figure 1.3.2. A depiction of cell types within human prostate epithelium.

The second epithelial cell types are basal cells. These cells are located between the luminal cells and the basement membrane and are able to express cytokeratins 5 and 14, as well as CD44. Liu *et al*, (1997) reported that basal cells express low levels of androgen receptor protein, and that basal cells do not produce secretory proteins. However, they do express autocrine factors such as *Bcl-2* which have a protective function against DNA damage (Abate-Shen and Shen, 2000). Additionally, it is believed that the basal cell layer acts as a stem cell reservoir in order to generate all three types of cells (Foster and Ke, 1997).

The third cell type is the neuroendocrine cell, which is found interspersed among basal cells. These cells provide paracrine signals that support luminal cell growth and proliferation. They appear to be androgen independent cells able to express Chromogranin A, and serotonin (Abate-Shen and Shen, 2000). Within the normal prostate, neuroendocrine cell populations are relatively low. However, neuroendocrine cell differentiation, the accumulation of cells with neuroendocrine characteristics and increased Chromogranin A expression, is a mark of increased cancer aggression.

1.3.3 Prostate cancer initiation

Prostatic Intraepithelial Neoplasia (PIN) refers to a sub stage of cellular transformation from a normal to a malignant prostatic epithelium (Foster *et al.*, 1999). In the USA, over 1,300,000 biopsies are studied to detect 198,500 new cases of prostate cancer annually. Prostatic Intraepithelial Neoplasia represents abnormal proliferation of premalignant cells without invasion into surrounding stroma, and can be characterised by a variety of architectural and cytological aspects (Foster and Ke, 1997) resulting in minimal changes to modifications that make it undistinguishable from carcinoma (Montironi *et al.*, 2000).

McNeal and Bostwick, (1986) identified PIN lesions by histopathological studies of prostate cancer tissue. These lesions were grouped into a series of four architectural types: Tufting, Micropapillary, Cribriform and Flat and are mainly located in the peripheral zone of the prostate (Bostwick and Brawer, 1987). Likewise, the morphological appearances can be as low grade or high grade PIN. Low grade PIN cell nuclei are enlarged and have increased chromatin content whereas high grade PIN cells have large nuclei, distinctly visible nucleoli, and coarsely increased chromatin content.

During development and growth of PIN, the epithelium may remain static or may increase in cell-stratified layer depending on the balance between cellular proliferation and apoptosis. Morphologically, a loss of the two cell thick epithelium, followed by a loss of basal layer is observed. This is an important factor as an absence of basal cells indicates the ability of cells to develop past organ confinement.

Chromosomal mutation studies (Haggman *et al.*, 1997; Sakr *et al.*, 1994) have shown that high grade PIN is multifocal and endures the same chromosomal mutations observed in early invasive carcinoma. The appearance of high grade PIN generally precedes the manifestation of carcinoma by approximately 10 years (Haggman *et al.*, 1997; Sakr *et al.*, 1994) and is an important morphological marker for detection of potential carcinoma of the prostate.

1.4 TUMOUR SUPPRESSOR GENES

Cancer is a genetic disorder arising from mutation or malfunction of a set of genes. These malfunctions can either be inherited or can be caused by carcinogenic stimuli as seen in sporadic cancer cases. It is also possible for cancer to occur as a result of epigenetic mechanisms such as DNA methylation or genomic imprinting.

Tumour suppressor genes (TSG) act antagonistically to oncogenes. Whereas oncogenes act to promote cellular proliferation, TSG operate to actively keep a cell at a steady state and control proliferation urges of oncogenes. The significant difference between oncogenes and TSG is that oncogenes require only a single allele to be activated in order to be a possible carcinogen, hence are deemed dominant. In contrast, TSG are involved in control and regulation of normal cellular function and require only a loss of an allele in order to suffer haploinsufficiency, resulting in partial or total loss of gene function and malignant transformation (Foster, Cornford *et al*, 1999).

Several tumour suppressor genes have been linked to the malignant progression of prostate cancer, and are identified using methods such as comparative genome hybridisation (CGH) and loss of heterozygosity (LOH). Comparative genome hybridisation is a process of identifying candidate genes for specific diseases. As the loss or gain of chromosomal regions by tumour cells occurs in a non random manner and is governed by underlying mechanisms, this method identifies candidate genes by comparing tumour DNA with normal DNA in order to pinpoint lost or gained chromosomal regions. Loss of heterozygosity is a higher resolution method of candidate gene detection compared to CGH. Whereas CGH is used to locate the region of mutation, LOH enables detailed study of the process by which a mutation in an allele results in loss of heterozygous expression of that gene, leading to homozygosity or hemizygosity.

1.4.1 Loss of Chromosome 8p and *NKX3.1*

Loss of specific regions of chromosome 8p is a common hallmark in early prostate carcinogenesis and is seen in approximately 80% of prostate tumours. Two chromosomal hot-spots for hereditary prostate cancer mutation have been identified on chromosome 8p12.21 and 8p22. Loss of 8p12.21 occurs in early stages of prostate cancer onset as this region is also lost in PIN and early invasive carcinoma. Loss of region 8p22 is thought to be a late occurring event in tumour progression as it is commonly seen in more advanced grade carcinoma. The *NKX3.1* gene is thought to be the candidate gene to the 8p12.21 locus as it is located within the chromosomal region lost in human prostate cancers (Voeller *et al.*, 1997). Targeted disruption of this gene resulting in *NKX3.1* homozygous deficient mice caused malformation of prostatic ducts and disruptive secretory protein production (Bhatia-Gaur *et al.*, 1999). Furthermore, mutant *NKX3.1* mice have been shown to develop human like PIN lesions suggesting that loss of *NKX3.1* expression may be responsible for PIN in humans. Interestingly, prostatic epithelial hyperplasia and dysplasia phenotypes are presented in heterozygote mice, indicating a haploinsufficiency mode of action for this gene.

1.4.2 Loss of Chromosomal Region 9p.21

The cylin dependent kinase N2 gene (*cdk-2*) is located on 9p21 and can be inactivated by deletion, point mutation, or CpG hypermethylation. This gene product has a very useful function in the cell as it enables progression past the G1 cell cycle phase. Consequently, in their inactivated phase, they may allow genetically unstable cells to progress through the cell cycle and propagate. Research in *CDKN2* has shown involvement in prostate cancer in both the primary and secondary phase of the disease. Jarrard *et al.*, (1997) reported that 13% of

primary tumours and 8% of metastatic tumours demonstrated hypermethylation in their promoter region; whereas 20% of primary tumours and 46% of metastatic tumours had deletions near the *CDKN2* gene. This indicates a dual action mutation event of methylation and deletion in these cancer cells resulting in malignant progression of the cell.

1.4.3 Loss of Chromosome 10q and *PTEN*

Loss of chromosome region 10q is a common event occurring in approximately 50 – 80% of cases tested. Loss of region 10q is believed to be a late stage occurring event in cancer progression as it is found in a greater number of carcinomas relative to PIN. The *PTEN* gene maps to chromosome 10q23, a region frequently lost in prostate and other carcinomas such as breast and endometrial cancer.

PTEN is widely expressed during mouse embryonic development and adulthood. A homozygous disruption of the gene results in embryonic lethality (Luukko *et al.*, 1999), whereas *PTEN* heterozygotes show severe dysplasia and carcinoma of the colon and skin. The *PTEN* gene was found to be mutated in some breast cancer cell lines, gliobastoma and LnCaP and Du145 prostate cancer cell lines (Li *et al.*, 1997). This was confirmed by other studies which demonstrated that this gene is frequently lost in prostate cancer (Vlietstra *et al.*, 1998) and that *PTEN* mutations are linked to advanced tumour stage (Suzuki *et al.*, 1998).

1.4.4 Loss of Chromosome 13q and *Rb1*

Loss of chromosome region 13q, including the region coding for the retinoblastoma gene (Rb1) commonly occurs in 50% of prostate tumours (Li *et al.*, 1998). The retinoblastoma gene was the first identified TSG and is located on chromosome 13q14.1 (Benedict *et al.*,

1990). Retinoblastoma loss of function mutations occur relatively early in tumour progression as mutations in the protein coding region have been identified in localised prostate carcinoma as well as advanced prostate cancer (Ittmann and Wieczorek, 1996). The loss of *Rb1* gene and subsequent onset of retinoblastoma was studied by Knudson, and formed the basis of his Two Hit Hypothesis of cancer development. This hypothesis was based on his studies and observations of inherited and sporadic cases of retinoblastoma between 1944 and 1969. Through statistical analysis, Knudson observed that the familial form of the disease generally occurred in children and produced a greater frequency of bilateral tumours in both eyes, whereas the sporadic form occurred significantly later in adults, and frequently produced a unilateral tumour in a single eye. This led Knudson to conclude that patients with the inherited form of retinoblastoma inherited a mutant *Rb1* gene congenitally, and the second hit or cancer causing mutation occurs in visual cells after birth. In sporadic cases, Knudson believed that the lag time in cancer incidence was a direct relationship to the rare occurrence of two cancer causing mutation events occurring in the same cell (Knudson, 1977).

Interestingly, reintroduction of exogenous *Rb1* gene into homozygous deficient prostate cancer cells caused a reduction in levels of tumourigenicity (Bookstein *et al.*, 1990). Additionally, LOH analysis demonstrated that approximately 48% of prostate cancer cases studied suffered from an allelic loss of the *Rb1* gene. From this number, one third demonstrated a loss of region 13q14 containing *Rb1*(Foster *et al.*, 1999).

1.4.5 Loss of Chromosome 17p and *p53*

The *p53* gene is located on chromosome 17. It is mutated in approximately 42% of advanced stage prostate cancers, whereas a low frequency (10-20%) of gene mutations has been

observed in primary prostate tumours. Normally functioning *p53* is a nuclear protein that is capable of controlling entry and movement through the cell cycle (Foster *et al.*, 1999). The *p53* gene safeguards cells against mutation by increasing *bax* and *p21* gene expression to promote the apoptotic pathway and decrease cyclic dependent kinases (*cdk2*). The *p53* gene binds to DNA to enable downstream signalling and increased activity of *p21*, which in turn interacts with a cell division stimulating protein (*cdk2*). The formation of a *p21-cdk2* complex halts a cells progression to the next stage of the cell cycle. However, in its mutant form, loss of *p53* gene expression results in a reduction in binding efficiency to target DNA. This causes a loss of *p21* gene expression and loss of regulation of the cell cycle. This enables mutated cells to divide in an unchecked manner, promoting replication errors and ultimately, increased tumourigenic potential.

Loss of chromosome region 17p occurs in advanced stages of prostate cancer and metastasis. Within the deleted region of 17p is the *p53* gene coding region. Mutations in the p53 gene rarely occur in early invasive carcinoma, and are more commonly mutated in advanced recurrent and metastatic prostate cancers (Abate-Shen and Shen, 2000).

1.4.6 Bcl-2 and cell-mediated apoptosis

The protein family Bcl-2 comprises an integral part of the mechanism which controls cell-mediated death. Four of the family members *Bcl-2, Bcl-XL, Bcl-W* and *Mcl-1* are anti-apoptotic favouring genes, whereas *Bax, Bak, Bcl-Xs, Bad* and *Bik* are apoptotic favouring genes (Lu *et al.*, 1996). These protein groups function by interacting with each other. Their individual concentrations as well as their proportion of expression relative to other members of the family determine a cell's fate when faced with apoptotic stimuli such as an anticancer drugs or androgen deprivation (Reed, 1994). Using immunohistochemistry, the expression of

Bcl-2 was detected in androgen independent basal cells, but not in the adjacent androgen dependent luminal secretory cells (Krajewski *et al.*, 1994a; Krajewski *et al.*, 1994b). *Mcl-1* and *Bax* are expressed in both basal and luminal cells, with the latter cell type having the higher level of expression. *Bcl-X* is equally expressed in both cell types.

McDonnell *et al*, (1992) demonstrated that transfection of *Bcl-2* into androgen dependent LNCaP cells enabled the survival of those cells during androgen deprivation. Furthermore, reduction of the level of *Bcl-2* via antisense technology resulted in an increased sensitivity to the cytotoxic drug Etoposide due to an increase in cellular proliferation as a result of androgen signalling (Berchem *et al.*, 1995). The results of the two above experiments suggest that *Bcl-2* over expression is related to androgen independence in cells as well as building up resistance to chemotherapy and radiotherapy.

1.4.7 Pathways of Tumour Suppressor Gene (TSG) activity

Tumour suppressor genes share common functions and interact with each other in many cases to provide regulatory function in cells. Their importance is such that losses of function mutations result in breakdown of cellular order and control deregulation.

The *PTEN* TSG acts by dephosphorylating a phosphate group from 3–phosphorylated inositol lipids that, in turn, acts as messengers to protein kinase AKT otherwise known as protein kinase B (Feldman and Feldman, 2001). Activation of this pathway initiates an anti-apoptotic activity in cells. In normal cell function, *PTEN* expression blocks activation of the AKT pathway and initiates programmed cell death. In tumour cells, this ability is lost. Reduced *PTEN* expression increases AKT activity, thereby blocking apoptotic signals (Feldman and Feldman, 2001) (Figure 1.4.7). Cancer cells commonly show mutations of the PTEN gene, and more specifically, mutations in the phosphatase catalytic domain of PTEN.

This suggests that loss of PTEN function mutations is manifested as an inability to dephosphorylate phosphatidylinositol 3,4,5-trisphosphate (PIP_3) leading to unfettered activation of the AKT pathway.

The Bcl-2 protein family, especially the *Bcl-2* gene, plays an important role in programmed cell death. Pro-apoptotic members of the Bcl-2 family include Bax, Bid, Bim, and Bik contain an alpha helical "death domain" that enables complex formation with the hydrophobic domain of anti-apoptotic members of the BcL-2 family such as *Bcl-2* and *Bcl-*x_L. This heterodimer formation inhibit the anti apoptotic activity of *Bcl-2* and the proapoptotic proteins are able to interact with mitochondrion, resulting in excretion of cytochrome C and activation of down stream mediators of the caspase cascade, and apoptosis. However, relative levels of pro and anti-apoptotic members of the Bcl-2 family determine a cells susceptibility to programmed cell death (Figure 1.4.7).

The *p53* gene acts as a cell cycle regulator. This TSG has the ability to halt the cell cycle in order to ensure DNA repair, or failing that, programmed cell death. The p53 gene is able to regulate p21 gene expression. This p21 gene binds to and inhibits cyclin dependent kinase activity, causing the blocking of G1-S phase transition to enable DNA repair. p53 genes can also initiate programmed cell death through caspase cascade mentioned above.

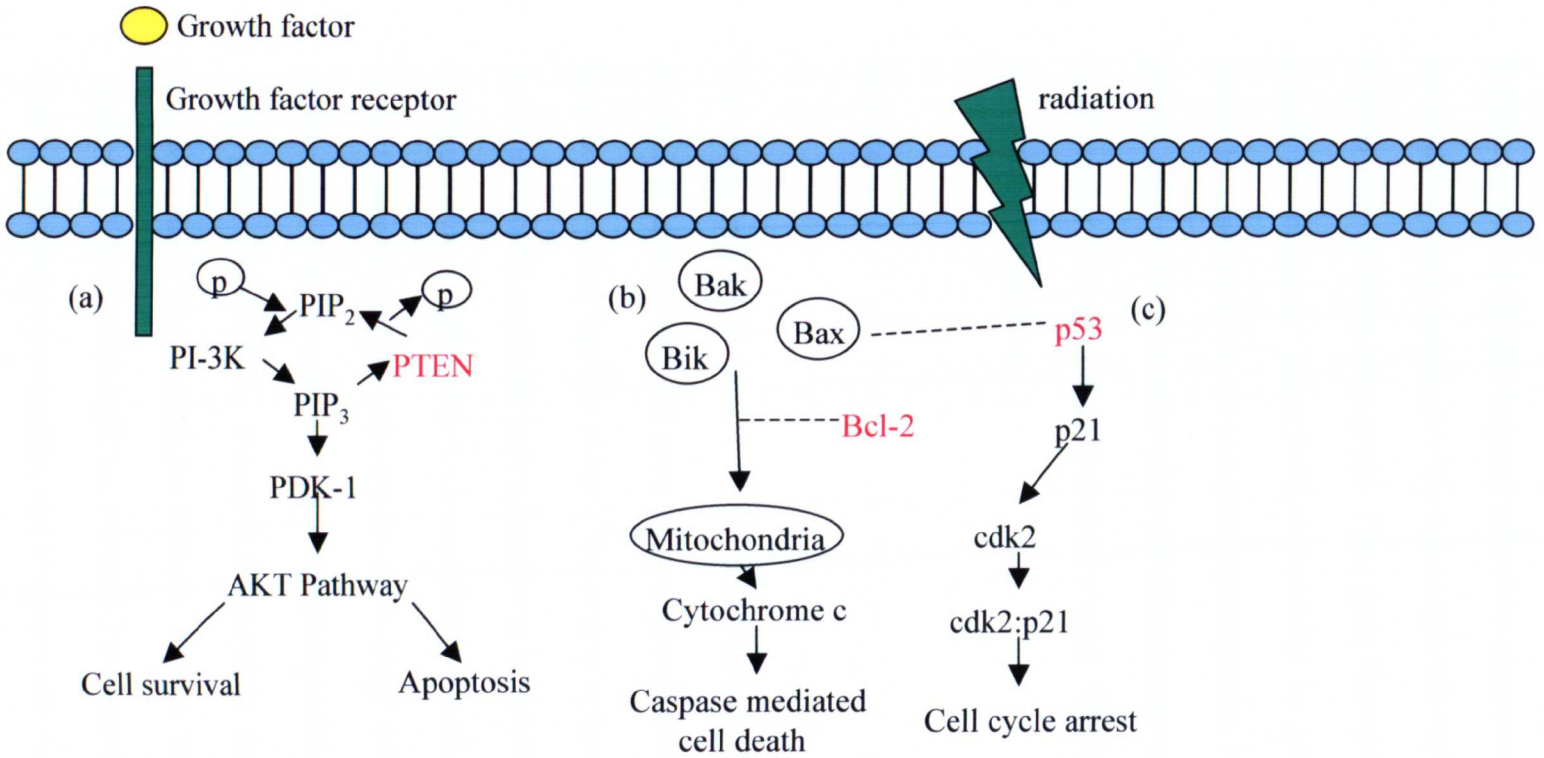

Figure 1.4.7 Tumour suppressor gene pathways of *PTEN* (a), *Bcl-2* (b) and *p53* (c)

(a) The Phosphatidyl inositol 3-kinase (PI3-K) product, phosphatidylinositol 3,4,5-trisphosphate (PIP_3), is dephosphorylated by *PTEN* which ultimately blocks activation of AKT pathway, resulting in apoptosis. Mutations to PTEN result in increased AKT signalling and activation of AKT pathway and cell survival.

(b) *Bcl-2* is an anti-apoptotic protein that is antagonised by pro-apoptotic members of the *Bcl* family such as *Bak* and *Bax*, Loss of *Bcl* function results in caspase mediated cell death.

(c) The *p53* gene is a cell cycle regulator. Normally functioning *p53* up-regulates *p21* activity which complexes with cdk2 to halt the cell cycle. However, loss of p53 function causes unregulated cell cycle progression.

1.5 ONCOGENE ACTIVATION

Oncogenes can be defined as genes carried by tumour viruses expressed by cancer cells and are partly or solely responsible for tumourigenesis (Lawrence, 1997). Oncogenes are the mutated form of proto-oncogenes. Their main function within the cell is to stimulate cell growth and division. Oncogenes are activated by genetic alterations in gene sequences caused by base deletions, substitutions, rearrangement, over expression or amplification. At present, there is a vast number of identified oncogenes in cancer. However, only a relatively small number has been linked to prostate cancer. These include H, K, and N-ras, Myc, Bcl, and Her2/neu oncogenes.

1.5.1 *Ras-p21*

The *ras-p21*protein is located on the inner surface of a cell's plasma membrane and is involved in transduction and processing of growth factor signals. The *ras-p21* protein can exist in active and inactive phases. The protein is inactivated by interacting with GTPase activating protein, and loses a phosphate group to become an inactive *ras-p21* GDP.

GTPase activity is reduced in the mutant form. A reduction in GTPase signalling results in *ras-p21* gene activation. Continued downstream interaction results in accumulation of cellular protein kinase and an increase in cellular proliferation (Moul *et al*, 1994).

H-ras gene expression is increased in androgen insensitive cells relative to androgen sensitive cells. This correlation between mRNA levels and tumour progression is not repeated in *N-ras* or *K-ras* mRNA, yet it has been reported that transfection of non-metastatic dunning rat prostatic cancer cells with *H-ras* provides increased metastatic potential.

1.5.2 *Myc*

The *Myc* gene is another oncogene that has been functionally associated with prostate cancer. The gene is differentially expressed in normal, BPH and prostate cancer cases as a result of an increase in gene copy number caused by amplification or chromosomal gain (Nipponon *et al*, 1998). Activation of the *Myc* oncogene results in increased cell proliferation and transformation. This activity can be seen in 8% of primary prostatic cancers, and about 30% of prostate cancer metastaes.

1.5.3 *Her – 2 Neu*

Her–2/Neu gene is located at chromosome 17q11-21, and codes for a protein that is similar to epidermal growth factor receptor (EGF). Its normal gene function is to increase signalling activity of androgen receptor during periods of low androgen levels. Consequently, it may be that the *Her–2/Neu* is responsible or closely involved in the onset of androgen independent tumours through the out law pathway of androgen independence (Feldman and Feldman, 2001). *Her–2/Neu* has been observed to be consistently over-expressed in androgen independent prostate cancer cell lines generated from xenografts implanted in castrated mice (Craft *et al.*, 1999). *Her–2/Neu* is capable of activating androgen dependent genes in the absence of androgen receptor ligands such as steroid hormones; however, androgen dependent gene activation cannot be activated in the absence of androgen receptor. This is interesting since Casodex, an anti-androgen agent, blocks activation of androgen receptor by EGF growth factors, yet cannot block outlaw androgen receptor produced by *Her–2/Neu* over-expression. This indicates that either *Her–2/Neu* signalling cascade produces a molecule that binds at a competitively higher affinity than Casodex (Craft *et al.*, 1999).

Furthermore, Signoretti *et al.*, (2000) failed to observe amplification in gene copy number of *Her-2/Neu* genes whereas amplification has been observed in other studies (Ross *et al*, 1997; Kaltz-Whittmer *et al*, 2000). In a later study, Savinainen *et al*, (2002) assessed the role of *Her-2/Neu* in prostate cancer through analysis of *Her-2/Neu* gene expression in breast and prostate cancer cell lines, and tumours by chromogenic in situ hybridisation (CISH). This study observed over-amplification of *Her-2/Neu* gene in breast cancer but no change in prostate tumour gene expression was observed.

1.5.4 Transforming Growth Factors-α (TGF-α) and Epidermal Growth factor (EGF)

The family of growth factors include epidermal growth factor (EGF), fibroblast growth factor (FGF); and platelet derived growth factors (PDGF). Growth factors bind to their cell surface receptors and facilitate cellular proliferation and differentiation.

Transforming growth factors-α (TGF-α) and epidermal growth factors (EGFs) are members of a superfamily of cell-surface receptors that includes the bone morphogenic protein (BMP) receptors, which, after ligand activation, transduce signals mainly through the Smad family of transcription factors and co-activators. They regulate proliferation, growth arrest, differentiation, and apoptosis of prostatic stromal and epithelial cells as well as the formation of osteoblastic metastases.

These growth factors exert their influence on the cell by binding to cell surface epidermal growth factor receptors (EGFR) to enable intrinsic tyrosine kinase activity and facilitate cellular communication and signal transduction (Lenferink *et al.*, 1997) TGF-α and EGF bind with equal affinity to EGFR, however, upon internalisation, the growth factors follow different intracellular routes(Ebner and Derynck, 1991).

In advanced prostate cancer, EGF and TGF-α as well as the EGFR receptor are observed to be over-expressed (Culig *et al.*, 2000; Culig *et al.*, 1994; Culig *et al.*, 2002). In addition, it was observed that in primary androgen dependent tumours, a paracrine relationship exists between tumour cells, which expressed EGFR, and surrounding stromal cells, which expressed TGF-α. However, in androgen independent metastases, tumour cells established an autocrine functionality that enabled expression of both EGFR and TGF-α (Scher *et al.*, 1995).

Such results suggest a close relationship between androgen receptor signalling, growth factor expression and prostate cancer progression. Previous studies have suggested that polypeptide growth factor signal transduction pathways can stimulate androgen receptor amplification (Gioeli, 2005) and also increase their hypersensitivity or independence towards androgen ligands (Culig *et al.*, 2000; Culig *et al.*, 1994; Culig *et al.*, 2002)

1.6 MOLECULAR BIOLOGY OF PROSTATE CANCER METASTASIS

1.6.1 Mechanism of prostate cancer metastasis

Mid to late tumours in humans and animals are heterogeneous, and consist of different subpopulations of cells with varied biological characteristics. Malignant progression of cancers is matched by increasing genetic instability. Cifone and Fidler, (1981) demonstrated that increased metastatic potential was closely related to genetic instability. It was also reported that cancer cells develop in a sequential manner to achieve a metastatic state. From a population of cancer cells, only a few will achieve mutations appropriate to enable invasion, dissemination and survival at a new location.

Metastasis is the migration of cancer cells from a primary location or organ to colonisation of a secondary location or organ. In a clinical sense, cancer metastasis presents a bleak outlook for patients as current medical management and associated techniques fail to deal with the heterogeneity of metastasising cancer cells.

The full mechanism of metastasis remains unclear. However, since the presentation of the "Seed and Soil" hypothesis (Paget, 1889) to explain the apparent non-random pattern of metastatic displacement, our knowledge and strategies for combating this mechanism is increasing. The crux of the theory obtained by examining over 900 autopsies of patients with a variation of different types of primary cancer, was that certain cancer cells had an affinity for certain environments provided by certain organs, and would strive to reach this destination.

Cancer metastasis represents a specific phase in a sequential process requiring the involvement of several hormones and growth factors interacting with a cancer cell. Each stage is as important as the previous. Failure to successfully negotiate hurdles set up by cell

regulatory mechanisms result in retarding the malignant progression of a cancer cell (Figure 1.6.1).

Fidler, (1970) demonstrated that within a 24hr period of invasion into the blood stream, less than 0.1% of tumour cells are viable, and from this number, only 0.01% produce sustainable metastases. This clearly indicates that tumour cell metastasis is a highly selective mechanism that requires expression of specific genes in order that a cell achieves its metastatic potential. Not all primary tumour cells have the ability to metastasise due to an inability to successfully navigate different metastatic stages. Breast and prostate cancer cells have been reported to exhibit a high affinity for bone. Approximately 95% of cases result in osteoblastic metastasis (Harris *et al*, 1994). However, the question remains, why is bone tissue a favoured metastatic site for prostate cancer cells?

1.6.2 Factors governing osteoclastic metastasis

Osteoclasts and osteoblasts closely regulate bone growth, remodelling and management. Osteoclasts are large multi-nuclear cells derived from macrophages and exhibit an ability to destroy calcified or cartilaginous matrix. Osteoblasts are cells responsible for the formation of bone by secretion of non-mineralised bone matrix. Osteoclasts exist in the two states of inactive and active. Inactive osteoclasts are derived from precursor cells of a monocyte macrophage lineage, whereas in their active form, osteoclasts enable absorption of bone by stimulating hormones such as parathyroid hormone (PTH), and Dihydroxy vitamin D3.

Osteoclastic production is managed by an interaction of growth factors and cytokines. Of these, the most prominent is the Receptor Activator of Nuclear Factor - κβ ligand (RANKL) produced by osteoblastic cells.

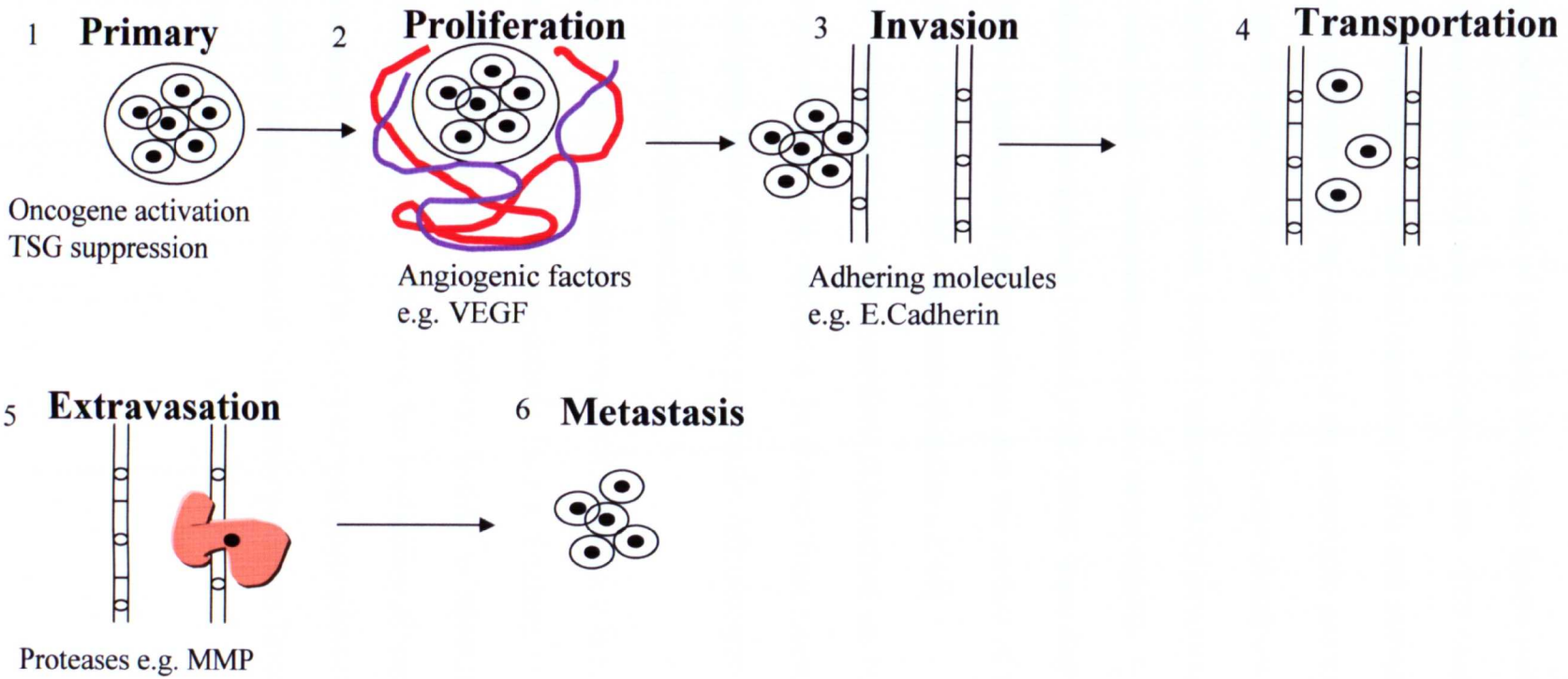

Figure 1.6.1 shows the metastatic pathway by which primary tumour cells are able to disseminate from a primary tumour site to a secondary location. Initially, cellular alterations occur within a cell that leads to tumour growth and loss of proliferative control **(1).** Additional mutations instigate increased mobility and invasiveness of a tumour. An increase in angiogenic activity, represented by neovascularisation, facilitates increased tumour growth **(2)**. The enhanced expression of proteases and an enhanced invasive trait enable penetration of carcinoma cells into circulation **(3)**. Once within the circulation, these tumour cells form micro clots that are trapped in capillary beds **(4)**. In order to establish a secondary metastatic site, tumour cells anchor and start to invade into surrounding tissue **(5)**. These tumour cells establish a microenvironment and proliferate to become productive metastasis **(6)**.

RANKL are located on the cell surface stromal cells and on osteoblasts. They are up-regulated by a variety of different osteotropic factors including prostaglandin E2, 1, 25 dihydroxyvitamin D3, and parathyroid hormone. This causes the release of RANKL from the cell surface of stromal and osteoblastic cells, and enables them to bind onto their RANK receptors situated on the surface of the osteoclastic precursors. Formation of osteoclasts occurs by signalling through the NF-κβ pathways (Roodman, 2004).

Regulation of osteoclastic levels is maintained by osteoprotegrin, a member of the tumour necrosis family. Osteoprotegrin acts as a decoy receptor for RANKL and inhibits RANKL induced osteoclastogenesis (Edlund *et al.*, 2004). Bone degradation and absorption occur by release of proteases from osteoclasts onto the surface of bone causing a breakdown and release of bone mineral components (Roodman, 2004).

The mechanisms by which osteoblasts differentiate are less well understood. However, osteoblasts have been reported to be formed from mesenchymal stem cells, and that a transcription factor crucial to the osteoblastic differentiation process is a core-binding factor α - 1 (CBFA1) (Roodman, 2004).

Approximately 90% of prostate cancers metastasise to bone (Harris *et al.*, 1994). Of these metastases, 95% present osteoblastic lesions, resulting in a net gain of bone formation. Present understanding of the pathway leading to osteoclastogenesis is well documented (Keller, 2004; 2002). However, the mechanism of osteoblastogenesis is less clearly understood. What is clear is that in the metastatic pathway, osteoclastic metastasis causes increased secretion of minerals which act as precursors for osteoblastic activity in production of bone metastasis.

1.6.3 Factors governing osteoblastic metastasis

In a situation where bone absorption precedes bone production, a good many factor are likely to play an important role in the acquisition of an osteoblastic metastatic state.

1.6.3.1 Parathyroid Hormone Related Protein (PTHrP)

Parathyroid hormone related protein (PTHrP) has 70% homology to parathyroid hormone (PTH), and is capable of binding to the PTH receptor and eliciting the same biological activity as PTH. PTHrP was isolated from human lung, breast and renal cell carcinomas and characterised through its role as a hypercalcemic factor (Gohji and Kitazawa, 2003). Hypercalcemia is a condition characterised by high concentrations of calcium compounds in circulating blood, and is detected using biochemical markers such as pyridinoline and deoxypyridinoline. Parathyroid hormone augments osteoclastic activity, increases PTH activity and results in elevated osteoclastic activity. However, PTHrP/PTH ratios do not consistently equate to elevated levels of hypercalcemia in the circulation as the expression of calciton, a hormone responsible for metabolism of calcium, secreted by the thyroid gland and in neuroendocrine cells of the prostate gland, reduces circulating levels of calcium.

PTH is an osteoclastic promoting factor, and operates by binding to the PTH receptor to stimulate differentiation and activity of osteoclastic precursor cells. Increased osteoclastic activity results in increased bone absorption, resulting in the release of calcium from degraded bone. In tumour initiated bone metastasis, osteolysis is regarded as the first stage in osteoblastic metastasis. Hence, certain biochemical markers such as an increase in blood calcium and phosphate levels are displayed in non-prostate cancer patients and patients with prostate cancer. Ikeda *et al.*, (1996), and Takeuchi *et al.*, (1996) demonstrated a marked difference in calcium and phosphate levels in patients with metastatic prostate cancer

compared to patients with organ confined prostate cancer, 89.3% and 5.9% respectively. The level of deoxypyridinoline, a hypercalcemic marker, was 0% in BPH cases.

1.6.4 Peroxisome Proliferator Activator Receptor (PPAR)

1.6.4.1 Structure of PPAR

The Peroxisome Proliferator Activated Receptor (PPAR) is a member of a group of nuclear hormone receptors. At present, 3 different subtypes have been identified: α, δ, and γ. Each is encoded by a different gene (Bilson *et al*, 2002). There is a great homology between members of the nuclear hormone receptor family, and isoforms of the PPAR protein. PPARα, δ, and γ show conserved DNA and ligand binding domains. The PPAR structure consists of a ligand independent and ligand dependent transactivation function, AF1 and AF2 respectively (A/B), followed by a DNA binding domain (C), which consists of two zinc motifs. Within these motifs are well-conserved P and D boxes that enable interaction with specific DNA sequences, and the dimerisation of receptors respectively (Bilson *et al*, 2002). Domain D is referred to as a variable hinge region, which enables structural changes as a result of DNA, sequence interaction or receptor dimerisation. Section E is the ligand-binding domain.

Figure 1.6.4.1 Structure of Peroxisome Proliferator-Activated Receptor (PPAR)

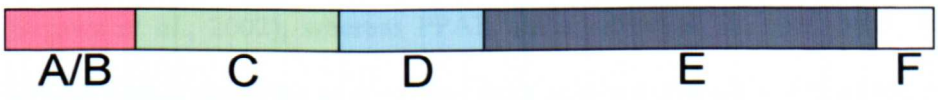

A/B – Ligand activation function
C – DNA binding domain
D – Variable hinge region
E - Ligand binding domain
F – Unknown function

PPARs form heterodimer complexes with the retinoid-X receptor and enables binding of the complex to specific DNA elements known as peroxisome proliferator response elements (PPRE). Peroxisome proliferator response elements are made up of two repeat sequences separated by a 1 base pair spacer nucleotide (AGGTCA-n-AGGTCA). Peroxisome proliferator response element polarity is governed by a short sequence upstream to the first repeat sequence, and PPRE functional units have been identified in several genes linked with protein metabolism. Such proteins include lipid processing and uptake protein lipoprotein lipase (LPL), fatty acid translocase (FAT/CD36), fatty acid transport protein (FATP), and fatty acid metabolism such as acyl-CoA Oxidase and Acyl-CoA synthetase (van Bilsen *et al.*, 2002).

Peroxisome proliferator activated receptor is a ligand activated transcription factor and has three isoforms: α, δ, and γ. A high level of homology exists among the three subtypes, especially in the DNA binding domain of PPARα and PPARγ, sharing 86% and 85% amino acid homology respectively relative to PPARδ. Furthermore, a high homology rate is observed in the ligand-binding domain that produces a 70% and 68% amino acid homology of PPARα and PPARγ respectively compared to PPARδ. PPAR activity is initiated by ligand binding to a plethora of ligands including fatty acids (PPARα and PPARβ) and prostaglandins and leukotrienes (PPARγ).

A region of great diversity is the A/B region that is poorly understood, but is believed to enable ligand independent transactivation function (as reviewed in Rosen, (2001). PPAR gamma, predominantly found in adipose tissue, is up-regulated in prostate cancer cells (Segawa *et al.*, 2002), whereas PPAR alpha, observed in liver, heart, muscle and brown adipose tissue, functions as a nuclear fatty acid and steroid hormone transporters (Collett *et al.*, 2000).

1.7 ANGIOGENESIS AND PROSTATE CANCER

1.7.1 Angiogenesis

The malignant progression of a cell is dependent on interaction of two main classes of genes; oncogenes and tumour suppressor genes. Also, it is now widely accepted that due to inherent heterogeneity of a sub cellular tumour populations, only a small number of cells undergo sufficient genetic instability to achieve a metastatic phenotype. Angiogenesis is a crucial factor of metastasis, and as such, may act as a rate-limiting step in progression of a metastatic phenotype.

Angiogenesis is described as "the development of a network of blood vessels (neo-vascularisation) in an oxygen deficient environment". Within the scope of cancer, angiogenesis represents an important milestone in tumour progression as it indicates development and maturation of the tumour.

During vascularisation, changes in tumour environment and cellular signalling attract endothelial cells. Migrating endothelial cells aggregate to form tubules that surround peri-endothelial support cells, enabling development of a network of vessels to support and nurture tumour growth (Hanahan and Folkman, 1996). Tumours have been shown to actively mould their environments and induce physiological changes such as neo vascularisation by emitting or releasing autocrine and paracrine factors such as vascular endothelial growth factor (VEGF), fibroblast growth factor (FGF), matrix metalloproteinase, insulin like growth factor I and angiopoietin-I (Zetter, 1998). To date, it is firmly believed that angiogenesis and neo-vascularisation are a physiological response to an inducer known as Hypoxia Inducing Factor (HIF), which in turn up regulates the expression of a very potent mitogenic growth factor, VEGF.

1.7.2 Hypoxia Inducing Factor (HIF)

Hypoxia inducing factor 1 is a α–β–heterodimer and acts as a DNA binding factor capable of controlling hypoxia related activities. HIF-α together with HIF-β subunits exist as a series of isoforms, of which, HIF-1β subunit is a constitutively expressed nuclear protein, whereas HIF-α is expressed as a result of hypoxic conditions.

There are three HIF- α isoforms, HIF-1α, HIF-2α, and HIF-3α, of which HIF-1α, and HIF-2α are closely conserved.

.

1.7.3 Hypoxia Inducing Factor and Prostate cancer

Previous studies have associated low levels of oxygen post radiotherapy as resulting in poor patient prognosis. This suggested a role of hypoxia in tumourigenicity and metastasis. Studies in human and animals reported a level of hypoxia in prostate carcinoma, and that hypoxic regions are linked with higher clinical stages (Cvetkovic *et al.*, 2001). Thus it is believed that hypoxic condition acts as a stimulator of angiogenesis. At a critical mass, simple oxygen diffusion is inadequate in providing oxygen to tissues; and a more efficient delivery system is required. At this stage, changes in tumour environments are observed, and a hypoxic signalling pathway is activated to release angiogenic growth factors. Hypoxia has been shown to increase the expression of platelet derived growth factor, and VEGF mRNA in tissue culture (Shweiki *et al.*, 1992). They reported that VEGF expression in tumours was highest in regions surrounding hypoxic tissue, thereby indicating a possible mechanism by which hypoxia regulates blood vessel growth in tumours.

1.7.4 Vascular Endothelial Growth Factor (VEGF)

New vessel growth and development is a complex and complicated mechanism requiring an interaction of several factors and receptors. Neo-vascularisation is stimulated by the release of autocrine and paracrine factors such as matrix metalloproteinase and other tumour promoting factors. However, one of the more important growth factors involved in the angiogenic framework is VEGF. VEGF is a member of a group of closely related proteins that are all pro-angiogenic factors (Huss *et al.*, 2001). There are five members of the VEGF family; VEGF-A B, C, D, and E, and three receptors, VEGFR-1, 2, and 3 (Chevalier *et al.*, 2002).

VEGFR-1 and 2 are expressed in vascular endothelium, whereas VEGRF-3 is expressed in lymphatic endothelium in adults. VEGF-A, and B bind to VEGFR-1, whereas VEGF-C and D bind to VEGFR-2 and 3 (Sato, 2003).

1.7.5 VEGF Isoforms

The human VEGF-A gene consists of eight exons separated by 7 intronic regions. Alternative splicing produces four different isoforms; VEGF121, 165, 189 and 206, numbered for the different amino acids present. VEGF165, the predominant isoform, lacks residues coded for by exon 6, whereas VEGF121 lacks residues coded for by exon 6 and 7 (as reviewed in (Ferrara *et al.*, 2003). Neufeld *et al*, (1999) identified two other VEGF isoforms (VEGF145 and VEGF183).

Native VEGF is a heparin binding homodimeric glycoprotein 45kDa in size, and is similar to VEGF165. VEGF121 is an acidic polypeptide that does not bind protein, whereas VEGF189 and 206 are basic and bind with great affinity to heparin. VEGF121 and 165 are freely

diffusible whilst 189 and 206 are used within the extra cellular matrix (as reviewed in (Ferrara *et al.*, 2003).

1.7.6 VEGF and Prostate cancer

VEGFR signalling has a very complex mechanism consisting of several signalling proteins. Interestingly, a VEGFR1 induces endothelial cell migration, but does not induce endothelial cell proliferation, nor does it signal through the mitogen activated protein kinase pathway (MAPK) cascade (Waltenberger *et al.*, 1994). However, VEGFR2 does signal through the MAPK cascade, enabling endothelial cell proliferation.

As there are angiogenic factors, equally, there are antiangiogenic factors such as angiopoietin-2, thrombospondin, and tissue inhibitor of metalloproteinase-1. It is believed that tumour vascularisation occurs as a result of disruption in the balance of pro and anti angiogenic factors.

VEGF is a potent pro-angiogenic factor, and is over expressed in human and rat prostate cancer cells (Chen *et al.*, 2000; Ferrer *et al.*, 1997). VEGF is differentially expressed in normal, benign and prostate cell line models. Urine tests of patients with BPH and organ confined prostate cancer failed to detect VEGF expression in all cases, however, in Dunning R3327 PAP tumour models, expression of VEGF, VEGFR1 and VEGFR2 mRNA were up regulated relative to normal ventral prostate. Furthermore, serum levels of VEGF were also detected in mice orthotopically grafted with DU-145 and PC3M prostate cancer cell lines (as reviewed in (Huss *et al.*, 2001).

Huss *et al*, (2001) measured the expression of VEGF isoforms in normal, benign and prostate cancer tissue sections, and reported that VEGF mRNA expression was detected in PIN, well differentiated and poorly differentiated tissues, but not in normal prostate tissue. This led

them to conclude that the angiogenesis switch was not a straight on/off signalling, but a more complex sequential graded switch consisting of an early initiating phase that is linked to hypoxia, and a late progression phase for tumour development. The initiating phase is associated with HIF 1α and VEGFR1 expression and rising levels of hypoxia, whereas the progression phase is linked to VEGFR2 expression and stimulates tumour progression.

1.8 ANDROGENS AND PROSTATE CANCER

Testicular synthesis accounts for approximately 90% of testosterone-derived dihydroxytestosterone (DHT) within the prostate. The remaining 10% is formed by adrenal androgens and dietary supplementation (Bruchovsky *et al*, 1971). Testicular-synthesised testosterone is an important factor in the development and function of the prostate gland *in utero*, postnatal and in adulthood.

1.8.1 Androgen independence and prostate cancer

Growth and development of prostate cancer from a primary phase to a secondary metastatic phase is dependent on tumour cells attaining androgen independence. Metastasis of prostate tumour cells results in poor patient prognosis; hence, the main therapeutic outcomes are aimed at tackling the cancer at its primary androgen dependent stage. Androgen ablation, whether by surgical or pharmacological castration, deprives androgen dependent cells of androgen, thereby resulting in a suppression of androgen signalling and androgen receptor activated target gene transcription. Blockage of androgen signalling in androgen dependent cells is thought to initiate compensatory proliferation, a selection pressure, by which cells that are able to tolerate a low androgen environment are able to stabilise and gradually

increase their rate of proliferation till eventually a greater population of cells with more and more independence to androgen are presented as the remaining progeny (Prehn, 1999).

1.8.2 Mechanism of androgen action

The growth of prostate cancer depends on the ratio of cells proliferating to cells undergoing apoptosis. This ratio is regulated by androgens that are capable of stimulating proliferation, and inhibiting apoptosis (Feldman and Feldman, 2001). Androgen ablation causes a shift in this balance, lowering the rate of proliferation, and increasing cell death. This results in a gradual reduction of cell numbers, leading to extinction. The great majority of testosterone exists in a bound form with sex-hormone binding globulin and albumin, however, the unbound form diffuses into a target cell cytoplasm where it is converted into dihydroxy – testosterone by a 5-alpha-reductase enzyme. DHT binds to androgen receptors at a higher affinity than testosterone, resulting in regulation of specific gene transcription (Figure 1.8.2).

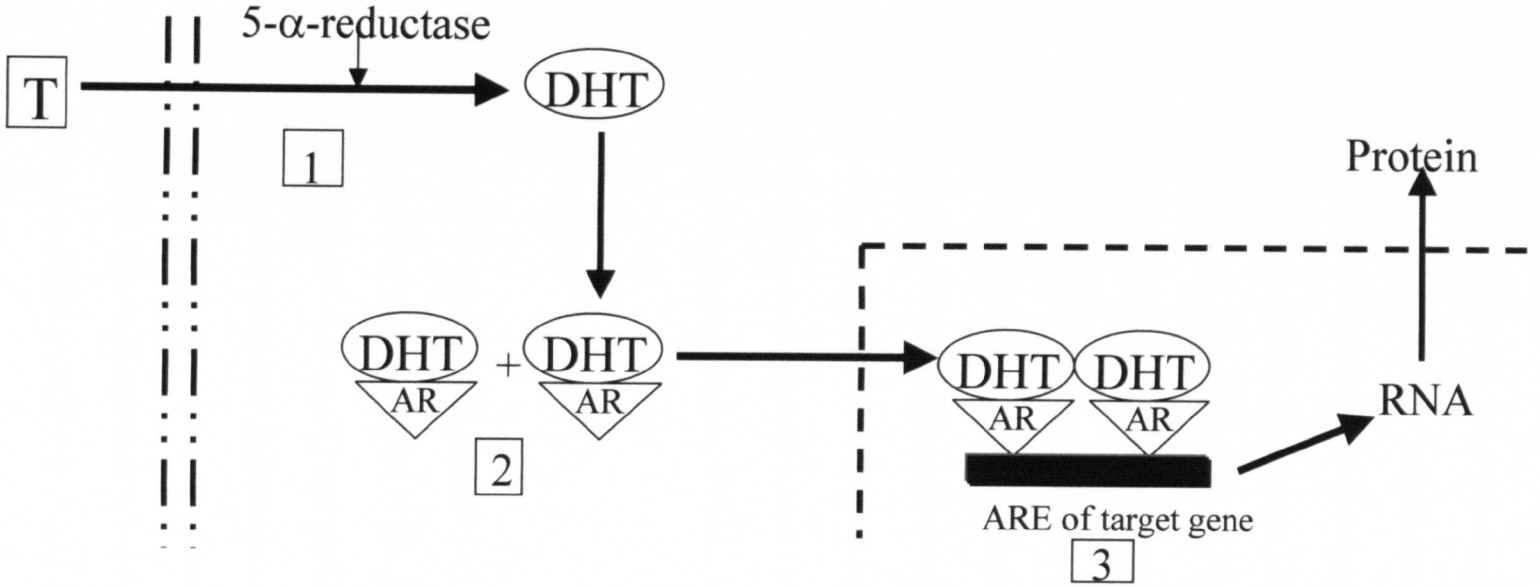

Figure 1.8.2 Conversion of testosterone to DHT, and activation of androgen response element

1. Testosterone (T) is converted in Dihydroxy-testosterone (DHT) by 5alpha-reductase enzyme
2. DHT binds at a higher affinity to androgen receptor (AR) than testosterone to form DHT complexes
3. These complexes pass through the nuclear membrane and attach to the androgen response element of target gene, enabling gene specific transcription

1.8.3 Trigger points of androgen independent prostate cancer

One of the key trigger points for tumour progression is a genetic alteration that may serve to provide the cell with an advantage. The earliest genetic alteration to occur in sporadic prostate cancer is the phase II detoxification enzyme, glutathione S-transferase (GST). These enzymes act as intracellular detoxifiers of electrophiles and carcinogens and environmental carcinogens. Loss of function by hypermethylation of the GST promoter region, as observed in 90% of prostate cancers, increases carcinogenic potential of cells. (Feldman and Feldman, 2001). Inability to nullify electrophiles and carcinogens increases the cells relative risk of further mutation events occurring that would lead to loss of androgen status

Cher *et al*, (1996) demonstrated that metastasising tumours had the requisite chromosomal aberrations required for successful growth during androgen deprivation. This indicates that the requisite androgen independent prostate cancer (AIPC) mutations must occur prior to androgen deprivation (Feldman and Feldman, 2001).

1.8.4 The Hypersensitive Pathway of AIPC

The concept of androgen independence in prostate cancer cells is a misnomer as it is clear that prostate cancer cells faced with declining levels of androgen evolve coping strategies that enable increased sensitivity to low level androgen signalling, or receptor activities that are stimulated by more generic steroids or signalling pathways. Consequently, when talking about androgen signalling, this has to be taken into account.

The mechanism of change that occurs to enable a tumour cell to move from an androgen dependent phase to an androgen independent stage is not fully understood. A clearer understanding of this pathway is essential in order to improve longevity of androgen ablation

therapy, and to increase our understanding of the malignant progression of a prostate cancer tumour cell.

1.8.5 Androgen Receptor amplification

One of many different theories that have been proposed as a possible pathway to low androgen level tolerance is the hypersensitive pathway (Feldman and Feldman, 2001). This pathway maintains androgen receptor amplification increases sensitivity to low levels of circulating androgens. To test this, a study was performed that verified that 30% of tumours had increased levels of androgen receptor gene expression after testosterone ablation therapy. In contrast, none of the primary tumours, taken from patients prior to ablation therapy, had androgen receptor amplification. Furthermore, patients with androgen receptor amplification, post-androgen ablation, survived for longer periods than patients with no androgen receptor amplification (Chen *et al.*, 2004; Hobisch *et al.*, 1995; Hobisch *et al.*, 1996). These results fit with the compensatory hyperplasia model which suggests that tumour cells with appropriate mutations adapt, stabilise and eventually proliferate in low androgen conditions. Tumours that use this method continue to depend on low level androgen signalling and androgen receptor amplification (Feldman and Feldman, 2001).

1.8.6 Increased androgen levels

Another coping strategy of cells confronted with androgen deprivation is to increase androgen production or increase the efficiency of conversion of testosterone to DHT. This proposed mechanism was supported with evidence which, after androgen ablation, showed a 95% decrease in serum levels of testosterone, and a decrease in DHT of prostate tissue of

only 10% (Labrie *et al.*, 1986), clearly indicating an increase in efficiency of DHT conversion.

Epidemiological studies have shown that individuals and ethnic groups with high 5-α-reductase enzyme activity have higher incidence of prostate cancer (Labrie *et al.*, 1986; Makridakis *et al.*, 1997). Furthermore, Labrie *et al*, (1993) highlighted individual cases whereby patients with very low levels of serum testosterone were failing ablation therapy. This was attributed to the efficient conversion of adrenal steroids into potent androgens, which enabled continued androgen signalling allowing tumour cell growth.

1.8.7 The promiscuous pathway

The promiscuous pathway maintains that androgen receptor signalling is upheld in cells with androgen receptor mutations by decreasing receptor specificity towards innate ligands. Consequently, cells containing mutated androgen receptors are able to bypass apoptosis and continue proliferation via the use of other circulating steroid hormones after androgen ablation therapy (Feldman and Feldman, 2001).

In the hypersensitive pathway, androgen independent prostate cancers cells are not truly androgen independent; but are maintained by low-level androgen signalling, efficient 5-α-reductase activity, and androgen receptor amplification. The promiscuous pathway is maintained by mutations in the androgen receptor gene, which results in non-specific ligand activation.

1.8.8 Androgen mutations

The androgen receptor gene is located on the X chromosome. Germ line mutations commonly result in androgen receptor insensitivity. However, due in part to the heterogeneity of tumours, the incidence of somatic mutations is not fully known. What is clear however is that primary tumours have a low level of androgen receptor mutation compared to metastatic tumours after androgen ablation therapy (Marcelli *et al.*, 2000; Taplin *et al.*, 1995). These finding suggest that gaining such mutations may be a driving factor leading to androgen independence. These results contrast with another study which reported that requisite mutations required for growth during androgen deprivation were already acquired by metastatic tumours, and were not instigated by androgen ablation (Cher *et al.*, 1996).

LNCaP cells were one of the first cell lines to be identified with a missense mutation in the ligand-binding domain of androgen receptor (Veldscholte *et al.*, 1992). These cells demonstrated high androgen receptor levels that resulted in increased growth and prostate specific antigen levels. The promiscuous pathway maintains that these androgen receptor mutations in LnCaP cells enabled ligand binding with generic steroid hormones, such as progestins and oestrogens, as well as androgen agonists such as flutamide, leading to an increase in androgen receptor expression and tumour cell proliferation. A study by Gaddipati *et al*, (1994) reported that 25% of metastatic prostate cancer patients studied matched to a missense mutation in the ligand-binding domain.

There is a phenomenon in androgen ablation therapy known as Flutamide Withdrawal Symptoms. Individuals with this condition may show signs of deterioration when treated with Flutamide, an androgen agonist. However, upon withdrawal of the agonist, the patient shows clinical signs of improvement. Upon further investigation it was observed that

patients with a wild type androgen receptor responded well to the ablation therapy, however, patients with a T877 mutation demonstrated rapidly increased levels of PSA levels (Small and Srinivas, 1995). As tumour cells are heterogeneous, wild type androgen receptor cells die out due to testosterone deprivation, whereas cells containing T877 mutation thrive and continue proliferating.

Androgen receptors are known to be active in androgen independent cancer cells (Zegarra-Moro *et al.*, 2002) as androgen receptor dependent molecules such as prostate specific antigen are continually produced in patients that have endured androgen ablation (Craft *et al.*, 1999). Clearly, loss of androgen sensitivity is linked with the malignant progression of prostate cancer, and understanding the mechanisms by which prostate cancer cells lose their sensitivity to androgens is of utmost importance.

1.9 FATTY ACIDS, FATTY ACID BINDING PROTEINS AND PROSTATE CANCER

1.9.1 Introduction to Fatty Acids

Fatty acids have a structural arrangement that is predetermined by their hydrophilic head group and a hydrophobic tail section. They exist in an unbound water insoluble phase or as a complex to albumin that transports fatty acids to specific target sites on the cell membrane. Fatty acids are an important component in the cells metabolic system as they act as a secondary source of energy which can be tapped to produce energy in the liver and muscle cells (Valette, 1991). Adipocytes store intracellular supplies of neutral esterified lipids, which are released as fatty acid acyl residues when the cells' need for fatty acid increases. The fatty acyl residues are released from the triacylglycerol pool, and secreted by fat cells into extracellular space (Glatz and Vusse, 1996). The unbound free fatty acids cross the plasma membrane either by passive diffusion or though an active protein mediated transport

(Hamilton and Kamp, 1999). Fatty acid complexes undergo a dissociation step that liberates fatty acids and enables their movement into the cell by passive, protein mediated or FAT transfer. From here, fatty acids either enter a metabolic pathway or are bound to an intracellular fatty acid binding protein (FABP).

1.9.2 Dietary fatty acid and prostate cancer

The incidence of latent cancer is uniform around the globe. However, western developed nations have a higher incidence of clinical prostate cancer. Given that approximately 40% of total energy intake is obtained from fat in a westernised diet, this provides a rationale for studying the link between dietary fat intake and prostate cancer (Frohnert and Bernlohr, 2000; Pandian, 2000).

Epidemiological studies (Aronson *et al.*, 2001; Cook *et al.*, 1999; Crawford, 2003) show a link between prostate cancer and the two main factors of age and diet. Such studies suggested that the difference in prostate cancer incidence between North America and Japan was a direct link to the type and quantity of fatty acids ingested. They also showed an increase in relative risk of an individual from a country of low prostate cancer incidence to that of high prostate cancer incidence.

The human body is capable of synthesising certain fatty acids. Yet those acquired solely through diet are defined as "essential" fatty acids. These make up the precursor of two classes of polyunsaturated fatty acids, linoleic acid – an omega 6 fatty acid derived from vegetable, seed and corn oils, and linolenic acid, an omega 3 fatty acid derived mainly from fish oils. The methods by which polyunsaturated fatty acids (PUFA), such as eicosanoids, are thought to influence and promote cancer progression in not fully understood, however it is believed that conversion of the precursor linoleic acid into arachidonic acid by desaturation plays an integral part. Arachidonic acid is catalysed into prostaglandin and thromboxanes by

the cyclooxygenase enzyme. Studies have shown the existence of two forms of cyclooxygenase enzymes. Cox-1, which is constitutively active, and Cox-2, an inducible gene observed to be over expressed/up regulated in prostate cancer biopsies (Gupta, 2000).
In contrast, fish oils containing eicosapentanoic acid act in an antagonistic fashion by actively binding to the substrate of cyclooxygenase and lipoxygenase, thereby producing series 3 and 5 prostaglandins which reportedly cause less tissue inflammation, and reduce the production of the more active arachidonic acid metabolites (Bagga *et al.*, 1997).

1.10 FATTY ACID BINDING PROTEIN (FABP) FAMILY

Fatty acid binding proteins (FABPs) are members of a multigene family of intracellular lipid binding proteins, and have a molecular mass of around 15kDa. They are highly conserved and share a common ancestry in vertebrates and invertebrates (Schleicher *et al*, 1995).
There are four distinct sub families of intracellular lipid binding proteins (iLBD) expressed in vertebrates. These are sub family I – a family consisting of proteins specific for vitamin A, cellular retanoic acid binding protein I and II, and cellular retanoic binding proteins I – IV. Sub family II – consisting of protein families with larger binding sites which enable binding to larger ligands such as long chain fatty acids, heme and acyl CoA. Sub family III – contains intestinal FABP; and sub Family IV – consists of the greatest variety of FABP including heart, adipocyte, epidermal, brain, myelin and testis – type FABP (Ross, 1993) (Table 1.10).
Heart and epidermal FABP are the most widely expressed of iLBPs. Heart FABP is found in kidney, lung, mammary tissue, placenta, testis, stomach, ovary and brain whereas epidermal FABP is widely expressed in skin, lung, heart, skeletal muscle, kidney, testis, adipose tissue, brain, and retina (Haunerland and Spencer, 2004)

Table 1.10 The FABP family

iLBD type	Gene	Expression	Ligands
Subfamily I			
CRBP I, II, III, IV		Ubiquitous in mammalian cells	Retinol
CRABP I and II		Ubiquitous in mammalian cells	Retinoic acids
Subfamily II			
L-FABP	*Fabp1*	Liver, intestine, kidney, lung, and pancreas	Long -chain fatty acids, acyl-CoAs, and heme
I-BABP	*Fabp6*	ileum	bile acids
Lb-FABP	*Fabp10*	Fish and bird liver	Long-chain fatty acids
Subfamily III			
I-FABP	*Fabp2*	Intestine, liver	Long-chain fatty acids
Subfamily III			
H-FABP	*Fabp3*	Heart, skeletal muscle, brain, kidney, lung, mammary, placenta, testis, ovary and stomach	Long-chain fatty acids
A-FABP	*Fabp4*	Adipose tisse and macrophages liver	Long-chain fatty acids
E-FABP	*Fabp5*	Skin, adipose tissue, lung, brain, heart, skeletal muscle, testis, retina and kidney	Long-chain fatty acids
B-FABP	*Fabp7*	Brain, glia cells, and retina	Long-chain fatty acids and docosahexanoic acid
M-FABP	*Fabp8*	Brain and Schwann cells	Long-chain fatty acids
T-FABP	*Fabp9*	Testis	Long-chain fatty acids

Haunerland and Spencer, 2004.

1.10.1 Fatty Acid Binding Protein (FABP) structure

The structure of FABP has been studied using X-ray crystallography (Banaszak *et al.*, 1994). This group reported that FABPs have varied sequence homology ranging from 20 – 70%, but are greatly conserved in their tertiary structure. The region of greatest homology is in the β-barrel, which is formed by 10 folded anti-parallel β-strands. These strands vary in length, from 4 to 10 amino acid residues, which are linked by hydrogen bonds and two short α helices at the first and second β-strands. These β-strands are arranged to form two 5 stranded sheets in which one sheet runs perpendicular to another, thus providing a central cavity within the flattened β-barrel structure (Glatz and Vusse, 1996).

Fatty acids enter binding proteins carboxyl group first, through a portal area flanked by two alpha helical segments. These helical capped regions confer ligand-induced flexibility, and act as a lid for entry and release of ligands from binding proteins. Once docked within proteins, fatty acids are secured by hydrogen bonding networks between the carboxyl group and arginine and tyrosine (Glatz and Vusse, 1996). The FABP β-barrel, which encapsulates the FA, is structurally very stable, and does not undergo significant conformational changes.

1.10.2 FABP function

Long chain fatty acids are virtually insoluble in an aqueous environment due to their hydrophobic nature. Hence, an efficient transport system for cellular entry and intracellular locomotion is required. One such transport system is the fatty acid binding protein.

FABPs are soluble non enzymatic proteins of low molecular weight, approximately 15kDa, and have the ability to bind to long chain fatty acids (Owada, 2002), and have been proposed as intracellular fatty acids transporters. As yet, there is no direct proof of such activity, but

several indirect studies point to its intracellular transporting function. One such study (Binas, 1999) demonstrated that mice lacking the FABP gene had reduced fatty acid uptake, and the fatty acid usage was greatly reduced. In another recent study, (Liu, 2001) adipocyte – type FABP was transfected by electroporation into preadipocyte cells, and showed an increase in the rate of palmitate uptake compared to control cells.

Fatty acids have also been proposed to be involved indirectly in the regulation fatty acid mediated genes. However, there are a limited number of studies to verify this claim. What is observed however are the regulatory role of fatty acids, and a possible secondary role of FABP in gene transcription regulation. Studies have shown that FABP is regulated by fatty acids (Clarke, 2000; Martin *et al.*, 1997). Fatty acids are known ligands of PPAR, a family of nuclear hormone receptors. Furthermore, FABP expression has been detected in the nucleus of hepatocytes (Fahimi *et al.*, 1990), and cardiac myocytes (Borchers *et al.*, 1989), clearly suggesting that nuclear transportation of fatty acids and nucleus-directed signalling by fatty acids control gene expression (Zimmerman and Veerkamp, 2002).

1.10.3 C-FABP in prostate cancer

The role C-FABP in malignant progression of prostate cancer is an emerging area with few data yet published. Nevertheless, the available literature is very compelling. A study of differentially expressed genes in prostate cancer as identified by micro-quantity differential display (Jing *et al.*, 2000b) identified a number of candidate genes. Further characterisation and subtractive selection of these genes identified a candidate gene, C-FABP to be differentially expressed in normal, benign and malignant breast and prostate cell lines (Jing *et al.*, 2000a). C-FABP was reported to be able to induce metastasis in benign non metastatic rat mammary cell Rama37 cells, and to regulate the expression of a potent angiogenic factor,

VEGF (Jing *et al.*, 2001). Similarly, C-FABP expression was observed to be over-expressed in bladder and pancreatic malignancies (Celis *et al.*, 1999; Ostergaard *et al.*, 1997; Sinha *et al.*, 1999). These results clearly suggest that C-FABP up-regulation is involved in the malignant progression of prostate cancer either as a signalling molecule or as transporters of fatty acids.

1.11 AIM OF THESIS

This overview has identified the potential core role of FABP in the biology of prostate cancer metastasis. Previous studies in this laboratory reinforced this view and provided the foundation for the studies now proposed. Thus, the objectives to be addressed in this Thesis will include:

- **To study the role of C-FABP expression on prostate cancer tumourigenicity.**

- **To investigate the association between elevated levels of C-FABP expression and loss of androgen sensitivity in prostate cancer cells.**

- **To explore the therapeutic possibilities of suppressing C-FABP expression combined with androgen depletion in a nude mouse model.**

CHAPTER – 2

METHODOLOGY

2.1: INTRODUCTION

This chapter is divided into two sections. The first section describes experiments utilised to study the role of C-FABP on prostate cancer tumourigenicity, whereas the second section describes experiments conducted to investigate any potential association between C-FABP over-expression and loss of androgen sensitivity in highly malignant prostate cancer cells; and to explore the therapeutic possibilities of C-FABP suppression and androgen ablation in a nude mice model.

The first section of the methodology, referred to as the antisense section, details protocols used to suppress C-FABP expression by antisense oligonucleotides to generate several single-cell-cloned transfectant cells in highly malignant prostate cancer cell lines, PC3M. The invasive potential of cells was assessed *in vitro*, and tumourigenicity assessed *in vivo* by inoculation into male immuno-compromised nude mice. At autopsy, mice were culled and tumour tissues immunohistochemically stained for C-FABP, VEGF and factor VIII related antigen.

The second section of the methodology, referred to as the siRNA section, details the protocols used to suppress C-FABP activity in highly malignant androgen independent PC3M cells to generate several single-cell-cloned transfectant cells with reduced levels of C-FABP expression. Proliferation rate and colony formation were assessed *in vitro* in androgen positive and negative conditions, likewise, *in vivo* tumourigenicity assays were performed in androgen negative and

positive conditions in male immuno-compromised nude mice. At autopsy, primary tumours (where available), heart, lungs and liver tissues were dissected. These tissue sections are processed and stained with haematoxylin and eosin for detection of secondary tumour cells in liver, heart and lungs of mice.

By doing this, it was anticipated that a classification of the role of C-FABP in tumourigenicity and loss of androgen sensitivity will be defined and a potential mode of therapy in nude mouse explored.

2.2 SECTION ONE: ANTISENSE METHODOLOGY

2.2.1 Immunohistochemical staining for the detection of C-FABP expression

Archival human prostatic tissues were held within the surgical pathology archive in the Department of Pathology, University of Liverpool, UK. Ethical approval was obtained from the Liverpool University Ethics Committee in accordance with the Medical Research Council guidelines.

Histological sections of paraffin-embedded tissues were cut and processed as described in Deshmukh *et al,* (1997). Haematoxylin and eosin is a widely used method of histological staining and involves the application of the basic haematoxylin dye to bind and stain basophilic structures such as nucleic acids and ribosomes blue-purple. The eosin dye is an acidic dye that binds and stains eosinophilic structures such as intracellular and extracellular proteins.

All materials and reagents used in Section 2.2 can be found in Appendix 1.1

2.2.2 Tissue sectioning

1) A water bath was filled with distilled water and heated to 37°C.
2) The microtome was cleaned with xylene and a new disposable blade was fitted to the machine.
3) The paraffin-embedded tissue blocks were pre-cooled in a container filled with ice.
4) Tissue sections were cut at 4μm thickness and mounted onto labelled twin frosted microscopic slides.

5) The slides were allowed to dry overnight at 37 °C.

2.2.3 Haematoxylin and eosin staining of sections

1) Haematoxylin sections were deparaffinised in 3 x washes of xylene and hydrated in water
2) The sections were stained in haematoxylin for 5 minutes and washed in running water.
3) Following this, sections were differentiated in 1% acid alcohol for 5 seconds and washed in water
4) The sections were submerged in Scotts tap water till "blue", and washed in running tap water
5) Stained in alcoholic eosin for 30 seconds, and washed in running tap water.
6) These sections were dehydrated in 95% and absolute alcohol for 2 minutes respectively.
7) Sections were cleared in 2 washes of xylene for 2 minutes respectively, and mounted using DPX synthetic resin.
8) Tissue sections were examined independently by two qualified pathologists and classified by Gleason grades as normal, benign prostatic hyperplasia (BPH) and carcinomas.

2.2.4 Immunohistochemistry for the detection of C-FABP in human prostatic tissue

1) Following tissue section classification by Gleason grading, tissue sections were prepared for immunohistochemistry for the detection of C-FABP expression.
2) Mounted tissue sections were prepared as detailed in Section 2.2.2 using (3-Aminopropyl)triethoxy-silane (APES) coated slides.

3) The following day, the mounted sections were dewaxed in two changes of xylene for 3 minutes and 30 seconds respectively, and rinsed in 90% alcohol and absolute ethanol respectively.
4) Slides were incubated in hydrogen peroxide/methanol for 12 minutes to block endogenous peroxidase activity.
5) The sections were rinsed in running tap water, then in deionised water
6) Antigen retrieval was conducted by microwaving tissue sections for 25 minutes in 10mM Tris-EDTA buffer (pH 9.0) at full power.
7) Following antigen retrieval, sections were placed in running water before being racked into sequenza immunohistochemistry trays
8) Tris-Buffered Saline (TBS) was added to each racked section allowed to flow through over a period of 4 minutes.
9) Then 100µl of 5% Bovine Serum Albumen in TBS (BSA/TBS) was added to sections and left to incubate for 10 minutes.
10) Sections were incubated with primary anti-C-FABP sera (Iwaka Glass Corp, Niigata, Japan) at a dilution of 1:500 in 100µl BSA/TBS for 1 hour. Negative controls were incubated with 100µl BSA/TBS alone for the same period of time.
11) Sections were washed in two changes of TBS for 4 minutes respectively, and then incubated in 100µl anti rabbit horse radish peroxidase (HRP) -conjugated polymer (Dako Ltd, Ely, UK) for 30 minutes
12) These sections were washed with TBS for 4 minutes.
13) 100µl of 3,3' Diaminobenzidine (DAB) is mixed with 1µl chromogen was added to the tissue sections for 10 minutes, and washed in deionised water for 4 minutes.

14) The sections were removed from the sequenza plates, and washed in running tap water for 2 minutes.

15) The sections were counterstained in Haematoxylin solution, washed briefly in running water and incubated in Scott's Tap Water blueing agent.

16) Following Blueing, the sections were washed thoroughly in tap water before being dehydrated in rising concentration 80%, 95% and absolute alcohol.

17) The sections were visualised using an EnVision detection procedure (Dako Ltd)

18) Sections were cleared of any remaining water by incubating in xylene. Following this, slides were mounted using DPX synthetic resin.

19) The C-FABP stained sections were observed, and graded negative, weakly positive, moderately positive and strongly positive based on the scale used by Watanabe *et al*, (1997).

2.3 CELL LINES AND CELL CULTURE CONDITIONS

2.3.1 Introduction to cell lines

The cell line used throughout this study was the highly metastatic human prostatic cancer cell line PC-3M (Kozlowski *et al.*, 1984). The PC-3M cell line is derived from a prostate adenocarcinoma cell line, PC-3. It was originally isolated from liver nodules that were formed from direct intrasplenic injection of PC-3 cells (Kaighn *et al.*, 1978). In studies performed to assess tumour forming ability of these newly isolate PC-3M variant cell lines, results demonstrated increased tumour forming abilities and increased micro-metastases relative to

parental PC-3 cells. The PC-3M metastatic cell variants represent the malignant metastatic phase of prostate cancer cell line models. Additionally, these cells have been shown to express the greatest level of C-FABP (Jing *et al.*, 2000), making them ideal candidate cell lines to use within this study.

All reagents, media compositions and materials are detailed in Appendix 1.2.

2.3.2 Cell culture conditions

Human prostate cancer cell lines and transfected cell lines were cultured in RPMI 1640 medium (Invitrogen Life Sciences). These cells were maintained in a humidified environment at 5% CO_2 at 37°C.

2.3.3 Routine subcultures

1) The prostate cancer cell lines were washed with PBS once.
2) Cells were incubated with Trypsin / EDTA (TE) at 3ml/9cm plate at 37°C for 3 minutes, or until cells were rounded and detached from the surface of the plate.
3) At this stage, cells were removed from the incubator and T/E was inactivated using an equal volume of routine cell culture medium.
4) Resuspended cells were centrifuged for 2 minutes at 110xg, and the supernatant was discarded.
5) Cells were resuspended in routine cell culture medium and plated out at the required concentration.

2.3.4 Cryopreservation of human prostate cancer cells

Cryopreservation of cells is a means of ensuring an ample stock of cells. Cells were initially harvested and aliquoted into $1x10^6$ concentrations before placing in a Cryobox (Nalgene, UK) filled with isopropanol (IPA), and placed in a -80°C freezer. The slow cooling rate of cells within the cryobox (-1°C per minute) in conjunction with "freezing medium" inhibit formation of ice crystals within cells during cryostasis and cell damage upon reanimation.

1) Cells to undergo cryostasis were incubated with trypsin / EDTA (TE) at 3ml/9cm plate at 37°C for 3 minutes, or until cells were rounded and detached from the surface of the plate.
2) At this stage, cells were removed from the incubator and T/E activity was inactivated using an equal volume of cell culture medium.
3) Resuspended cells were centrifuged for 2 minutes at 110xg, and supernatant was discarded. Cells were resuspended in 10mls of PBS.
4) 10µl of cell suspension was mixed with 10µl of trypan blue, mixed and added to haemocytometer to quantify cell numbers.
5) Having established cell concentrations, cryo-medium was added to cells to make $1x10^6$ cells/ml dilution. 1ml was pipetted into cryotubes (Nunc).
6) These cryotubes were placed within a cryobox and into a -80°C freezer overnight and transferred to liquid nitrogen the next day.

2.3.5 Reanimation of cryopreserved cells

1) Cryogenically preserved cells were thawed by removal of cryotubes from liquid nitrogen and placing in a 37°C water bath to thaw.
2) Cells were resuspended in 10ml of routine cell medium.
3) This cell solution was centrifuged at 110 x g for 2 minutes and supernatant was discarded.
4) Cell pellets were resuspended in 10mls of RPMI medium and decanted into 9cm plates. These cells are maintained in a humidified environment at 37°C and 5% CO_2 to grow.

2.4 CONSTRUCTION OF ANTISENSE C-FABP DNA

2.4.1 Generating reverse-C-FABP (C-FABPr) recombinant vector

Previous work within the department had amplified a 436 base pair fragment of the protein-coding region of C-FABP by RT-PCR from mRNA isolated from PC-3 cells. These fragments were amplified using the forward primer sequence 5'- ACC ATG GCC ACA GTT CAG CA -3'; and the reverse primer 5' – CCT GTC CAA AGT GAT GAT GGA A - 3'. Amplified C-FABP products were T-A cloned into a PGEM-Teasy plasmid. The C-FABP fragment was removed from the PGEM-Teasy vector and inserted into pBluescript Vector in sense and antisense orientation. C-FABP fragment orientation was confirmed by automated DNA sequencing, after which, the fragment was excised from the pBluescript vector and into the pSV-Neo expression vector (Glaxo Wellcome). The following methodology describes this process. All reagents and materials can be found in Appendix 1.3

2.4.2 Amplification of C-FABP in pSV-Neo plasmid vector

1) 100µl glycerol stocks of C-FABP, inserted in the forward and reverse orientation in pSV-Neo plasmid vectors, were streaked onto liquid broth (LB)-agar plates, and incubated overnight at 37°C
2) The following morning, five colonies were picked up from the forward and reverse agar plates respectively.
3) These colonies were transferred to individual conical flasks containing 10mls of LB-medium and ampicillin (Sigma) at a concentration of 100µl/ml. These colonies were incubated at 37°C and 121rpm in an incubator shaker (New Brunswick Scientific) overnight.
4) The following morning, bacterial cells were pelleted at 14,500x g for 8 minutes at room temperature. Extraction of plasmid from bacterial cells was performed using the Qiaprep ® Miniprep method (Qiagen).
5) The bacterial pellets were resuspended in 250µl of resuspension buffer P1 and transferred to microfuge tubes.
6) The bacterial cells were lysed with the addition of cell lysis buffer P2, and inverted 6 six times to aid mixing and lysis.
7) Following this, 350µl of neutralising buffer N3 was added cells and inverted six times.
8) These cells were centrifuged for 10 minutes at 14,500-x g in a microfuge, and supernatants were added to QIAprep Spin Column by pipetting.
9) Supernatants in spin column were centrifuged for 1 minute and the flow-through was discarded.

10) The QIAprep Spin Columns were washed by adding 750µl of buffer PE to remove excess salts, and centrifuged for 1 minute, after which, the flow through was discarded.

11) The QIAprep columns were transferred to clean 1.5ml microfuge tubes, and DNA was eluted with the addition of 50µl of elution buffer EB. The Spin Column was left to stand for a minute, before being centrifuged for 1 minute.

2.4.3 Excision of CFABP fragment from pSV-Neo plasmid

Having successfully isolated pSV-neo plasmids from DH5-α bacterial cells, the forward and reverse orientated C-FABP fragments were excised from the plasmid. This was performed using restriction enzymes HindIII and Xba1.

The following restriction digest reaction was set up in the following order to restrict the forward and reserve C-FABP fragments:

Buffer B	12.5%
DNA (1µg/µl)	6µl
dH_20	9.5µl
Xba1 (10U/µl)	1µl
HindIII (20U/µl)	1µl
Total reaction Volume	20µl

1) The above restriction enzyme reaction volume was prepared and incubated at 37°C in a water bath for 1 hour.

2) Following the completion of restriction digest reaction, the enzymes were inactivated at 65°C for 5 minutes.

3) Following heat inactivation, 15µl of the forward and reverse C-FABP fragments were ran on a 0.8% agarose gel (containing 1µl ethidium bromide) against DNA marker III at 80V for 90 minutes.

4) Analysis of fragment dispersion under UV conditions demonstrated two clear bands corresponding to the linearised pSV-Neo plasmid (2500bp), and the excised C-FABP fragment (500bp).

2.4.4 Automated DNA sequencing of C-FABP forward and reverse fragments

The sequencing analysis is conducted by using 5' - GTC CAA TTA TGT CAC ACC ACA G - 3' located within the vector sequence. Primers, C-FABP forward and reverse samples were required at a concentration of 200ng/µl. The samples were transferred to the Liverpool School of Tropical Medicine for sequencing.

2.5 CALCIUM PHOSPHATE CO-PRECIPITATION TRANSFECTION OF REVERSE C-FABP EXPRESSING CONSTRUCT

2.5.1 Transfection of human prostate cancer cells

The calcium phosphate method of introducing exogenous material into mammalian cells is a well characterised methodology (Davies *et al.*, 1994; Jamieson *et al.*, 1990) that has been standardised and implemented in previous research conducted within the department (Chen *et al.*, 1997; Ke *et al.*, 1998). The calcium phosphate method of mammalian cell transfection enables the formation of precipitates of calcium phosphate to DNA by the slow mixing of HEPES-buffered phosphate solution with a solution containing calcium chloride and DNA. These precipitates are attracted to phospholipid membrane layers and form clusters on the cell surface. Precipitates enter the cell via endocytic mechanisms. All materials and reagents can be found in Appendix 1.3.

1) Prior to transfection, cells were cultured up to 50-60% confluence in 9cm plates.
2) Cell medium was changed using routine cell medium, and incubated in an incubator at 37°C and 5% CO_2 for a period of 4 hours.
3) During the cell incubation period, solutions in tubes 1and tubes 2 were prepared.
4) The two tubes were mixed by pipetting up and down to ensure a thorough mix, then tube 2 was added to tube 1 in a drop wise manner, whilst air was being bubbled through the contents of tube one with a needle and syringe to aid precipitate formation.
5) Likewise, Tubes 3 and 4 were prepared during the cellular incubation period, and each tube was mixed thoroughly by pipetting up and down.

REAGENT	TUBE 1	TUBE 2
2x HBS	500µl	/
1M CaCl2	/	125µl
pSV-Neo DNA	/	20µg
pSV-C-FABPr DNA	/	/
dH2O	/	Make up to 500µl

6) Tube 4 was added to tube 3 in a drop wise manner whilst air was being bubbled into the contents of tube 3 with a needle and syringe to aid precipitation.

REAGENT	TUBE 3	TUBE 4
2x HBS	500µl	/
1M CaCl2	/	125µl
pSV-Neo DNA	/	2µg
pSV-C-FABPr DNA	/	20µg
dH2O	/	Make up to 500µl

7) Tubes 2 and 4 were discarded, and tubes 1 and 3 were left to stand at room temperature for 45 minutes to aid DNA calcium-phosphate precipitate formation.

8) After a 4-hour incubation period, cells were removed from the incubator and the DNA solution in tube 1 (control transfection) and tube 3 (recombinant transfection) were added to two separate cell dishes.
9) Cells were incubated at 37°C and 5%CO_2 for 4 hours.
10) Following this, cells were removed and replaced with transfection medium (9mls routine cell medium and 1ml DMSO).
11) Cells were incubated at room temperature for 90 seconds before the transfection medium was aspirated and cells washed with PBS.
12) Routine cell culture medium was added to cells and incubated at 37°C and 5% CO_2 for 24 hours.
13) The following day, both cell dishes were split into 10 separate 9cm plates and cultured in selective medium containing 1mg/ml geneticin.
14) The cell medium was changed every 3 days.

2.5.2 Ring cloning of transfected cells

The proportion of cells successfully transfected within a population was relatively low (approximately 10 colonies per plate), consequently, cloning was used to isolate sub-colonies of transfected cells of approximately 3mm in diameter within a population of cells on a 9cm plate. Ring cloning was used to isolate five stably transfected single cell clones.

1) The tips of 1ml pipettes were cut to equate to the number of transfectant colonies in the petri-dishes.
2) 1ml pipette tips, forceps, and silicone grease were sterilised by autoclaving.

3) The 9cm Petri dishes were removed from the incubator and the medium was aspirated. The cells were washed with PBS.
4) Using forceps, the tops of the 1ml pipettes were dipped in silicon grease and placed over the colonies within the 9cm plate to form a seal around the cell colony.
5) Then, 75µl of trypsin and 50µl of versene were added to isolated colonies, incubated for 2 minutes or until cells were rounded or detached.
6) Detached cells were transferred to sterile 1.5ml microfuge tubes and trypsin was inactivated by adding an equal volume of routine cell medium.
7) The microfuge tubes containing cell colonies were centrifuged for 2mins at 16,000 x g, after which, the supernatant was discarded.
8) Cell pellets were washed in 75µl PBS and centrifuged again at 16 000 x g for 2 minutes.
9) The resulting cell pellets were resuspended in 1ml selective medium containing 1mg/ml geneticin and plated into a 24 well plate. The cells were transferred into an incubator at 37°C and 5% CO_2.

2.6 DETECTION OF C-FABP PROTEIN EXPRESSION IN TRANSFECTANT CELLS

A Western blot assay was used to detect the expression of C-FABP in antisense transfectant cells. Western blotting are commonly performed using an anionic detergent such as sodium dodecyl sulphate (SDS), and heat to dissociate proteins into individual polypeptide subunits before they are loaded in a polyacrylamide gel electrophoretic system (PAGE). The denatured polypeptides bind to SDS, becoming negatively charged. As the proportion of bound SDS is relative to the size of the polypeptide, SDS-polypeptide complexes are separated in PAGE

according to size and charge ratio. Separated polypeptide units are transferred from gel to nitrocellulose membranes, and probed for amino acid sequences specific to C-FABP antibody (Burnette, 1981; Towbin *et al.*, 1979). C-FABP protein expression levels were assessed in control transfectant cells, PC-3M-pSV, transfectant pool cells (PC-3M-C-FABP-P), and antisense PC3M-C-FABP-1 – 5 transfectant cloned cells relative to parental PC-3M cells. All materials and reagents can be found in Appendix 1.4

2.6.1 Protein extraction by cell lysis

1) Parental and transfectant cells were removed from the incubator and the medium aspirated from cell plates. Cells were rinsed in 10mls PBS per 9cm plates.
2) PBS was aspirated and trypsin/EDTA was added to cells 3ml per 9cm plate. These plates were incubated at 37°C for 3 minutes, or until cells were rounded and detached from the plate surface.
3) Trypsin/EDTA was inactivated using an equal volume of routine cell culture medium, and cells were collected by centrifuging at 110 x g.
4) The supernatant was discarded and cells were resuspended in 10mls of PBS.
5) 10µl of cell suspension was mixed with 10µl of trypan blue, mixed and added to haemocytometer to quantify cell numbers.
6) Cell density was adjusted to $2x10^6$, collected by centrifuging at 110 x g, and resuspended in equal volumes of PBS and lysed with an equal volume of hot (>95°C) 2x lysis buffer.

7) Cell lysates were thoroughly vortexed and boiled for 5 minutes, and samples were vortexed thoroughly before being homogenised for 20 seconds at high speed using a Polytron Homogeniser (Kinematica, Swizterland).
8) Any contaminating nucleic acids were sheared by sonicating for 3 x 30 second cycles at room temperature at a mid level power range on a Bandolin Sonoplus (Bandelin scientific, Germany), and placed on ice.

2.6.2 Protein fractionation by SDS-PAGE

1) Proteins were separated using 10% polyacrylamide resolving gels in a Protean III system (Bio-Rad, Germany) in 500mls of 1x running buffer.
2) Protein samples were boiled in 5µl Double strength sample buffer (DSSB) for 10minutes before being electrophoresed.
3) Protein markers were used to estimate protein sizes
4) The gel was run for 15 minutes at 140 V and at 200V for an additional 30 minutes.

2.6.3 Transfer of proteins from SDS-Gel to nitrocellulose membrane

Proteins were transferred from polyacrylamide gels to Hybond-ECL membranes in 1x transfer buffer using Trans-Blot electrophoric transfer cells (Bio-Rad, Germany).

1) Six sheets of whatman 3MM filter paper and nitrocellulose membrane were cut according to the dimension of gel and soaked in 1x transfer buffer (pH 8.3).

2) Following completion of SDS-gel electrophoresis, the SDS-gel was soaked in 1x transfer buffer for a period of 5 minutes.

3) To aid protein transfer, three sheets of whatman 3MM filter papers were placed on the anode electrode of the transfer rig. The SDS-gel was placed on top of the 3MM papers, and nitrocellulose membrane was placed on top of the SDS-gel. Using a pipette, air bubbles were squeezed out, and three sheets of 3MM filter paper were placed on top of the membrane, and the cathode electrode was placed on top of the stack.

4) Transfers of proteins from gel to membrane were performed at 4°C overnight at 30V.

5) The following day, the membrane was stained with 10% Ponceau S solution for 15 minutes and destained with PBS solution. The gel was stained with coomassie blue for 10-15 minutes and destained with destaining solution. Both staining phases were conducted to assess the efficiency of transfer of proteins from gel to membrane.

2.6.4 Immunoblotting for detection of C-FABP protein expression

1) In preparation of immunoblotting, membranes were incubated in 10mls of 5% protoblock for 1 hour in order to prevent non-specific binding of primary C-FABP antibodies.

2) The membrane was then incubated in rabbit anti-human C-FABP antibody at a 1: 200 dilution for 2 hours, and washed 3x 15 minutes in T-TBS.

3) The membrane was incubated in secondary antibody (horseradish peroxidase-conjugated swine anti-rabbit immunoglobulin) at a 1:1000 dilution for 1 hour.

4) The membrane was washed for 3x 15 minutes in T-TBS.

5) Probed antigens were visualised by Electro Chemical Luminescence system™ (ECL), (Amersham). Reagents 1 and 2 were mixed 1: 1 and pipetted onto protein face of membrane for 1 minute.
6) Excess reagents were drained, and membrane was wrapped in saran wrap, placed in a film cassette and exposed to Kodak film from 1minute to 20 seconds.

2.6.5 Immunoblotting for detection of actin protein expression

Antibodies against constitutively expressed actin protein were used to normalise any variation in loading of protein samples.

1) Following detection of primary antibody expression by ECL detection, the membrane was washed for 2x 15 minutes in T-TBS, and blocked for 1 hour with 5% protoblock.
2) After blocking, the membrane was incubated in actin antibody for 45 minutes at a 1:5000 dilution in 10mls 5% protoblock.
3) Post actin binding, the membrane was washed for 3x 15 minutes to remove all non-specific bound antibodies.
4) The membrane was incubated with rabbit anti-mouse horse radish peroxidase conjugate secondary immunoglobulin for 1 hour at 1: 1000 dilution in 10mls 5% protoblock.
5) The membrane was washed 3 x 15 minutes in T-TBS and bound actin probes were visualised using ECL detection method

2.7 SOUTHERN BLOT ASSAY FOR DETECTION OF C-FABPr EXPRESSION

Identification of sequences within genomic DNA is commonly achieved by the method of transfer described by Southern, (1975). This process involves restriction of genomic DNA by restriction enzymes and separation of DNA fragments according to size by agarose gel electrophoresis. DNA fragments are denatured within the gel, and transferred onto nitrocellulose membrane. Relative positions of DNA fragments are maintained upon transfer by cross linking attached DNA to membrane via ultra violet light fixation. Attached DNA is then probed with radio-labelled probes that are complementary to a specific fragment. Exposure of the membrane to film identified the size, position and relative intensity of targeted sequence relative to a control sample.

All materials and reagents used within this section are found in Appendix 1.5.

2.7.1 Extraction of genomic DNA from antisense transfectant and parental PC3M cells

Cells were harvested using tissue culture techniques described in Section 2.3.3. Extraction of genomic DNA was achieved using Qiagen Genomic DNA extraction kit according to the manufacturer's instructions.

1) Cells were counted and resuspended in PBS at a concentration of 10^7 cells /ml.
2) 2ml of ice cold cell lysis buffer C1 and 6ml of ice cold distilled water were added to cell suspension, mixed by inverting several times and incubated for 10 minutes on ice.

3) Lysed cells were centrifuged at 1300 x g for 15 minutes at 4°C to pellet the nuclei, and supernatant was discarded.

4) 1ml of ice-cold lysis buffer C1 and 3 ml of ice-cold distilled water was added to lysed cells to remove all residual cell debris from nuclear pellets.

5) Nuclei pellets were resuspended by vortexing before being spun at 4°C for 15 minutes at 1300 x g.

6) The supernatant was discarded.

7) 5ml of nuclear lysis buffer G2 was added to nuclei pellets to release genomic DNA and homogenised by vigorous vortexing for 10–30 seconds at maximum speed.

8) 95µl of Qiagen Protease was added to resuspended nuclei and incubated at 50°C for 60 minutes.

9) Genomic-tip 100/G was equilibrated with 4ml of equilibration buffer QBT and left to empty by gravity flow.

10) The extracted Genomic DNA samples were vortexed thoroughly at maximum speed for 10 seconds before being applied to the Qiagen genomic- tip. The solution was allowed to enter the resin by gravity flow.

11) The Qiagen Genomic-tip was washed with 2 x 7.5 ml of wash buffer QC.

12) The genomic DNA was eluted with 5 ml of elution buffer QF.

13) The eluted DNA was precipitated by adding 3.5 ml room temperature isopropanol (0.7 volumes of eluted DNA) to eluted DNA. DNA recovery was by centrifugation at 25000 x g for 30 minutes at 4°C.

14) Supernatant was carefully removed.

15) The DNA pellet was washed with 2 ml of cold 70% ethanol, vortexed briefly and spun at 5000 x *g* for 10 minutes at 4°C.

16) Supernatant was carefully removed without disturbing pellets and left to air-dry for 10 minutes.

17) DNA pellets were resuspended in 0.5 ml of a TE Buffer (pH 8.0) and incubated at 55°C for 1 hour to dissolve the pellet.

18) The yield and purity of extracted DNA from each cell line was determined using an optical light spectrometer at 260nm and 280nm.

2.7.2 Digestion of genomic DNA from parental PC3M and antisense transfectant cells

A restriction digest was performed on PC3M parental cells, control PC3M-pSV transfectant cells, pool of transfectant cells (PC-3M-P), and antisense transfectant PC3M-C-FABP 1 and PC-3M-C-FABP 3 cells respectively.

1) A 50µl restriction digest reaction was prepared. This consisted of 15µg of genomic DNA from cell lines digested in 3µl of HindIII (20U/µl). 5µl of 10x buffer was added and the remaining volume was made up using sterile deionised water. Restriction digest mix was gently mixed before being incubated at 37°C for 2 hours.

2) Following digestion, the restriction digest reaction was heat inactivated at 65°C for 5 minutes.

2.7.3 Agarose gel electrophoresis of digested DNA samples

Parental PC-3M cells, control transfectant cells, pool of transfectants and antisense transfectant cells were separated by fragment size using agarose gel electrophoresis. A 0.8% gel was set up using 1x Tris-borate buffer (TBE buffer) and ran against DNA marker III at 80V for 1 hour.

2.7.4 Southern blotting of DNA from gel to Hybond-N Membrane

1) DNA samples were denatured by placing the gel in 0.05M NaOH solution and left to soak for 20 minutes with gentle agitation.
2) The gel was placed in 1x SSC solution for 45 minutes with gentle agitation.
3) During this incubation period, the transfer rig was set up (Figure 2.7.4).

Figure 2.7.4 Set up of Southern blot transfer of DNA from gel to membrane

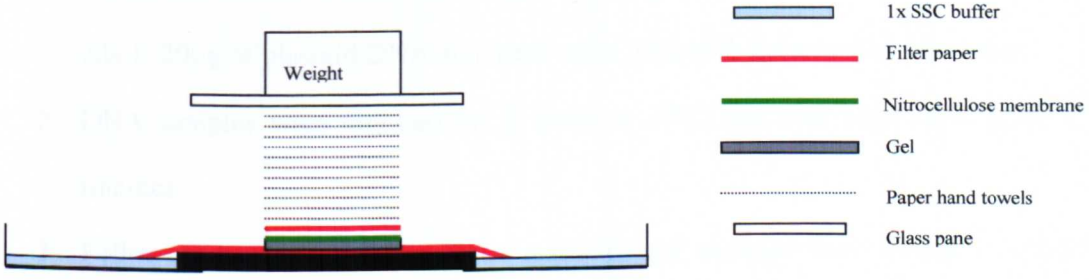

4) 3MM filter paper was measured to fill the length and breadth of the transfer rig. 1x SSC buffer was poured into the reservoir until the filter paper was wet through. During this period, nitrocellulose membrane was soaked in 1x SSC for 5 minutes
5) Following gel incubation, the gel was placed on top of the filter paper and a sheet of nitrocellulose membrane was placed on top of the gel.
6) To aid capillary action, a stack of dry paper towels were stacked on top of the filter paper, and a heavy weight placed on this stack.
7) Transfer was left to blot over night for a period 15 hours.
8) Following overnight transfer, the membrane was washed in 6x SSC for 20 minutes and then subjected to UV light fixation of DNA to membrane for 3 minutes.

2.7.5 Excising C-FABPr fragment from pSV-Neo plasmid

The pSV-Neo plasmid containing a reverse C-FABP fragment was restricted to liberate the reverse C-FABP fragment using XbaI (10U/μl) and HindIII (20U/μl) restriction enzymes.

1) A reaction volume of 60μl was set up consisting of 6μl 10 x buffer, 2μl of HindIII, 4μl of XbaI, 20μg of plasmid DNA and made up to 60μl with deionised sterile water.
2) DNA samples were digested for 2 hours at 37°C and heat inactivated at 65°C for 5 minutes.
3) Following heat inactivation, DNA restricted the samples were loaded in a 0.8% tris-acetate (TAE) low melting point agarose (LMA) gel and ran for 1 hour 45 minutes at 80V.

4) Using ethidium bromide staining, C-FABP fragment was identified and cut out of the gel in order to extract genomic DNA from the gel slice (Figure 2.7.5).

Figure 2.7.5 Double digestion of pSV-C-FABPr and separation of samples by agarose gel electrophoresis

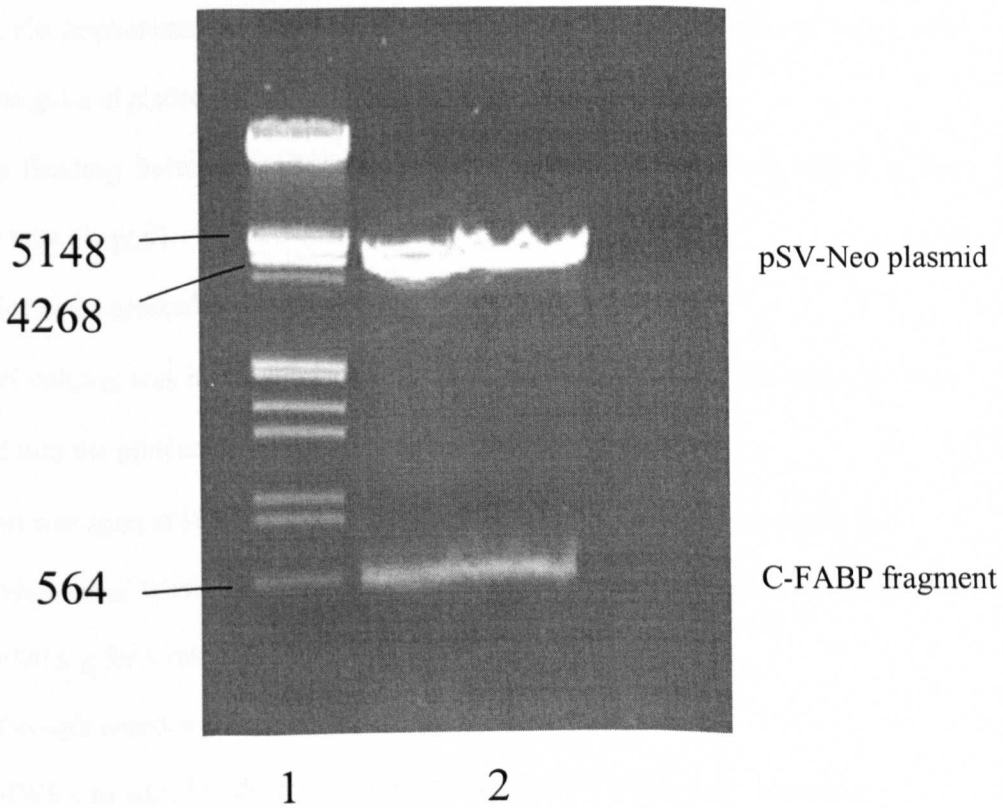

Lane 1 - DNA Marker III
Lane 2 – pSV-C-FABPr digested with HindIII and Xba1

2.7.6 Isolation of C-FABPr genomic DNA from agarose gel

Isolation of C-FABP DNA fragment from the pSV-Neo plasmid was conducted using the Wizard® SV Gel and PCR Clean-Up System (Promega) and the protocol followed as specified by the manufacturer.

1) Following electrophoresis, the DNA band corresponding to base pair size of insert was cut from the gel and placed within a 1.5ml microfuge tube and weighed
2) Membrane Binding Solution (MBS) per 10mg weight of gel slice was added to the microfuge tube (1μg/μl)
3) The gel slice was vortexed and incubated at 50-65°C to dissolve LMA.
4) A SV Mini column was inserted into a collection tube and the dissolved LMA gel was transferred into the mini column.
5) The column was spun at 16 000x g for 1 minute and the flow through was discarded.
6) 700μl of Membrane Wash Solution (MWS) was added to the mini column, which was spun at 16000 x g for 1 minute.
7) The flow through was discarded.
8) 700μl of MWS was added to the minicolumn and spun at 16 000 x g for 5 minutes.
9) The minicolumn was transferred to a sterile 1.5ml microfuge tube and 500μl of nuclease free water was added to the minicolumn.
10) The column was incubated at room temperature for 1 minute, and then spun at 16 000 x g for 1 minute.
11) The minicolumn was discarded and eluted DNA was stored at -20°C.

12) 2µl of eluted DNA against DNA Marker XIV and was run in a 0.8% agarose gel using 0.5 x TBE buffer. The results from this gel enabled quantification of eluted DNA.

2.7.7 Random-Primed Labelling of Probes

The C-FABPr probes were labelled with ^{32}P-γ-dCTP using a Random-primed labelling kit (Boehringer Mannheim). Probe preparation was performed in accordance with the manufacturers guidelines (Feinberg and Vogelstein, 1983; Feinberg and Vogelstein, 1984).

1) Probe DNA (25ng) was denatured by boiling for 10 minutes.
2) Denatured probes were then cooled on ice for 2 minutes to prevent reannealing and mixed with the following reagents in a microfuge tube on ice:
    a. 0.5mM of dATP, dGTP and dTTP respectively
    b. 2µl of reaction buffer
    c. 20U Klenow enzyme
    d. 30µCi ^{32}P-γ-dCTP
3) The reaction mixture was incubated at 30 minutes at 37°C, then boiled for 10 minutes, and placed immediately on ice before being added to hybridisation solution.

2.7.8 Southern Hybridisation

To prevent non-specific binding, membranes were incubated in prehybridising solution. The use of Denhardts reagent in the prehybridisation buffer enables blocking of non-specific attachment of probes in future steps.

1. The membrane was incubated with 25ml of pre-warmed prehybridisation buffer for 4 hours in a Techne glass tube at 42°C.
2. Following this incubation period, prehybridisation buffer was decanted, and replaced with hybridisation buffer containing the radio-labelled probe and incubated overnight.

2.7.9 Washing membrane

Following incubation of radio-labelled probes, the membrane was washed in a series of stringent washes to remove non-specific hybridised probes.

The membrane was washed in a series of washes. After each washing stage, the intensity and localisation radio-labelled probes to RNA fragments were assessed using a Series 900 mini-monitor GH.M Tube. When background signalling was sufficiently reduced (to between 5 – 10 counts/second), the membrane was washed in 3x SSC, blotted dry and wrapped in Saran cling film wrap and exposed to Kodak film at -80°C.

Reagent	Temperature	Time (minutes)
2x SSC, 0.5% SDS	Room Temp	5 minutes
2x SSC, 0.5% SDS	Room Temp	15 minutes
0.1x SSC, 0.5% SDS	37°C	30 minutes
0.1x SSC, 0.5% SDS	68°C	30 minutes
0.1x SSPE	Room Temp	5 minutes

2.8 SOUTHERN BLOT ANALYSIS FOR DETECTION OF NEOMYCIN GENE

Southern blot analysis for the detection of neomycin gene expression was performed as described in section 2.7. Neomycin resistance gene probes were prepared by restriction digest of pSV-Neo plasmid with B*ssH*II and HindIII to provide an 881bp DNA fragment.

2.9 CELL INVASION ASSAY

A cellular invasion assay was performed to assess the invasiveness of antisense transfectant cells relative to highly malignant parental PC3M cells. The protocol used was based on previous work performed by Smith *et al,* (1998). All materials and reagents used in this Section can be found in Appendix 1.2.

2.9.1 Preparing standard curve for invasion assay

1) Cells were harvested as described in Section 2.3.3, and their numbers adjusted to 4 x 10^4 cells/ ml.
2) Using doubling dilutions, a standard curve for each cell line was prepared in a 24-well plate (Nunclon). The cell numbers in the standard curve were as follows:
    a. 4 x 10^4 / ml
    b. 2 x 10^4 / ml
    c. 1 x 10^4 / ml
    d. 5 x 10^3 / ml
    e. 2.5 x 10^3 / ml

f. 1.25×10^3 / ml

g. 6.25×10^2 / ml

h. 3.125×10^2 / ml

3) The cells were incubated for 24 hours at 37°C.

4) 200µl of 5mg/ml 3-[4,5-dimethylthiazol-2-yl]-2,5-diphenyltetrazolium bromide (MTT, Sigma) was added to each well, and incubated for 4 hours at 37°C. MTT solution was aspirated from wells and 400µl of dimethyl sulphoxide (DMSO) was added to each well to dissolve the formazan crystals at 37°C for 10 minutes.

5) Aliquots of 195µl were transferred from each 24 well into a 96 well plate in duplicate.

6) The optical absorbance was measured using a Multiskan MS plate reader at 570nm.

2.9.2 Invasion assay

1) 15µl of extra-cellular matrix (ECM, Sigma) was applied to the membrane of 12mm diameter filter inserts with a pore diameter of 12µm (Millipore) and evenly distributed with a glass rod.

2) The inserts were heated at 37°C to polymerise the gels.

3) Cells to be assessed were harvested using T/E and adjusted to 6.40×10^4 / ml.

4) 0.4ml of each cell suspension was placed in triplicate into each Millicell filter insert in a 24 well plate, and 0.6ml of routine cell culture medium, supplemented with 5% dialysed stripped foetal calf serum, was added to each filter insert and incubated at 37°C for 48 hours.

5) Following the incubation stage, the surface of each filter insert was wiped thoroughly with cotton buds.
6) 120µl MTT was added to each well and incubated for 4 hours at 37°C
7) The MTT solution was aspirated and formazan crystals dissolved with the addition of 400µl DMSO at 37°C for 10 minutes.
8) Aliquots were transferred from each well into a 96-well plate in duplicate and the optical absorbance measured with a Multiskan MS plate reader at 520nm. This enabled regression analysis to be performed on absorbance values in order to determine cell number.

2.10 TUMOURIGENICITY OF ANTISENSE TRANSFECTANT CELLS

2.10.1 Introduction *in vivo* work

In vivo assay was performed on 8-week-old male immuno-incompetent ICRF-Nude mice (Harlan Ltd). Male ICRF nude mice were the *in vivo* model of choice as they had T-cell deficiency. This characteristic proved to be favourable as an inhibited immune system reduced the possibility of immune rejection.

Three groups of 8 mice were inoculated subcutaneously into the shoulder region of male ICRF mice with control transfectant cells, PC3M-C-FABP-1 and PC3M-C-FABP-3 cell clones respectively. Measurements of tumour growth were taken weekly over the course of the experiment by measuring tumour length, width and height. These measurements were applied to

a formula: *L x W x H x 0.5236* (Janik *et al.*, 1975) that enabled tumour volume to be calculated. All materials and reagents used in this section can be found in Appendix 1.6.

2.10.2 Inoculation of male immunoincompetent nude mice

1) Control transfectant cells and antisense transfectant PC3M-C-FABP 1 and PC3M-C-FABP-3 cells were sub-cultured as described in section 2.3.3, and resuspended in $25x10^6$ cells/ml respectively in PBS.
2) Mice were inoculated subcutaneously in the shoulder region with 0.2ml ($5x10^6$ cells) cell suspension.
3) Tumour growth at site of inoculation was measured over a period of 6 weeks.
4) At 6 weeks, animals were culled and tumour tissue (where present) was removed and fixed in 10% formalin for a period of 24 hours.

2.10.3 Processing of tumour tissue derived from mice

Tumour tissues dissected from mice were fixed in 10% formalin for a period of 24-hours. In order to conduct immunocytochemical analysis, tissues were dehydrated and impregnated with paraffin wax to preserve tissues and provide a solid support for tissue sectioning.

1) Animal tissues were fixed overnight in 10% formalin.
2) The following day, fixed tissue samples were trimmed and placed within embedding cassettes and processed on a Shandon processor.
3) Following this, the tissues were washed for:
    a. 1 x 1 hour wash in 70% ethanol

b. 1 x 1 hour wash in 90% ethanol

c. 4 x 1 hour washes in absolute ethanol

d. 3 x 1 hour washes in xylene

e. 2 x 1.5 hour washes in paraffin wax (60°C)

4) Processed tissues were embedded in paraffin wax at 60°C and cooled on ice.

5) Paraffin embedded tissues were cut into 4μm sections as described in Section 2.2.2.

6) Some of these sections were stained with Gill's haematoxylin and eosin as described in Section 2.2.3, and the other sections were immunohistochemically stained for the detection of C-FABP. This was performed as described in Section 2.2.4.

2.10.4 Immunohistochemistry for the detection of VEGF Expression in mice tumour tissue

Immunohistochemistry for the detection of vascular endothelial growth factor (VEGF) was performed on mouse tumour derived tissue sections, and utilised the same methodology as described in Section 2.2.2 and Section 2.2.4. Primary anti-VEGF sera (Santa Cruz Biotechnology) was used at a dilution of 1:500, and incubated in a HRP-conjugated polymer.

2.10.5 Immunohistochemistry for the detection of Factor VIII-related antigen in mice tumour tissue

Immunohistochemistry for the detection of Factor VIII-related antigen was performed on the same mouse tumour derived tissue sections using the methods described in Section 2.2.4 and 2.2.5. In this instance, an avidin-biotin complex (Dako Ltd, Ely UK) was used. These sections were stained with rabbit anti-Factor VIII-related antigen serum (Dako Ltd) at a dilution of 1:1000 and then with donkey anti-rabbit immunoglobulin conjugated to biotin (Amersham International), and visualised with an avidin-biotin complex system (Dako Ltd).

2.11 NORTHERN HYBRIDISATION ASSAY

Northern hybridisation enables separation of RNA by electrophoresis on a denaturing gel, Northern transfer onto nitrocellulose membrane (Goldberg, 1980; Seed, 1982; Thomas, 1980) and hybridisation of radio-labelled probes to RNA samples.

RNA was extracted from cells using a Qiagen RNeasy ® Midi preparation kit according to the manufacturers' instructions. All materials and reagents in the section can be found in Appendix 1.7.

2.11.1 RNeasy ® Midi preparation of RNA

1) Cells were harvested using tissue culture techniques described in section 2.3.3.

2) Cell pellets were then disrupted by the addition of 2ml Buffer RLT containing 20µl of beta-mecaptoethanol (BME).
3) The cells were then homogenised for at least 45 seconds at maximum speed then 2ml of 70% ethanol was added to the homogenised lysate and vortexed.
4) The samples were then applied to an RNeasy midi column and centrifuged for 5 minutes at 3000 –5000 x g at room temperature.
5) The supernantent was discarded and 4mls of Buffer RW1 was added to the column and spun for 5minutes at 5000 x g to wash the column.
6) The flow through was discarded and the column was washed twice using 2.5ml Buffer RPE and centrifuged for 5 minutes at 5000 x g.
7) Following this washing cycle, the RNA bound to the midi column was eluted by addition of 250µl of Rnase-free water into the column and left to stand for 1 minute at room temperature.
8) The columns were spun at 5000 x g, and the flow through was transferred back into the column, left to stand for a minute and then spun for 3 minutes at 5000 x g at room temperature
9) The eluted RNA was collected in 1.5ml sterile RNase free tubes and stored at -20°C.

2.11.2 Precipitation of RNA

1. Following isolation of RNA using Qiagen RNeasy midi kit extraction protocol, RNA samples were concentrated by addition of $1/10^{th}$ the eluted volume of 3 molar sodium acetate (pH5.0) and 2 x eluted volume of ice cold 100% ethanol.

2. This was vortexed to mix, and precipitated overnight at -20°C.
3. The RNA was pelleted 15 000 x g at 4°C for 10 minutes.
4. The supernatant was removed, and RNA pellet was resuspended in 32µl of RNase free water.
5. The concentration of each extracted RNA sample was obtained using a spectrophotometer at 260nm and 280nm.
6. Precipitated RNA samples were stored at -20°C.

2.11.3 Preparing denaturing gel electrophoresis

A 1% agarose denaturing gel containing formaldehyde was prepared. This method was adapted from Goldberg, (1980); Seed, (1982).

1) 0.5g of agarose powder was mixed with 40mls of diethyl pyrocarbonate (DEPC) treated water. This was heated in the microwave until agarose had melted.
2) 0.1M 3-(N-morpholino) propanesulphonic acid (MOPS, pH 7.0) and 4µl formaldehyde was added to melted agarose and cast into a gel rig to polymerise.

2.11.4 Sample preparation for denaturing gel

1) Each RNA sample (20µg) was prepared by the addition of 2µl of 10x MOPS buffer, 4µl of formaldehyde, 10µl of formamide respectively.
2) This was boiled for 10 minutes and cooled on ice for 2 minutes.

3) 5µl of loading buffer was added to samples, loaded into gel and run against an RNA marker for 15 minutes at 40V, and 1 hour at 75V.

2.11.5 Northern transfer of RNA

The transfer of RNA from gel to nitrocellulose membrane was based on Thomas, (1980); White and Bancroft, (1982) and follows the method detailed in Section 2.7.4. The transfer was left to run overnight. The following day, the membrane was removed from the transfer rig and washed in 6xSSC for 5 minutes. Excess liquid was drained, and RNA was fixed to the membrane by UV fixation. The membrane was stored at 4°C.

1) VEGF probe preparation was performed using random-primed labelling method (Boehringer Mannheim Biochemica). The probes (25ng) were radio-labelled with [α^{-32}P]dCTP as described in Section 2.7.7.
2) The membrane was prehybridised for 4 hours at 42°C in prehybridisation buffer to prevent non-specific probe attachment, then hybridised to radio-labelled VEGF probes overnight at 42°C in a Techne hybridisation oven.
3) The following day, the membrane was put through a series of washes as described in Section 2.7.9 and exposed to Kodak XAR-5 film with an intensifying screen for 24 – 36 hours.

2.12 SECTION TWO: RNA INTERFERNCE METHODOLOGY

2.12.1 Cell lines and cell culture conditions

The cells lines used in this section of the study were the PC-3 metastatic variants cells PC-3M (Section 2.3.1). Additionally, LNCaP prostate cancer cell lines were used within this thesis. These cell lines were derived from biopsies of lymph node metastasis from a patient with well-differentiated prostatic adenocarcinoma (Horoszewicz *et al.*, 1983; Webber *et al.*, 1997). These cells were classified as androgen dependent, weakly malignant, prostate cancer cells and represent early stage malignancy in prostate cancer cell line model (Horoszewicz *et al.*, 1983). Materials and reagents can be found in Appendix 1.8.

2.12.2 Introduction to RNAi

RNA interference (RNAi) works along similar principles of homologous sequence recognition and cleavage as antisense technology. RNAi is an evolutionary conserved defence mechanism used by eukaryotic cells to guard against exogenous nucleic acid or viral attacks. Introduction of long double stranded RNA into eukaryotic cells initiates the RNAi pathway in which RNase III, a member of the Dicer family of endonucleases, cleaves long double stranded RNA into small interfering RNA (siRNA) segments approximately 21 – 23bp in length. siRNA are incorporated into a RNA Induced Silencing Complex (RISC) (Caplen *et al.*, 2001; Elbashir *et al.*, 2001). The double strand is unwound, and the sense strand is discarded whilst simultaneously activating the RISC complex containing the remaining antisense strand. This strand acts as a locator for any

homologous sequences within the transcriptome and are subsequently cleaved to produce target specific long term gene silencing (Brummelkamp *et al.*, 2002).

All materials and reagent used in this section can be found in Appendix 1.9.

2.12.3 Designing siRNA Silencing Construct

Figure 2.12.3 siRNA silencing construct

1) A unique 19nt sequence located at the 5-prime end of the C-FABP gene was chosen as the siRNA target site. This site was immediately downstream from an AA dinucleotide sequence. The uniqueness of the 19nt sequence was confirmed by blast searching the sequence to ensure that it held no specificity towards any other human or mouse sequence. The silencing construct is homologous to the C-FABP gene 253bp from the 5 prime end. The entire C-FABP nucleotide gene sequence is 662bp in size.

3) Upon receipt of the synthesised oligonucleotides, they were resuspended in 60µl TE buffer at pH8.0 to a final concentration of 5.2µg/µl for the sense oligonucleotides and 6.91µg/µl for the antisense oligonucleotide

2.12.4 Annealing sense and antisense oligonucleotides

1) To anneal both oligonucleotides together, the oligonucleotides were diluted to 1µg/µl with TE buffer.
2) Then, 2µl of each oligonucleotide was added to 46µl of annealing buffer, mixed and incubated at 37°C for 1 hour.
3) The samples were stored in -20°C freezer.

2.12.5 Making competent DH5α bacterial cells

E.Coli (DH5α) competent cells were prepared in accordance with the method detailed in Cohen *et al.*, (1972).

1) *E.Coli* bacterial cell (DH5-α) glycerol stocks were streaked onto LB-agar plates and incubated at 37°C overnight.
2) The following day, plates were removed from the incubator and a single colony was transferred into individual conical flasks containing 10mls Liquid Broth (LB) medium.
3) This flask was incubated overnight in 37°C and 300rpm.
4) The following morning, overnight cultures were transferred into 100mls LB medium and incubated at 37°C and 300rpm for several hours until LB medium appeared cloudy.

5) Optimum bacterial yield was obtained when bacterial cells were judged to be proliferating in the log phase. This corresponded to an optical absorbance value (OD_{600})1-1.5nm.

6) Following this, bacterial cultures were divided into 4 x 25ml aliquots and left on ice for 10 minutes to cool.

7) After the incubation period, they were spun at 1100 x g for 10mins in 4°C in a centrifuge.

8) The supernatant was discarded, and bacterial cell pellets were resuspended in 8.25mls RF1 calcium chloride glycerol buffer and incubated on ice for 10 minutes.

9) Resuspended cells were spun at 1100 x g for 10minutes at 4°C. The supernatant was discarded and cell pellets resuspended in 2mls of RF2 calcium chloride glycerol buffer.

10) The resuspended cells were aliquoted into 1ml cryo-tubes and were flash frozen in liquid nitrogen, and stored in -80°C freezer.

2.12.6 Restriction double digest of pSilencer 1.0-U6 vector

The pSilencer 1.0-U6 vector was purchased in a circularised form from Ambion®. In order to insert the silencing construct designed in Section 2.12.2, the vector was linearised by a double digest using *Apa*I and *Eco*RI restriction enzymes. This produced two fragments of approximately 3249bp and 42bp. As *ApaI* and *EcoRI* restriction enzymes had different optimal temperature ranges, two sequential single digests were conducted. The digestion would leave the plasmid unable to reanneal as remaining nucleotide over hangs would lose complimentary (Figure 2.12.6).

plasmid unable to reanneal as remaining nucleotide over hangs would lose complimentary (Figure 2.12.6).

Figure 2.12.6 Restriction map of pSilencer vector

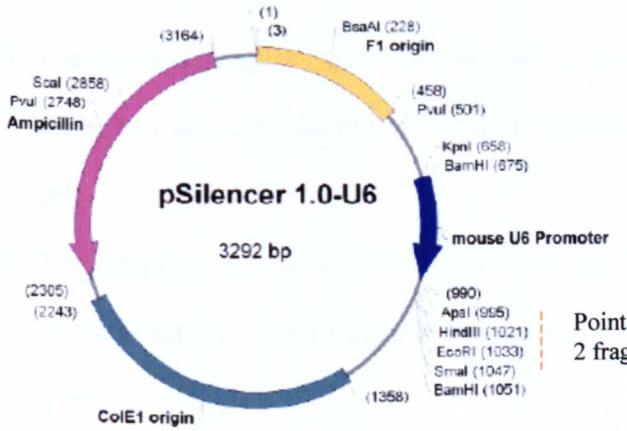

Restriction map of pSilencer vector. Linearising the vector enabled the insertion of the silencing construct, and re-circularising of the vector to form a recombinant vector.

1) To linearise the pSilencer vector, a restriction enzyme reaction mix was prepared. This consisted of 8µg of plasmid DNA in 35µl of water, 6µl of 10x buffer, and 30units of *EcoRI* restriction enzyme were added to the reaction mix. This was mixed thoroughly and incubated for 1 hour at 37°C
2) Following this, 60µg of BSA and 30units of *ApaI* were added to the reaction mix and incubated at 25°C for 1 hour.
3) Once the sequential single digest was completed, the enzymes were heat inactivated at 65°C for 5 minutes.

2.12.7 Agarose gel electrophoresis

1) A 0.75% agarose electrophoresis gel was prepared in 0.5x TBE and 5µl ethidium bromide.
2) The digested samples (5µl) were run against an undigested sample (5µl). 2µl of loading buffer was added to the digested and undigested samples respectively and loaded in the gel.
3) The samples were run at 80V for 1 hour using 1xTBE running buffer, and confirmation of predicted restriction fragment lengths was performed on a transilluminator at 302nm filter.
4) The digested samples were stored at -20°C for future use (Figure 2.12.7).

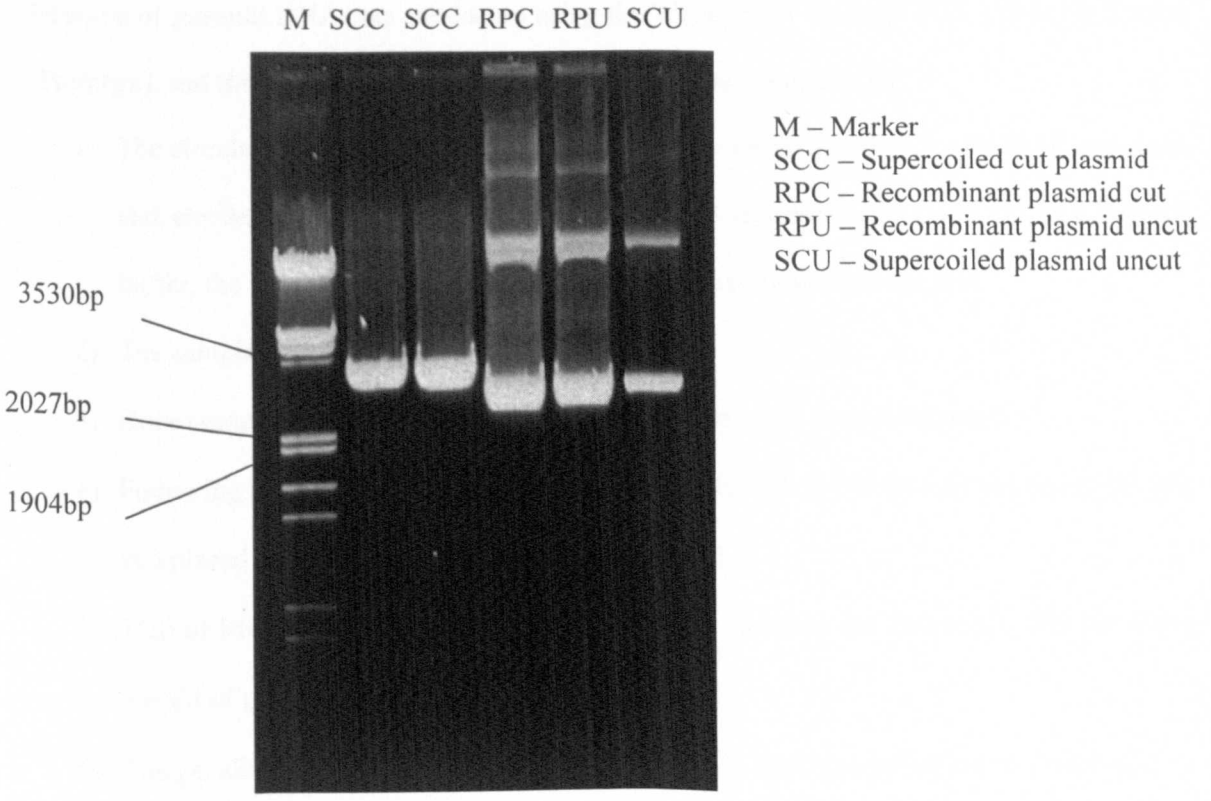

Figure 2.12.6 Gel electrophoresis showing generated recombinant pSilencer1.0 – U6 plasmid. To confirm insertion of silencing construct into pSilencer plasmid, a restriction digest was performed. Lanes 2 and 3 represent the super-coiled plasmids that were double digested with ApaI and EcoRI restriction enzymes to produce fragments of approximately 3249bp and 42bp (the smallest fragment cannot be seen). As insertion of the silencing construct occurred within the multiple cloning site, the ApaI and EcoRI restriction sites are lost and double digests of recombinant plasmids (lane 4) produce similar fragment dispersal patterns as unrestricted recombinant plasmids and super-coiled plasmids (lanes 5 and 6 respectively).

2.12.8 Isolation and purification of linearised pSilencer plasmid DNA from agarose gel

Isolation of plasmid DNA was conducted using the Wizard® SV Gel and PCR Clean-Up System (Promega), and the protocol followed is as specified by the manufacturer.

1) The circularised pSilencer plasmid is linearised by restriction digest with *Eco*R and *Apa*I, and electrophoresed using 1% low melting point agarose (LMA) and 1x TAE running buffer, the recommended buffer used for low melting point agarose gels.
2) The samples were loaded and ran for 1hr at 80V.
3) Once complete, the gel was visualised at 302nm on a UV transilluminator.
4) Following electrophoresis, the pSilencer1.0-U6 plasmid (3249bp) was cut out of the gel, and placed in a 1.5ml microfuge tube and weighed.
5) 10µl of Membrane Binding Solution (MBS) was added to the microfuge tube per 10mg weight of gel slice is added to the microfuge tube.
6) The gel slice was vortexed and incubated at 50-65°C until the gel slice was dissolved.
7) A SV Mini column was inserted into a collection tube and the dissolved gel was transferred into a mini column.
8) Each column was spun at 16 000 x g for 1 minute and the flow through was discarded.
9) 700µl of Membrane Wash Solution (MWS) was added to each mini column, and centrifuged at 16000 x g for 1 minute.
10) The flow through was discarded.
11) 700µl of MWS was added to the minicolumn and spun at 16 000 x g for 5 minutes.
12) The minicolumn was transferred to a sterile 1.5ml microfuge tube and 500µl of nuclease free water was added to the minicolumn.

13) The column was incubated at room temperature for 1 minute, and then spun at 16 000 x g for 1 minute.

14) The minicolumn was discarded and the eluted DNA was stored at -20°C.

2.12.9 Ligating silencing construct with pSilencer plasmid

To create a recombinant vector containing a silencing construct, the short DNA molecule was directionally cloned into plasmid DNA in the correct orientation. To do this, a ligation reaction experiment was performed in which the insert to plasmid ratio was at 3:1 to ensure that the rate-limiting step of this experiment was dependent upon the amount of plasmid present and not the insert.

1) This experiment was performed by the addition of 300ng of the short DNA molecule and 100ng of pSilencer vector to 12µl of deionised sterile water. 2µl of T4 DNA ligase buffer and 1µl of T4 DNA ligase were also added to the reaction mix.
2) The ligation reaction was incubated at 16°C overnight.

2.12.10 Transformation of DH5-α bacterial cells

1) A vial of competent cell DH5α bacterial cells was removed from the -80° C freezer and thawed on ice.
2) Once suitably thawed, 2x200µl aliquots were transferred into two separate tubes removed and placed in Falcon 20 tubes to make control and experimental groups.

3) Then, 20ng of recombinant plasmid DNA (formed by ligation of silencing construct, Section 2.12.8) was added to the experimental group vial. This was flicked gently to mix and both tubes were placed on ice for 30 minutes.

4) Both tubes were transferred to a 42°C water bath for exactly 90 seconds, and placed on ice again for a further 2 minutes.

5) 800µl of SOC medium was added to both tubes, gently shaken and incubated at 37°C for 1 hour at 200rpm.

6) During this period, LB-agar plates were removed from the fridge and placed in an incubating oven at 37°C to warm up.

7) 50µl from control and experimental groups respectively were plated on two separate plates containing 60µg/ml ampicillin.

8) The cultures were spread across the surface of the LB-agar and incubated at 37°C overnight.

9) The following day, a single colony was transferred into flasks containing 10mls LB medium and 60µg/ml ampicillin and left to grow overnight at 37°C and 200rpm to amplify bacterial cells.

10) The following day, bacterial cells grown in 10mls LB medium are transferred to 100mls LB medium containing 60µg/ml ampicillin, and grown for 3 - 4 additional hours in 37°C and at 200rpm. To ensure optimum plasmid extraction, bacterial cells were lysed when they were replicating in the log phase and had attained an OD_{600} of 1-1.3nm.

2.12.11 Midi-prep extraction of plasmid DNA

Extraction of plasmid DNA was conducted using an extraction kit prepared and distributed by Qiagen. The following protocol was carried out as specified by the manufacturers.

1) Transformed bacterial cells were amplified till OD_{600} value was within 1 – 1.3nm.
2) Following this, bacterial cells were harvested by centrifuging for 15minutes at 4°C at 6000 x g.
3) The supernatant was discarded and remaining bacterial pellets were resuspended in 4mls of buffer P1.
4) The bacterial cells were lysed with the addition of 4ml of lysis buffer P2, inverted 4 – 6 times and incubated at room temperature for 5 minutes.
5) After this incubation period, 4ml of pre-chilled P3 neutralising buffer was added, mixed immediately by inverting 4 – 6 times, and incubated for 15 minutes before being centrifuged at 20, 000x g for 30minutes at 4°C.
6) The supernatant containing plasmid DNA were promptly transferred to fresh tubes and spun at 20, 000 x g for 15 minutes at 4°C.
7) Whilst the centrifuge was running, the Qiagen 100 tips are equilibrated by applying 4ml equilibration buffer QBT and allowed to flow through under gravity.
8) Once the tip was equilibrated, the supernatants containing plasmid DNA were decanted into the Qiagen column and allowed to flow under gravity, enabling the plasmid DNA to be held by resin.
9) The flow through was discarded, and the Qiagen column was washed with 2x10ml wash buffer QC.

10) The DNA was eluted from the resin with 5ml of elution buffer QF.

11) The eluted DNA was precipitated with 3.5ml isopropanol, mixed and spun at 20 000 x g for 2hrs at 4°C.

12) The pellet was resuspended in 1ml of 70% ethanol, gently flicked to dislodge the pellet, and transferred into 1.5ml microfuge tubes, which are spun at 15 000 x g for 10minutes at 4°C.

13) The supernatant was removed and the pellet was air-dried and resuspended in 15µl TE buffer pH 8.0.

14) The concentration and quality of plasmid DNA was calculated using a spectrophotometer to measure the ratio of OD_{260}: OD_{280}.

15) Extracted plasmid was stored in -20°C.

2.12.12 Sequence analysis of recombinant pSilencer1.0-U6 plasmid

The sequencing analysis was conducted by using an internal pSilencer1.0 U6 T3 generic sequence primer to sequence the cloning site of the plasmid.

A T3 primer sequence was synthesised (5' – ATTAACCCTCAGTAAAGGGA – 3') by Invitrogen ™ before being diluted (200ng/µl) and prepared for sequencing at the Liverpool School of Tropical Medicine.

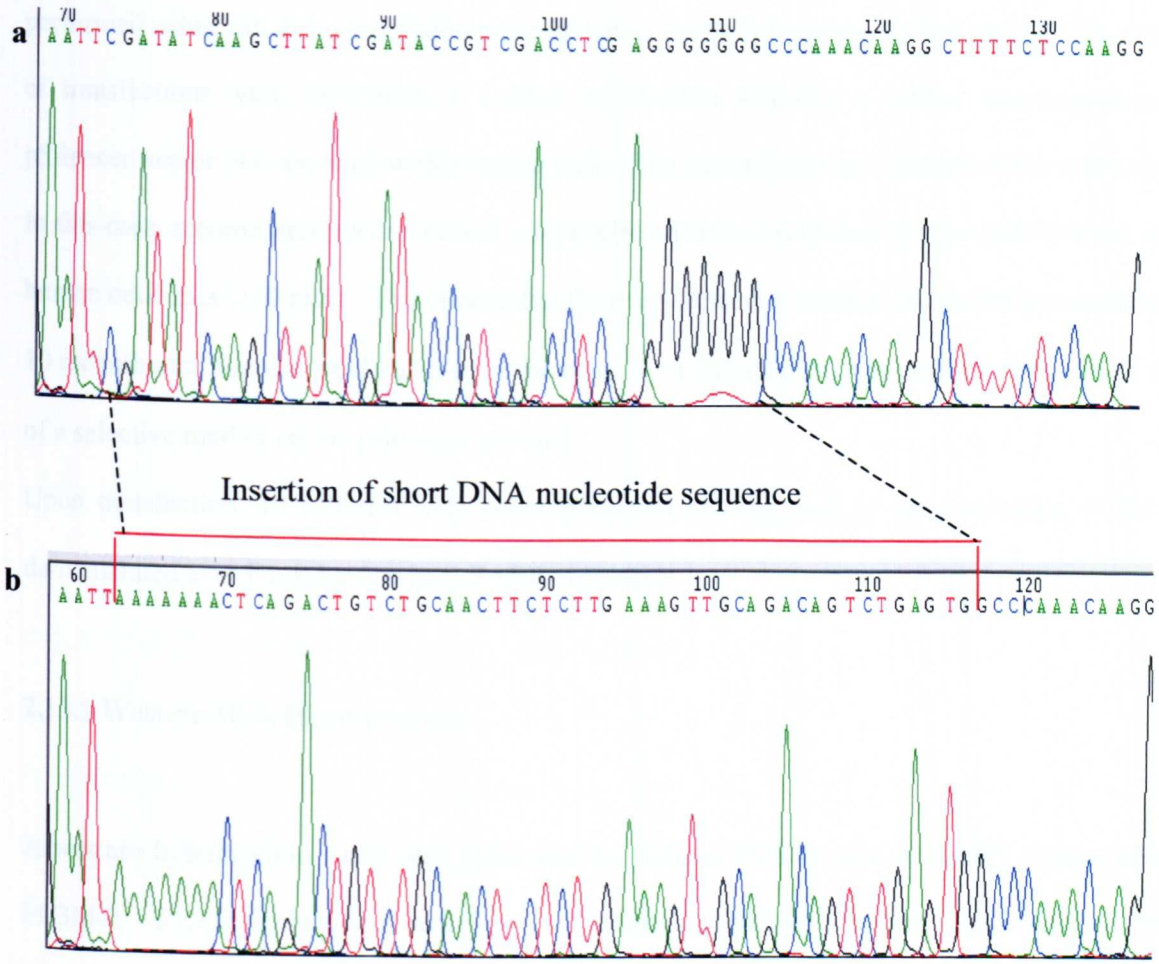

Figure 2.12.12 Electropherogram of control (**a**) and recombinant pSilencer plasmid (**b**).
(a) Control plasmid showing the regions of the multiple cloning site which were excised by restriction digestion and insertion of silencing construct **(b)**. The point of insertion and the sequence of insertion corresponds to the silencing construct. Automated sequencing was performed using internal primers in vector

2.13 TRANSFECTION AND IN VITRO ASSAYS OF siRNA TRANSFECTANT CELLS

Transfection of recombinant pSilencer plasmid into human prostate cancer cell lines, PC3M, was performed using calcium phosphate co-precipitation method described in Section 2.5. Two sets of transfections were performed, a control transfection whereby a control non-recombinant pSilencer vector was inserted within cancer cell. The second was an experimental transfection. In this case, recombinant pSilencer was co-transfected with a selective marker (pSV2-Neo) into human cells in a 1:10 ratio. This meant that for every selective marker successfully transfected, 10 recombinant vectors would also enter the cell. A co-transfection was performed due to a lack of a selective marker on the pSilencer plasmid.

Upon transfection, 10 colonies were isolated by ring cloning, and of these colonies, PC3M-3 demonstrated a >95% reduction in C-FABP expression.

2.13.1 Western Hybridisation assay

A western hybridisation assay was performed on parental PC3M cells, and siRNA transfectant PC3M-2 - PC3M-6 clones as described in Section 2.6 for the detection of C-FABP protein expression. The total cellular protein was isolated as whole-cell lysates from cell lines by lysis in hot 2x SDS lysis buffer. Proteins were run on a 10% SDS-PAGE gel, and transferred onto nitrocellulose membrane. Primary antibody immunoblotting was performed on proteins using rabbit anti human C-FABP at a 1:200 dilution, followed by horseradish peroxidase –conjugated swine anti rabbit immunoglobulin, diluted at 1:1000. Expression levels of C-FABP were determined by ECL detection.

2.13.2 Northern Hybridisation assay of siRNA transfectant cells

A Northern hybridisation assay was performed on parental PC3M cells, and siRNA transfectant PC3M-2, PC3M-3 and PC3M-6 clones as described in Section 2.11 for the detection of mRNA C-FABP expression.

15μg of total RNA per sample was electrophoresed under denaturing conditions, transferred to a nitrocellulose membrane and hybridised with [^{32}P]dCTP-labelled C-FABP cDNA probe. Radio-labelled C-FABP probes were prepared using a random primed labelling system (Boehringer Mannheim). The hybridised membrane was exposed to Kodak film for a period of 24-36 hours.

2.13.3 siRNA transfectant cell proliferation assay

2.13.3.1 Preparation of dialysed Foetal Calf Serum

Feasibility tests for cellular proliferation had shown that parental PC3M cells and siRNA transfectant PC3M-2 cells had rapid rates of proliferation in the initial phases of the assay. To counter this, foetal calf serum (FCS) was dialysed (Cellu-Sep, USA) and charcoal stripped of hormones. Dialysed and charcoal stripped medium lacks components required for cellular proliferation such as steroid hormones, resulting in reduced cellular proliferation and improved levels of comparison among parental PC3M and siRNA transfectant cells. All reagents and materials can be found in Appendix 1.2

Foetal calf serum was dialysed in the following way:

1) 100mls of frozen Foetal Calf Serum (FCS) was thawed at 37°C.

2) 5x 50cm strips of cellulose dialysis tubing membrane (molecular weight cut-off: 3.5kDa) were cut up and placed in a 500ml glass beaker and filled with 500mls of deionised water.
3) These strips were boiled for 3x 10minutes, replacing the quantity of water each time.
4) Upon completion, the strips were cooled in 500mls of fresh deionised water and tied at one end in a double knot.
5) The thawed FCS was added at 20ml/strip and double knotted at the other end, then placed in 5 litres of 1x dialysis buffer.
6) The dialysis buffer was placed in a cold room at 4°C and left to gently stir overnight.
7) The following day, the FCS filled cellulose membranes were placed in fresh 1x dialysis buffer and placed in a cold room at 4°C and left overnight to gently stir.
8) The following day, the serum was collected in a measuring cylinder and the volume noted; then activated charcoal was added to the volume of stripped FCS at 10mg/ml.
9) This mixture was left to stir at room temperature on a magnetic stirrer for 1hr.
10) Once time had elapsed, the mixture was centrifuged at 2800 x g for 10minutes to separate the charcoal from stripped FCS.
11) The supernatant was collected and filtered through a 0.22micron Millipore filter, divided into 20ml aliquots and stored in a -20° C freezer for future use.

2.13.3.2 Preparation of standard curve

1) Using 175cm^2 cell culture flasks, cells were cultured to 80% confluence.
2) Androgen positive medium was prepared. This consisted of RPMI 1640 cell culture medium (500ml) supplemented with Penicillin/Streptomycin 100IU, Hydrocortisone/ Testosterone 50ng/ml, 4% FCS and 8mM L-Glutamine. With the exception of hydrocortisone/testosterone, the androgen negative medium consisted of the same ingredients at the same concentration. In previous attempts at his experiment, cells were cultured in 10% FCS. However, they achieved confluence rapidly, and the experiment was discontinued. A 4% FCS supplementation was used to reduce cellular proliferation in order to attain a better resolution of cellular proliferation at the initial phase of the assay.
3) 24-hours before the onset of the assay, all cells were treated with an equal volume of androgen negative medium and incubated overnight at 37°C and 5% CO_2.
4) The following day, each cell line was harvested and resuspended in 1.0ml aliquots of PBS.
5) Each cell line aliquot was counted using a haemocytometer and adjusted to a density of $2.56x10^5$ /ml, then divided into two aliquots of $1.28x10^5$ /ml for the androgen positive and negative conditions respectively.
6) A standard curve was prepared in serial dilution fashion. In the androgen positive condition, 1ml of cells ($6.4x10^4$) were seeded into a 24-well plate. This represented the highest concentration of cells in the standard curve. The following concentrations serially diluted to correspond to the below dilutions:

a. $6.4x10^4$

b. $3.2x10^4$

c. $1.6x10^4$

d. $8x10^3$

e. $4x10^3$

f. $2x10^3$

7) Cells were plated in 24-well plates in duplicate and incubated overnight at 37°C and 5% CO_2.

2.13.3.3 Preparing cell proliferation assay

The proliferation assay was prepared on the same day as the standard curve was prepared. Each cell line was harvested, counted with a haemocytometer and plated in triplicate in 24-well plates at a cell density of $1x10^3$cells/well for the androgen positive negative and androgen negative condition.

1) Proliferation assay was set to run for 6 experimental days, colorimetric measurements were taken every day; hence 6 x 24-well plates were seeded to enable measurements on each experimental day.
2) The cells were incubated at 37°C and 5% CO_2.

2.13.3.4 MTT assay for standard curve and proliferation assay

On the following day, standard curve and proliferation assay measurements were performed by MTT assay. MTT is a yellow coloured liquid chemical that is incorporated into mitochondrion of a cells and oxidised into a soluble blue dye know as formazan. Formazan forms blue crystals in

the cell cytoplasm. Addition of DMSO causes the Formazan crystals to dissolve, leaving a coloured liquid. Optical density of cell population numbers was measured on a Multiskan MS plate reader at 570 nm. A standard curve was constructed by plotting OD (570nm) against cell density. The cell density of the test samples was determined by extrapolating from the standard curve.

1) MTT stock solution was prepared to a concentration of 1mg/ml and this was diluted to a working concentration of 1mg/ml.
2) MTT was added to standard curve cells and proliferation assay cells, incubated at 37°C and 5% CO_2 for 4hrs, and gently aspirated to avoid dislodging cells.
3) DMSO (400µl) was added to each well and incubated for 10 minutes until the formazan crystals had dissolved.
4) The DMSO in each well was mixed by pipetting up and down, and 2 x 195µl of the blue coloured liquid from each well of the 24 well - plate was transferred in duplicate to a 96-well plate.
5) Leaving one space blank into which 195µl DMSO was added, the optical density is measured at 570nm.
6) The results obtained from the Multiskan plate reader, a standard curve of optical absorbance against known cell numbers was constructed. Optical absorbance values obtained for the proliferation assays were converted into cell numbers per well per condition by regression analysis.

2.13.3.5 Soft agar assay

The soft agar assay is conducted in order to test tumourigenicity and ability parental and siRNA transfectant cells to form tumours in a sub strata free environment (Chien *et al.*, 1999). The more malignant a tumour cell, the greater its ability to form clusters of cells. In this experiment, parental PC3M cells and siRNA transfectant cells were cultured within an agarose suspension in order to determine their tumourigenic potential to migrate and form colonies of cells. This method describes the preparation of the androgen positive condition.

1) 50mls 2% low melting point agarose (LMA) gel using Tris-acetate buffer (TAE buffer) was prepared and left to cool in a water bath at 37°C .
2) After cooling, 3ml of 2% LMA was mixed with 3ml routine cell culture medium and plated in a 6-well plate in triplicate per sample under sterile conditions.
3) The gel was placed at 4°C to cool and solidify.
4) During this period, the untransfected PC3M and LNCaP; and siRNA transfected PC3M-2 and PC3M-3 cell lines were harvested using Trypsin/EDTA as described in Section 2.3.3 and adjusted to $5x10^3$ cells/ml.
5) 1ml of cells ($5x10^3$ cells) was mixed with 0.5ml routine cell culture medium and 0.5 ml 2% low melting point agarose, and plated on top of the preset bottom layer, then placed in 4°C to solidify the gel.
6) Once the top layer of gel was set, the 6-well plates were placed in an incubator at 37°C and 5% CO_2, and checked every 24hrs for colony formation for the duration of experiment.

This assay was conducted using androgen positive culture medium and androgen negative culture medium to determine whether testosterone supplementation affected tumour colony formation *in vitro*.

2.14 TUMOURIGENICITY OF siRNA TRANSFECTANT CELLS

2.14.1 Introduction to *in vivo* assay

The previous antisense tumourigenic assay was performed to assess the effect of suppressed levels of C-FABP on tumourigenicity using antisense transfectant cells. This assay was performed to determine whether a combination of suppressed C-FABP expression and inhibited androgen signalling affected tumourigenicity and metastasis in our test group relative to control group. 4 groups of 4 male immuno-incompetent CD-1 nude mice (Harlan, UK) were used in this study. Groups A and B consisted of non-castrated nude mice inoculated subcutaneously with parental PC3M cells and siRNA transfected PC-3M-3 cells respectively. Groups three and four consisted of castrated nude mice inoculated orthotopically into the prostate with parental PC-3M cells and RNAi transfected PC-3M-3 cells. Group A and B mice were inoculated with $2x10^6$ cells, whereas groups C and D were inoculated with $1x10^6$ cells. The difference in cell numbers was due to experimental error in which cell pellets were lost in the morning that groups C and D were to be inoculated.

2.14.2 Inoculation of male immunoincompetent nude mice

1) Parental PC3M cells and siRNA transfectant PC3M-C-FABP-3 cells were sub-cultured as described in Section 2.3.3, and resuspended in $10x10^6$ cells/ml respectively in PBS.
2) Mice were inoculated subcutaneously in the shoulder region with 0.2ml ($2x10^6$ cells)
3) The growth of tumours at the site of inoculation was measured over a period of 6 weeks.

2.14.3 Castration procedure of immunoincompetent mice

In order to create an androgen negative group, mice in groups C and D were castrated.

1) Mice were transferred to the bio-surgery department were they were administered anaesthetic (isoflurane and oxygen, nitrous oxide mix) and analgesia (temgesic-buprenophine 0.3mg/ml).
2) Mice were swabbed with iodine around the abdomen, hindquarters and genital area and two small incisions were made on either side of the scrotum, and each testis was gently eased out of the scrotum and a clamp was applied below each testis.
3) Suturing material was used to tie of the gubernaculums and the testis was removed.
4) The scrotum was sutured and mice were taken to the postoperative room for recovery.
5) The grooming, eating and excretory habits of each mouse were monitored post operatively to assess their recovery over the following week.

2.14.4 Orthotopic inoculation of immunoincompetent mice

Mice that were castrated a week previously were brought into the operating room to be othortopically inoculated with parental PC3M cells or siRNA transfectant PC3M-3 cells.

1) Each mouse was administered isoflurane anaesthetic gas and temgesic-buprenophine for pain relief.
2) Mice were swabbed with iodine around the abdomen, hind quarters and genital area, and an incision was made in the lower abdomen using a pair of scissors and forceps.
3) As the prostate gland is located just below the bladder it was used for orientation. Inoculation of parental cells and siRNA transfectant cells were targeted to the dorsal and lateral regions of mice prostate glands.
4) Upon cancer cell delivery, the wound was sutured and the mouse was placed in a post-operative recovery room and monitored.
5) Over the period of experimentation, mice were monitored twice weekly for loss of appetite, poor grooming or general malaise.
6) At the end of the experiment, mice were sacrificed by dislocation of cervical vertebrae. Dissections were performed to remove primary tumour tissue (where available), heart, lungs and liver and these were placed in 10% formalin tissue fixative.

2.14.5 Haematoxylin and eosin staining of mice tissue

Processing of mice tissues were performed as described in Section 2.10.3. The paraffin embedded tissue was sliced into sections 4μm thick and placed onto slides as described in Section 2.2.2, and stained with Haematoxylin and eosin as described in Section 2.2.3.
Two pathologists assessed the tissues in order to identify tumour cells within tissue.

2.15 STATISTICAL METHODS AND DATA ANALYSIS

The t-test was devised by William Gossett in 1908 and is a parametric test for calculating significant differences of means observed between two conditions. The t-test can be subdivided into independent t-tests in which participants or subjects participate in only one of two conditions; and a related or paired means in which participants are subjected to both conditions.
In this Thesis, the Student t-test was used to compare any differences observed within experimental groups and control groups. Data from proliferation assay, invasion assay and soft agar assay were all assessed using Students t-test. Similarly, comparison of tumour latent period, tumour incidence and tumour volume were all statistically assessed using Students t-test using Microsoft® Office Excel 2003. For all calculations, a value of $P<0.05$ was used to define statistical significance.

CHAPTER – 3 RESULTS

3.1 INTRODUCTION

The data presented within this Thesis were obtained in two separate rounds of experiments defined by antisense and RNA interference (siRNA) methods of gene silencing. The antisense section contains data obtained from experiments performed to assess C-FABP function in tumourigenicity and metastasis. To this end, antisense technology was used to suppress C-FABP protein expression in the highly malignant prostate cancer cell line, PC3M, to generate several single-cell-cloned transfectant cells. Western blot assay was performed to identify cloned transfectant cells expressing the lowest and mid-range level of C-FABP relative to control transfectant cells. These identified clones were used *in vitro* assays of tumourigenicity and metastasis and *in vivo* tumourigenic assays to better understand the involvement of C-FABP expression in prostate cancer development, progression and metastasis.

In the siRNA section, data are reported from experiments performed to further characterise C-FABP function in prostate cancer progression, and to determine whether androgen sensitivity is dependent upon C-FABP expression. To do this, RNA mediated interference was used to suppress C-FABP activity in highly malignant prostate cancer cell lines, PC3M, to create several single cell cloned transfectant cells. Confirmation of C-FABP suppression was performed by Western blot assays, and identified cloned transfectants were assessed *in vitro* for cellular proliferation and tumour formation in androgen positive and negative conditions. An *in vivo* assay was performed to observe any possible synergistic effects of C-FABP suppression and androgen depletion on tumour growth, development and metastasis.

3.2 ANTISENSE RESULTS SECTION

3.2.1 Differential expression of C-FABP in human prostatic tissues

Immunocytochemical staining for the detection of C-FABP expression in normal, benign and prostatic carcinoma tissues demonstrated a differential level of C-FABP expression (Figure 3.2.1a and 3.2.1b). From 7 normal cases stained, 7/7 (100%) failed to express C-FABP at a detectable level. In 35 Benign Prostatic Hyperplasia (BPH) cases, 25/35 (71.4%) stained negatively for C-FABP expression, whereas 10/35 (28.6%) showed a weak positive staining for C-FABP expression (Table 3.2.1).

In 34 prostatic carcinoma tissues used, 15 were classified as Gleason grades 1 – 3, and of these 15 cases, 4 /15 (26.7%) did not express detectable levels staining, 5 /15 (33.3%) expressed weak positive staining, 3/15 (20%) moderate and 3/15 (20%) strong positive staining for C-FABP expression. The 19 remaining prostatic carcinoma cases classified as being within Gleason grade 4 and 5 showed that C-FABP was nor expressed in 5/19 (26.5%) of cases, whereas 8 /19 (42.1%) stained weakly positive, 2/19 (10.5%) stained moderately strong and 4/19 (21.1%) stained strongly positive for C-FABP expression (Table 3.2.1).

Table 3.2.1 Expression of C-FABP in human prostatic tissue

Prostatic tissue	Number of cases	Negative Staining (%)	Weak positive staining (%)	Moderate positive staining (%)	Strong positive staining (%)	Total positive carcinoma staining (%)
Normal	7	7 (100%)	0	0	0	**0**
BPH[a]	35	25 (71.4%)	10 (28.6%)	0	0	**0**
Grades 1-3[b]	15	4 (26.7)	5 (33.3%)	3 (20.0)	3 (20.0%)	**11 (73.3%)**
Grades 4 & 5[b]	19	5 (26.3%)	8 (42.1%)	2 (10.5%)	4 (21.1%)	**14 (73.7%)**
Carcinomas (total)	**34**	**9 (24.5%)**	**13 (38.2%)**	**5 (14.7%)**	**7 (20.6%)**	**25 (73.5%)**

Immunocytochemical staining for each sample is graded negative, weak positive, moderate positive and strong positive. A grade of moderate positive staining corresponds to normal human epidermis. [a]Benign prostatic hyperplasia. [b]Gleason grades.

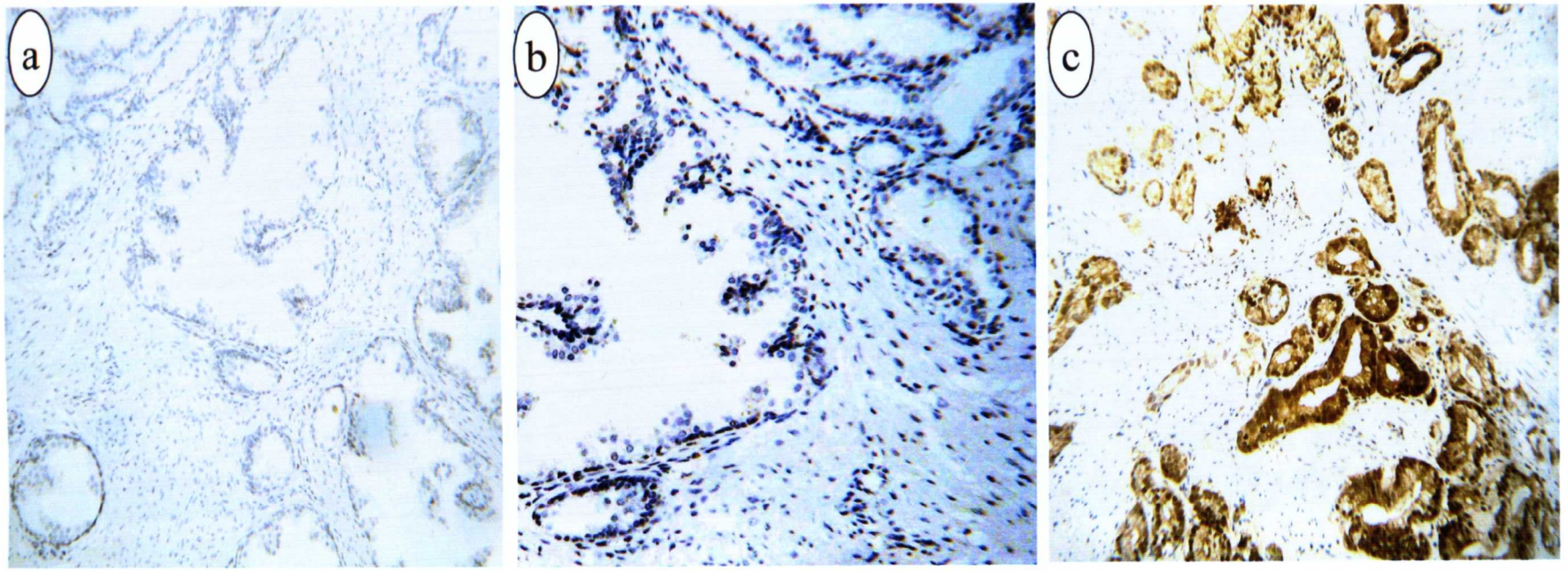

Figure 3.2.1a Immunocytochemical staining for the detection of CFABP in human prostate tissues. (**a**) Negative staining for C-FABP expression in normal tissue. (**b**) Negative staining for benign prostatic hyperplasia (BPH) cases. BPH tissues demonstrated negative to weakly positive C-FABP expression. (**c**) Moderately differentiated prostatic tissues demonstrated strong positive staining for C-FABP expression Magnification: a, b, and c, x120

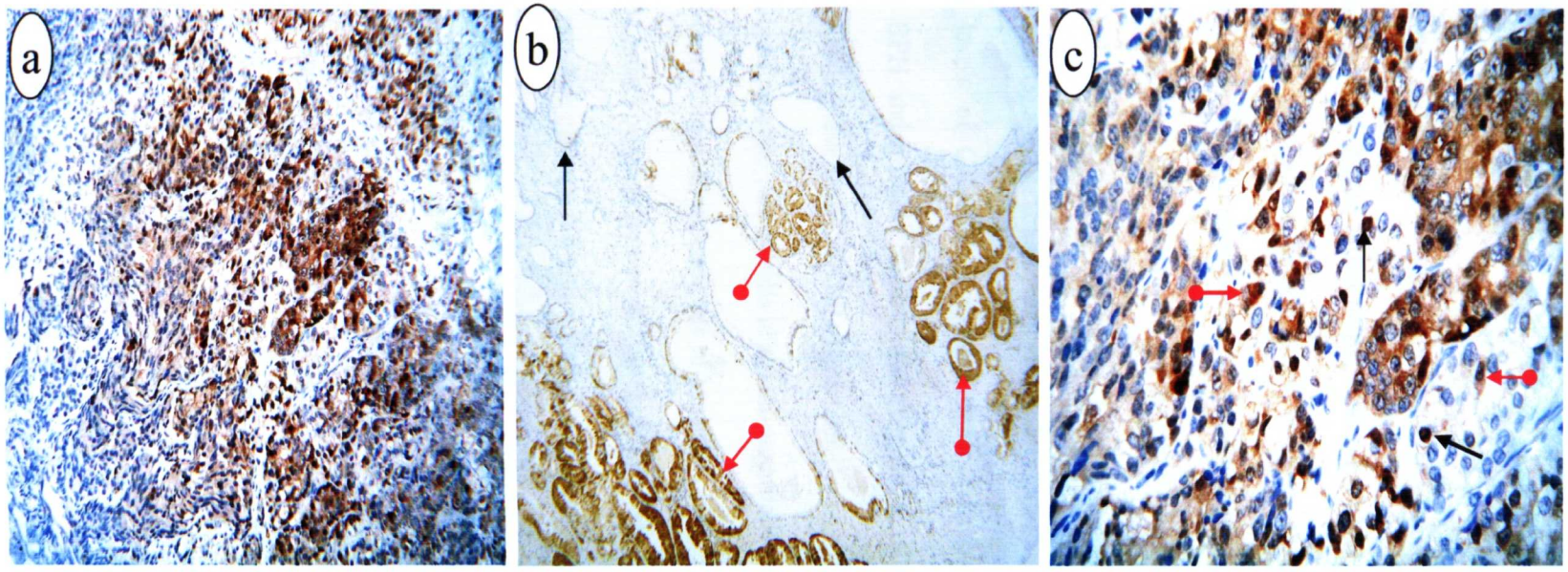

Figure 3.1b Immunocytochemical staining for the detection of CFABP in human prostatic tissues.
(**a**) Strong positive staining for C-FABP expression was observed in poorly differentiated prostatic carcinoma (grade 5)
(**b**) Positive staining for C-FABP expression observed in malignant carcinoma (red arrows), however, no staining was observed in adjacent areas of BPH (black arrows).
(**c**) The greater part of staining was observed in the cytoplasm of cells (red arrows), however, nuclear staining was also observed in some cells (black arrows).
Magnifications: a, and b, x 120; c, x 400

3.2.2 Discussion

This study reported differential expression of C-FABP in normal benign and prostatic carcinoma tissue. Normal prostate tissue failed to express C-FABP at a detectable level, whereas BPH tissue and prostatic carcinomas demonstrated weak to strong levels of C-FABP expression respectively as judged by immunocytochemical staining for C-FABP expression. This result is in keeping with previous studies reporting C-FABP over expression in bladder and pancreatic cancer (Celis *et al.*, 1999; Ostergaard *et al.*, 1997; Sinha *et al.*, 1999), cutaneous melanoma (Brouard *et al.*, 2002) and basal and squamous cell carcinomas (Masouye *et al.*, 1996). Absence of detectable levels of C-FABP in normal prostate tissue, relative to increased levels of expression in BPH and prostatic carcinomas suggests a relationship between prostate cancer progression and rising levels of C-FABP expression.

Gleason grading of prostate cancer cells is a semi-quantitative system that enables pathologists to categorise the morphological appearances of prostate cancer tissues, and allows prostate cancer prognosis to be based on prostate cancer morphology relative to normal prostate tissues. Well-differentiated prostate cancers (Gleason grades 1-2) resemble normal prostate gland with well-defined boundaries. Appearances within this scale are comparatively less aggressive than Gleason grade 3 prostate cancers. Grade 3 cells are the most commonly occurring type of prostate cancers and are characterised by less well-defined boundaries, and are considered to be moderately differentiated. Poorly differentiated cancers, typically comprise more aggressive cancer cells, and are characterised by poorly defined boundaries (Gleason grades 4 and 5).

Heterogeneity of prostatic carcinomas is commonly encountered by pathologists classifying tumour development, and can be countered by Gleason score values. Gleason score values are

the sum of the primary grade and the secondary grade, and is a number ranging from 2–10. The variation of staining observed in human prostatic tissue (Table 3.2.1) is an example of tissue heterogeneity.

Analysis of immunocytochemical staining for detection of C-FABP between Gleason grade samples 1-3 and grades 4 and 5 provided further evidence of C-FABP activity and action during prostate cancer progression. No significant changes were observed in levels of positive staining observed between samples of Gleason grade 1 – 3 and grades 4 and 5. This lack of difference observed between grades 1-3 and grades 4 and 5 prostatic carcinomas suggest that C-FABP activity is involved in tumour onset. However, lack of quantifiable differences in staining intensity of C-FABP observed in moderate to poorly differentiated tumours suggest that the C-FABP sphere of influence may be limited to malignant progression from a benign to a metastatic state, and may not influence the degree of tumour malignancy.

These deductions are in keeping with previous experimental findings by Jing *et al*, (2000b) who used microquantity differential (MDD) display to show that cutaneous fatty acid binding protein was over-expressed in breast and prostatic carcinoma cells when compared to normal prostate tissue (Jing *et al.*, 2000b). Furthermore, transfection of benign non-metastatic rat mammary cell lines, Rama-37, with C-FABP generated single-cell-cloned transfectant cells with over-expressed C-FABP activity. Inoculation of these transfectant cells into syngeneic Wistar-Furth rats produced significant numbers of metastases (Jing *et al.*, 2000c). This highlights the importance of C-FABP in malignant progression of prostate cancer from a benign state to a metastasising phase. A successive increase in C-FABP expression from normal through BPH to prostatic carcinoma indicates that C-FABP expression is limited to tumour development, progression and metastasis.

3.3 GENERATING ANTISENSE TRANSFECTANT CELLS WITH REDUCED C-FABP EXPRESSION

3.3.1 Introduction

A cDNA fragment of the protein-coding region of C-FABP was inserted into pSV-Neo plasmid in reverse orientation to form a plasmid construct expressing a reverse C-FABP transcript. This construct was transfected into highly malignant prostate cancer cell line, PC3M, to generate several single-celled-cloned transfectant cell lines expressing reduced levels of C-FABP. Control transfectant cells consisting of plasmid DNA alone, and pool of transfectants were also generated (Table 3.3.1).

Table 3.3.1 Nomenclature of transfectant cell lines

Cell line	Transfection protocol	Transfectant cell line nomenclature
PC3M	None	Parental PC3M
PC3M	pSV-neo plasmid	Control transfection (PC3M-pSV)
PC3M	Reverse C-FABP fragment in pSV-neo	Antisense transfectant clones 1–5 (PC3M-C-FABP 1–5)
PC3M	Pool of transfectants	Transfectant pool (PC3M-C-FABP-P)

Table 3.3.1 Nomenclature of transfectant cell lines.

This table shows the adopted nomenclature of PC3M cells following transfection.

3.3.2 Western Blot analysis of antisense transfectant cells for C-FABP expression

The level of C-FABP expression in parental PC3M, control transfection, pool of transfectants, and transfectant clones 1-5 was assessed using laboratory optimised Western Blot analysis (Figure 3.3.2). C-FABP expression of antisense transfectant cells were quantified relative to control transfectant cells using scanning densitometry.

No significant difference in C-FABP expression was observed between control transfectant cells and PC3M cells (Students t-test $P>0.05$). However, levels of C-FABP expression in pool of transfectants, and antisense transfectant clones 1-5 was significantly reduced (Students t-test $P<0.05$) by 59%, 74%, 29%, 85%, 77% and 45% respectively when compared to the expression of C-FABP in PC3M cells. Based on these findings, antisense transfectant clone 1 and 3 was used for further testing.

3.3.3 Southern Hybridisation of Antisense transfectant cells reverse-C-FABP and pSV-Neomycin expression

A southern hybridisation assay was performed to probe for pSV-neomycin and antisense C-FABP sequence in PC3M cells in order to confirm that silencing was due to antisense oligonucleotides and not an artefact.

Southern hybridisation assay did not detect neomycin gene expression in parental PC3M cells; whereas control and antisense clones 1 and 3 transfectants expressed positive neomycin expression (Figure 3.3.3a). Hybridisation of the same samples to reverse C-FABP transcript probes produced positive expression results for each of the samples (Figure 3.3.3b). However, signal intensity was 1.5 times stronger in transfectant pool cells compared to parental and control transfectant cells. Similarly, signal intensity for C-FABP expression in antisense clone 1 and

clone 3 cells was two fold and three fold stronger respectively than parental PC3M and control transfectant cells.

3.3.4 Northern Hybridisation of antisense transfectant cells for expression of VEGF mRNA

VEGF expression was observed in all cells. However, antisense transfectant cell clones 1 and 3 were significantly reduced to 0.41± 0.03 and 0.40 ± 0.04 (Students t-test $P<0.05$) relative to control transfectant cells. This represented a 2.5-fold reduction of VEGF expression in antisense transfectant cells relative to control transfectant cells (Figure 3.3.4a and 3.3.4b). Using scanning densitometry, the control transfectant was set as 1 and the relative intensity of the other cells lines were expressed as percentages to the control.

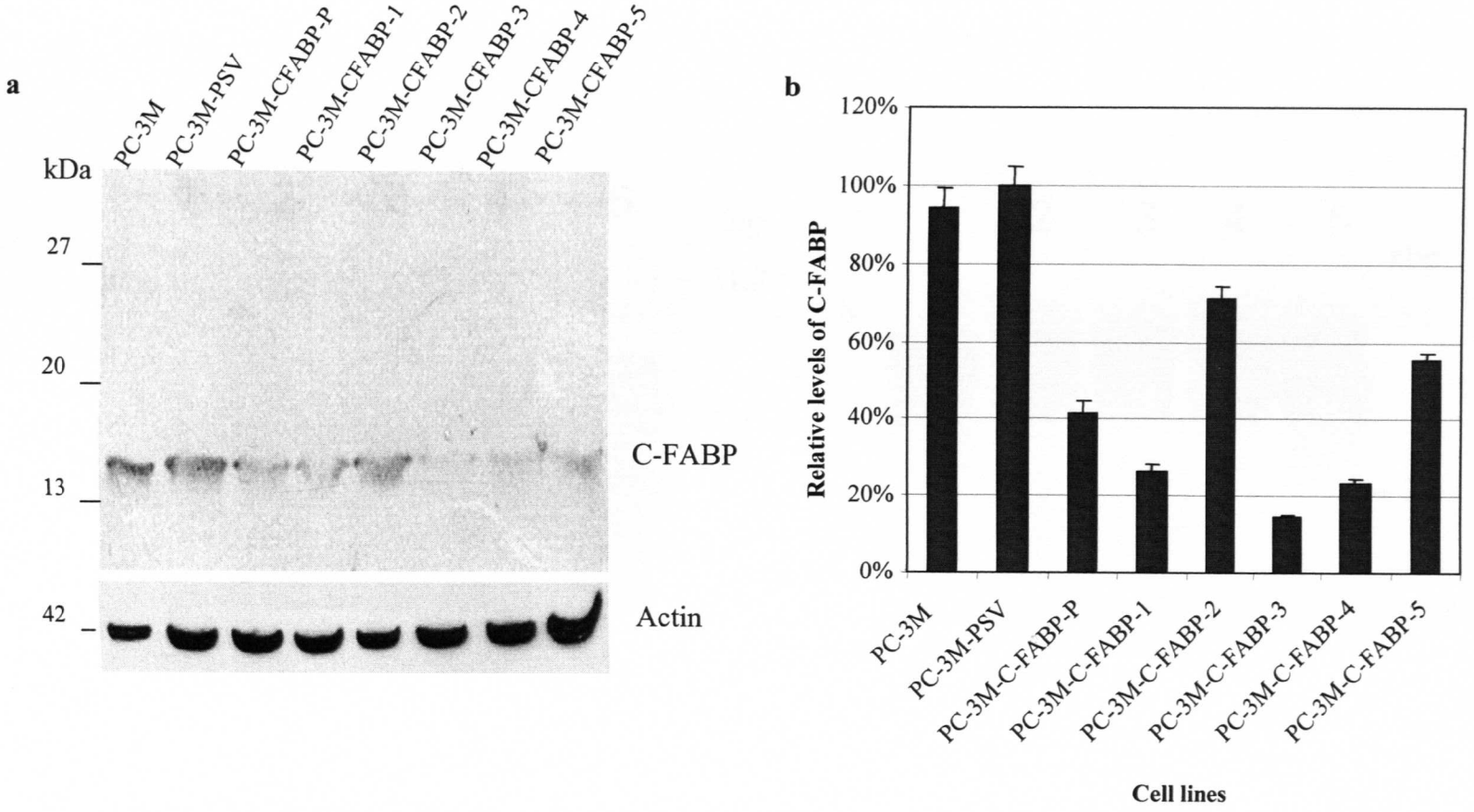

Figure 3.3.2 Expression of CFABP in antisense transfectant cell lines. (**a**) The Level of CFABP expression in antisense transfectant cell lines is assessed relative to parental PC3M and control transfectant cells. CFABP protein is found at 15kDa, whereas actin is found at 42kDa. (**b**) Relative levels of CFABP expression quantified by scanning densitometry. Actin expression is used to standardise any errors in sample loading, enabling accurate quantification of CFABP expression.

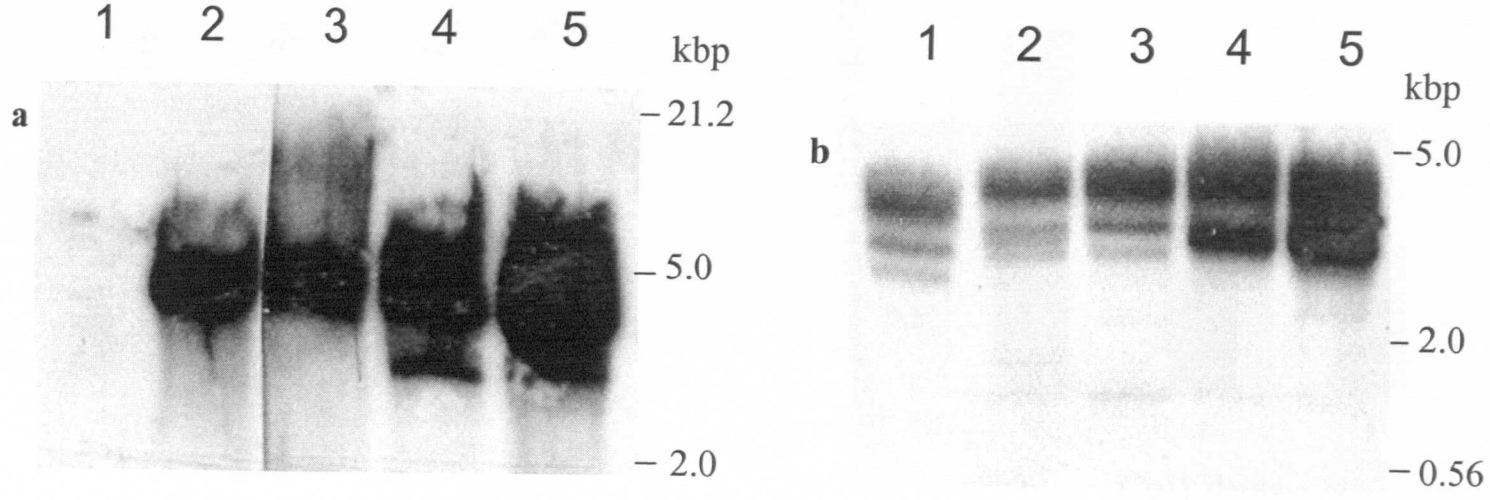

Figure 3.3.3 Southern hybridisation for detection of Neomycin and antisense C-FABP DNA in transfectant cells. DNA is extracted from each cell line and digested using HindIII restriction enzyme, transferred onto a nylon membrane and hybridised to *Neomycin* resistance gene probe (**a**) and CFABP gene probe (**b**). Parental PC3M (lane 1), control transfectant (lane 2), antisense transfectant pool (lane 3), and antisense transfectant clones 1 and 3 in lanes 4 and 5 respectively.

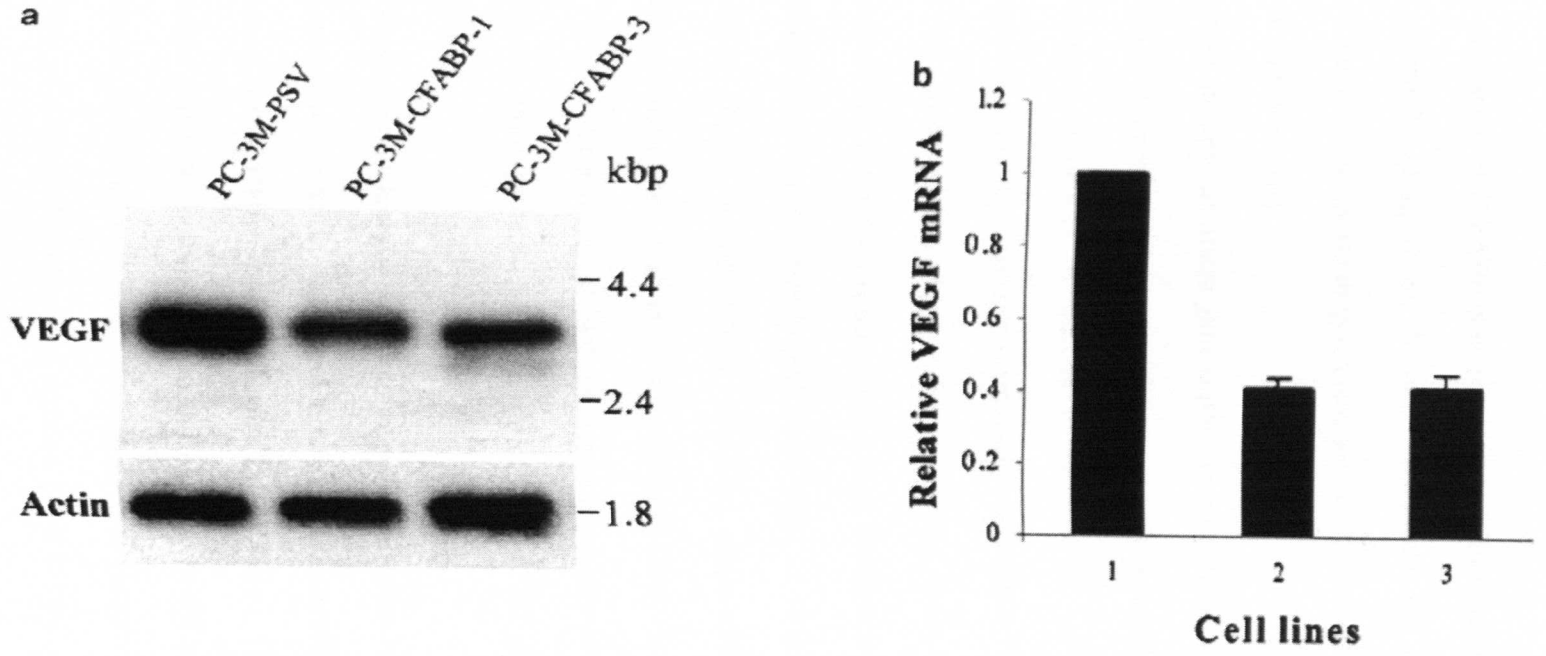

Figure 3.3.4 Expression of VEGF in antisense transfectant cell lines

(**a**) RNA was extracted from cell lines, electrophoresed on a denaturing formaldehyde- agarose gel, transferred to a nylon membrane and hybridised to radio-labelled VEGF and actin [32]dCTP cDNA probe. Following a stringent washing process, the membrane is left to expose to Kodak XAR-5 film for 72 hours for VEGF and 24 hrs actin. (**b**) The relative expression of VEGF in antisense transfectant cells to control transfectant cells were measured by scanning densitometry using a constitutively expressed actin probe. This enables standardisation of loading errors, enabling accurate measurements of the levels of reduction observed

3.3.5 Discussion of antisense technology

Over expression of C-FABP was observed to induce metastasis in non-metastatic rat mammary cells, Rama-37 (Jing *et al*, 2000a). To assess the role of C-FABP in prostate cancer tumourigenicity, antisense oligonucleotides of the protein-coding region of C-FABP was used to suppress gene activity.

Antisense therapy facilitates gene suppression through introduction of antisense oligonucleotide constructs that are homologous to the target gene in a cell model. The oligonucleotides bind to homologous sequences of mRNA to form DNA : RNA hybrids that initiate RNase H endonuclease activity, causing degradation of mRNA nucleotides and leaving the antisense construct intact and embedded within the mRNA chain. The insertion of a reverse orientated segment within the mRNA reading frame stops translation and ultimately, protein expression.

Antisense silencing is typically performed using 15 to 20 nucleotide long sequences to ensure specificity (Green *et al.*, 2000), however, oligonucleotide sequences as short as seven nucleotides have been used to initiate antisense silencing via RNase H degradation (Wagner *et al.*, 1996). As a result of high sequence homology shared between members of the FABP family, the entire protein-coding region of the C-FABP gene was used to synthesise a silencing construct.

Antisense oligonucleotides have had to overcome some limitations inherent with the transfer of exogenous nucleic acids. Such problems included premature degradation of oligonucleotides by nucleases before DNA : RNA formation could occur. This was tackled by making changes to the sugar and base moieties and to the phosphodiester backbone structure, however, the most successful modification was the development of phosphorothioates which increased the serum stability of oligonucleotides, and enabled them to maintain their hydrogen bonding ability to

mRNA and retain the ability to initiate RNase H activation and reduce indiscriminate nuclease digestion (Green *et al.*, 2000; Rubenstein *et al.*, 2002). Another problem facing researchers was a lack of sufficient quantities of oligonucleotides as a result of poor transfection efficiency and nuclease degradation. To compensate for this, many researchers used large concentrations of oligonucleotides. However, this fix was not without its own problems since mega doses of oligonucleotides, especially those modified with phosphorothioates, produced cytotoxic effects not attributable to antisense silencing (Green *et al.*, 2000). To combat this, oligonucleotides are typically contained within expression vectors, and transfected into cells using lipid-based protocols.

Antisense oligonucleotides have proven to be valuable tools in cancer research. The reported success of gene suppression studies in prostate cancer and other forms of cancer serve to highlight the robust nature of the technique in silencing a wide variety of genes. Equally, antisense technology was used successfully within the first section of this study to significantly reduce levels of C-FABP expression in highly malignant PC3M cells.

Antisense is a mature and established form of gene silencing whereas siRNA is in its infancy and will have to deal with its own inadequacies in years to come. As with all experiments, it is always best to choose the most appropriate method on a case-by-case process (Achenbach *et al.*, 2003).

3.3.6 Discussion of Southern Blot assay for pSV-Neo and C-FABP DNA expression

To ensure that suppression levels observed at the protein level were a direct result of antisense transfection, Southern hybridisation was conducted to assess pSV-neo DNA and antisense C-FABP in parental PC3M, control transfectant, transfectant pool and antisense transfectant cell lines.

No bands were present in parental PC3M cells, since they had not been transfected with the neomycin gene. Cells from the control and transfectant pools showed a strong level of pSV-Neo expression. However, both antisense transfectant cells demonstrated the highest intensity of neomycin gene expression. A 1.5-fold increase in pSV-Neo gene expression was observed in pool of transfectant cells relative to parental PC3M cells. A 2.0-fold and a 2.5-fold increase in pSV-Neo expression were observed in antisense transfectant cells PC3M-C-FABP 1 and 3 respectively compared to control transfectant cells.

Analysis of Southern hybridisation results for C-FABP expression in the same cell lines showed a positive expression of C-FABP in all samples. Differential expression of C-FABP was observed in transfectant pool cells (2.5-fold increase), with antisense transfectant cells PC3M-C-FABP 1 (3.9-fold) and PC3M-C-FABP-3 (6.9-fold) relative to control transfectant cells. This suggests a link between antisense C-FABP signal strength and quantifiable C-FABP gene suppression such that, the greater the antisense C-FABP expression, the greater the degree of silencing in transfected cells. This is expected as both antisense transfectant cell lines already contain a normal single copy of this gene. Therefore, additional integration of the antisense C-FABP construct within the genome result in a higher copy number of the C-FABP gene and subsequently, a stronger expression of antisense C-FABP.

3.4 *IN VITRO* ASSAYS FOR ANTISENSE TRANSFECTANT CELLS

3.4.1 Invasive potential of antisense transfectant cells

The rate at which antisense transfectant cells migrate through an extra cellular matrix and invade across a basement membrane is an indication of their metastatic potential. Comparison of metastatic potential of antisense transfectant cells relative to control transfectant cells was measured in a modified Boyden chamber over a fixed period of time (Figure 3.4.1). Migration of antisense transfectant clones 1 and 3 were significantly reduced to 7% ± 0.6% and 7% ± 1.2% respectively, when compared to pSV-PC3M control transfection (14% ± 3.8%) (Students t-test <0.05). This represented a 50% reduction in antisense transfectant clones 1 and 3 cell migration relative to control transfectant cells.

Cell proliferation assays and cell morphology comparisons between the pSV-PC3M control transfectants and antisense transfectants were also performed, although no significant differences were observed.

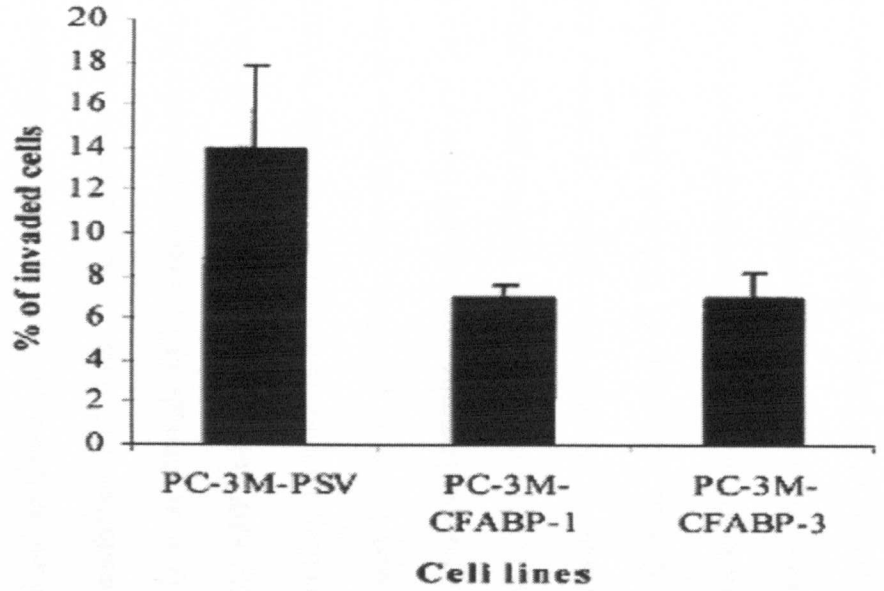

Figure 3.4.1 Invasion assay of antisense clones 1 and 3 transfectant cells *in vitro*. The invasive potential of the antisense transfectant cell lines was measured relative to control transfectant. The percentage of cells able to migrate through an extracellular matrix was assessed in three separate experiments. Analysis of the results show a significant reduction (Students T-test $P<0.05$) in invasive potential of antisense transfectant cells relative to control transfectant cells.

3.4.2 Discussion

Control and PC3M-C-FABP 1 and 3 antisense transfectant cell lines were used in an invasion assay to assess their *in vitro* invasive potential by measuring cell migration through an extracellular matrix (ECM). The data demonstrated a significant difference in the percentage of migrating cells between control and antisense transfectants 1 and 3, although none was observed between the two antisense transfectant cell lines. The similarities of migratory values of antisense transfectant cells migrating through ECM suggest that other signalling pathways existing outside the sphere of C-FABP influence may be involved in cell metastasis. This other pathway may still be active, enabling comparable levels of cell motility in antisense transfectant cells with differentially expressed levels of C-FABP. One possible pathway is the PPAR signalling pathway. PPAR is a nuclear hormone receptor, and functions as a ligand activating transcription factor. When bound to its fatty acid ligands, PPAR-α forms a heterodimer complex with retinoid-x-receptor to regulate target gene transcription. Antisense transfectant 3 cells demonstrated a 1.8-fold reduction in expression of C-FABP proteins relative to antisense transfectant-1 cells. Comparable levels of invasion were observed in antisense transfectant cells 1 and 3, indicating the involvement of a possible compensatory factor. This type of phenomenon has been commented upon by Owada *et al*, (2002) who observed a compensatory mechanism resulting in up-regulation of cardiac-fatty acid binding protein to compensate for suppressed C-FABP activity in C-FABP homozygous deleted mice.

Additionally, transforming growth factor-beta (TGF-β) has been implicated in mediation of cellular adhesion and motility (Shi and Massague, 2003). TGF-β receptor binding initiates signal transduction pathways that enable transduction of extra-cellular signals to the nucleus of cells to

regulate cellular proliferation and motility. Studies have demonstrated that TGF-β mediated increases in cellular adhesion in human prostate are dependent on Smad3 protein expression via the p38 mitogen activated protein kinase (MAPK) pathway (Hayes *et al.*, 2003), and that MAPK signalling is necessary for TGF-β-mediated up-regulation of matrix metalloproteinase-2 (MMP-2), and TGF-β dependent increases in prostate cancer invasion (Huang *et al.*, 2005). This suggests that tumour cell autocrine or paracrine growth factor signalling through the MAPK signalling pathway may enable tumour cells with reduced C-FABP expression to maintain an invasive phenotype. Consequently, C-FABP suppression may only have a partial effect on inhibiting the invasive potential of a cell.

3.5 *IN VIVO* ASSESSMENT OF TUMOURIGENIC POTENTIAL OF ANTISENSE TRANSFECTANT CELLS

3.5.1 Antisense transfectant cell tumourigenicity *in vivo*

To study the role of C-FABP in malignant progression of prostate cancer, control and antisense transfectant cells PC3M-C-FABP-1 and PC3M-C-FABP-3 were inoculated subcutaneously into the shoulder region of 8-week-old ICRF male immuno-compromised nude mice. Twenty-four of these mice were divided into three groups of eight and inoculated with $5x10^6$ cells/0.2ml PBS of control transfectant cells for group 1, antisense clone 1 cells for group 2 and antisense clone 3 cells for group 3. The incidence of tumours occurring in this model is presented in Table 3.5.1. Inoculation of control transfectant cells into mice produced 8/8 (100%) tumour incidences within a 3 - 4 day period after inoculation. Antisense clone 1 transfectant cells also produced 8/8 (100%) tumour incidence at a period of 3 – 7 days after inoculation, whereas, antisense clone 3 transfectant cells produced a 6/8 (75%) tumour incidence at a period of 3 – 9 days after inoculation.

Antisense clone 1 and clone 3 transfectant cells produced significantly reduced mean tumour volumes after 6 weeks, 524 $\pm 89mm^3$ and 356 $\pm 101mm^3$ respectively compared to control transfectant 1495 $\pm 295mm^3$. This represents a 2.9 - fold and 4.2 - fold reduction in mean tumour volumes for antisense transfectant clones 1 and 3 cells respectively (Figure 3.5.1).

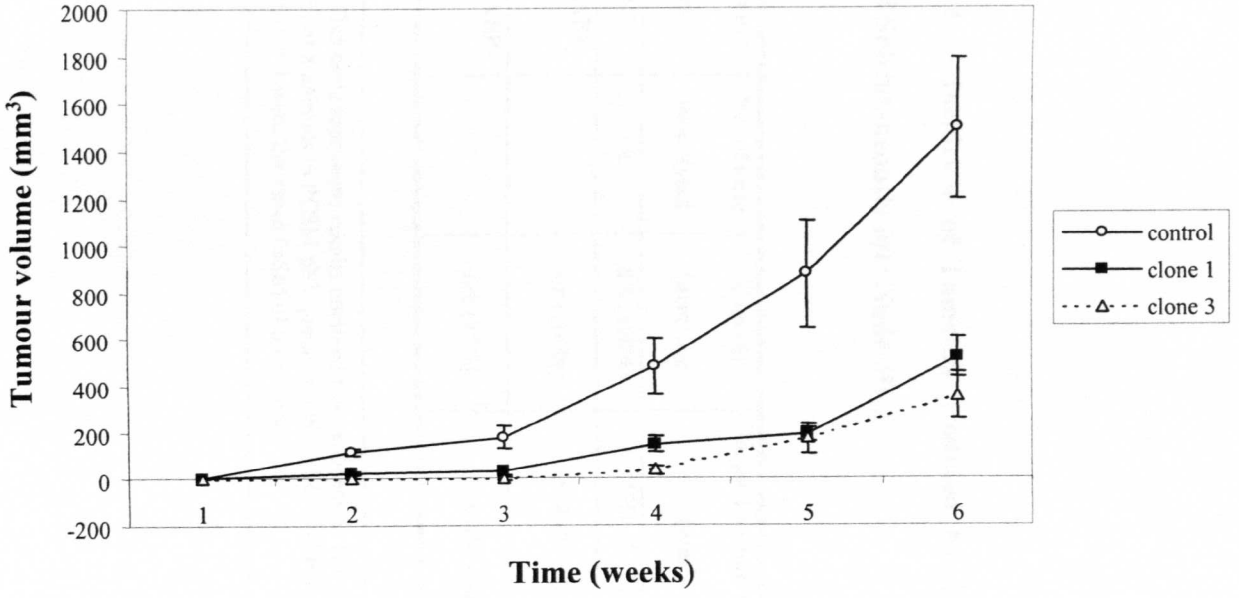

Figure 3.5.1 Tumourigenicity of antisense transfectant cells *in vivo*
Control and antisense clones 1 and 3 transfectants were inoculated subcutaneously into the shoulder fat pad of 3 groups of 8 male ICRF immunocompromised nude mice. A 100% tumour incidence is observed in control and antisense clone 1 transfectant groups, and a 75% tumour incidence rate in antisense clone 3 transfectants. At autopsy, 6 weeks, mean tumour volume is significantly larger in control transfectant cells compared to antisense transfectant cells (Students t-test $P<0.01$). There is also a significant difference in mean tumour volume between the two antisense cell lines (Students t-test $P<0.05$).

Table 3.5.1. – Incidence of Tumours produced by Antisense Transfectant Cell Lines Inoculated Subcutaneously into Nude Mice

Transfectant Cell lines	No. of mice inoculated	Tumour incidence	Mean Tumour Volume (mm^3)	Median latent period in days (range)
PC3M-pSV	8	8/8 (100%)	1495±295 (mm^3)	3.5 (3-4) days
PC3M-C-FABP-1	8	8/8 (100%)	524±89 (mm^3)	5 (3-7) days
PC3M-C-FABP-3	8	6/8 (75%)	356±101 (mm^3)	6 (3-9) days

Table 3.5.1. This table represents results obtained from antisense. The results shown were the mean tumour volumes (±SE) of 8 animals in PC3M-pSV group and PC3M-C-FABP-1 groups respectively, whereas those of PC3M-C-FABP-3 were the mean (±SE) of 6 animals.

3.5.2 Discussion

Subcutaneous inoculation of antisense transfectant cells into male immuno-compromised nude mice demonstrated noteworthy reductions in tumour incidence and tumour volume relative to the control group. This suggests that the tumour formation pathway is sensitive to C-FABP expression signalling and that suppression of C-FABP activity in highly malignant PC3M cells significantly reduces tumourigenicity of prostate cancer cells *in vivo* in relation to the control group.

The extent of C-FABP function can be inferred by the latency period of tumour development observed in antisense transfectant cells. The control transfectant cell line produced 100% tumour incidence in 3-4 days. The antisense PC3M-C-FABP 1, which demonstrated a 58.8% reduction in C-FABP expression at the protein level, also produced 100% tumour incidence within 3-7 days. The PC3M-C-FABP-3 antisense transfectant produced a 75% tumour incidence within the range of 3-9 days. A 3.8-fold difference in level of C-FABP protein expression in control and PC3M-C-FABP-1 transfectant cell lines was observed. However, in tumour latent period, this equates to a 3-day lag time for development of tumours in antisense PC3M-C-FABP-1, and no difference in tumour incidence.

The antisense transfectant cells, PC3M-C-FABP-3, had a 6.9-fold reduction in C-FABP protein expression relative to the control transfectant cells, resulting in a 25% reduction in tumour incidence. When compared to the antisense transfectant cell, PC3M-C-FABP-1, protein expression of C-FABP in PC3M-C-FABP-3 was reduced 1.8-fold and still produced a 25% reduction in tumour incidence. In addition, antisense transfectant PC3M-C-FABP-3 cells had a greater lag time to tumour incidence than control, and antisense transfectant PC3M-C-FABP-1

cells. These comparisons suggest that there is a threshold level of C-FABP expression that is sufficient to produce 100% tumour incidence in subjects. An increase in C-FABP expression above this threshold level, regardless of the amount of increase, would not be directly proportional to the tumour cells phenotype. This threshold limit is supported by results obtained by immunohistochemical staining for detection of C-FABP in Gleason grade samples 1-3 and grades 4 and 5 classified tissues discussed in Section 3.2. Those results demonstrated differential C-FABP expression among normal, BPH and prostatic carcinoma tissues. However, similar levels of C-FABP expression was observed between Gleason grade samples 1-3 and samples 4 and 5 classified tumours (Adamson *et al.*, 2003).

3.6 IMMUNOCYTOCHEMICAL STAINING FOR C-FABP, VEGF, AND FACTOR VIII-RELATED ANTIGEN

At 6 weeks, all mice were sacrificed. Primary tumours were extracted and fixed in 10% formalin in order to perform immunocytochemical staining of tumour samples. Immunocytochemical staining assessed primary tumours from animals from each group to detect C-FABP expression (Figure 3.6a). The data revealed strong staining for C-FABP in the control transfection cell sample, whereas groups 2 and 3, which had the mid level and lowest expression of C-FABP showed moderate to weak positive staining respectively.

This same pattern was repeated when samples were stained for expression of VEGF (Figure 3.6b). Primary tumour samples were also stained for Factor VIII-related antigen to assess microvessel density and angiogenic activity. A microvessel was defined as the presence of three or more adjacent Factor VIII-related antigen-expressing cells. The vessel numbers were recorded from 50 high-powered-fields (hpf) (x5) of 2.5 x 1.75mm. In each section, 10 random fields were counted and the mean number of vessels per hpf (mean ± SE) were calculated from all animals containing tumours in each group. Antisense transfectant cell derived tumours revealed moderate to weak staining respectively when compared with staining achieved by control transfectants. Average number of blood vessels per high-powered field (HPF) in antisense transfectant 1 and 3 derived tumours was 4.7±0.5 and 3.7±0.4 respectively compared to the control transfectant group (11.0 ±0.7) (Students t-test $P<0.05$) (Figure 3.6c). If micro-vessel count control transfectant derived tumours was set at one, the relative density of antisense transfectants 1 and 3 was 0.43 ± 0.1 and 0.34 ± 0.08, respectively.

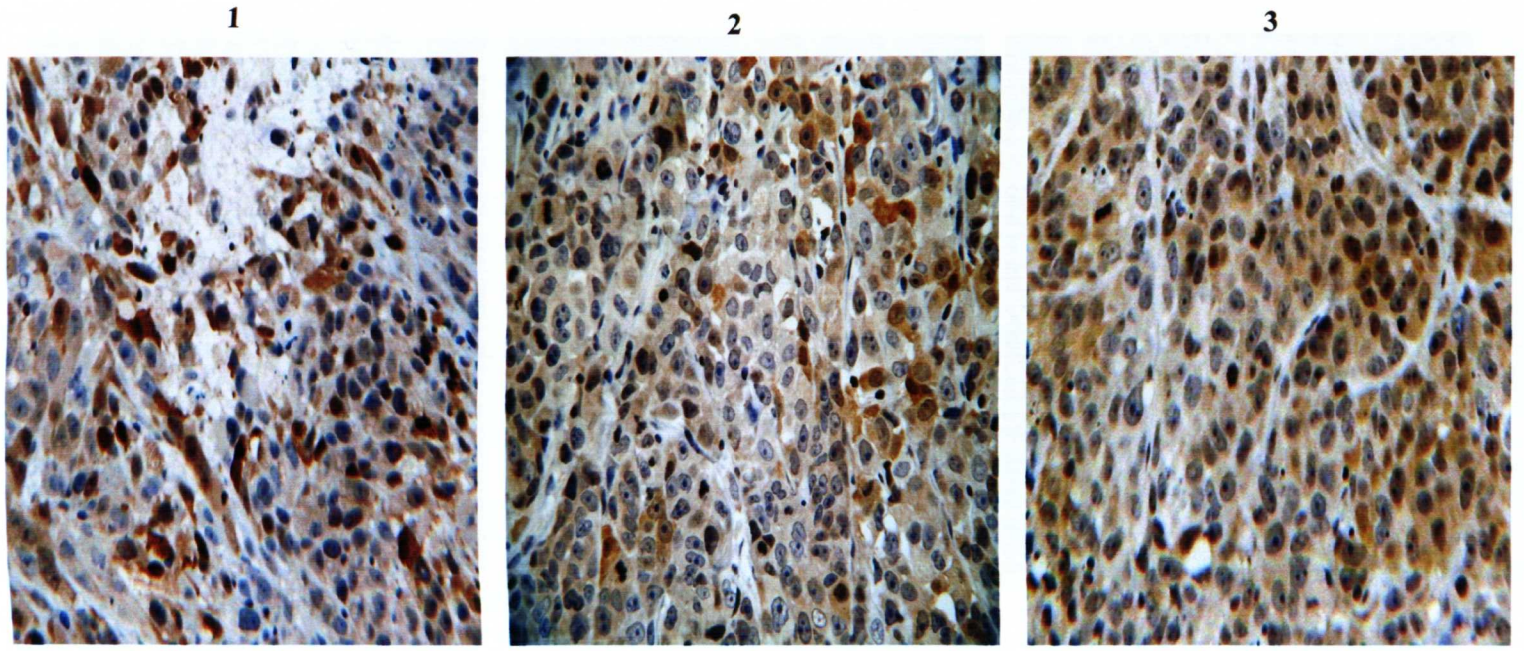

Figure 3.6a. Immunocytochemistry for detection of C-FABP protein expressed in nude mice tumours. **1,** this sample is derived from mice inoculated s.c. with control transfectant cells, PC3M-pSV. **2,** this sample is derived from transfectant cells, PC3M-CFABP-1cells, and (**3**) is from mice inoculated with PC3M-CFABP-3 cells.
Original magnification x400

1 2 3

VEGF antibody

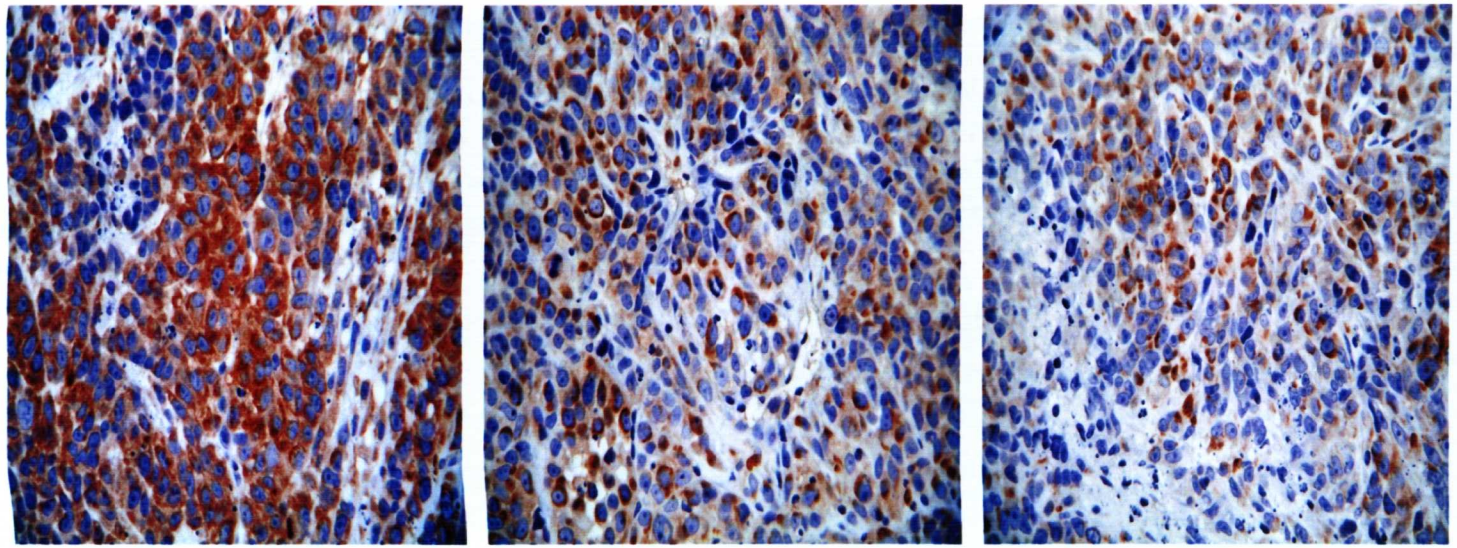

Figure 3.6b. Immunocytochemistry for detection of VEGF protein expressed in nude mice tumours. **1,** this sample is derived from mice inoculated s.c. with control transfectant cells, PC3M-pSV. **2,** this sample is derived from transfectant cells, PC3M-CFABP-1 cells, and (**3**) is from mice inoculated with PC3M-CFABP-3 cells.
Original magnification x400

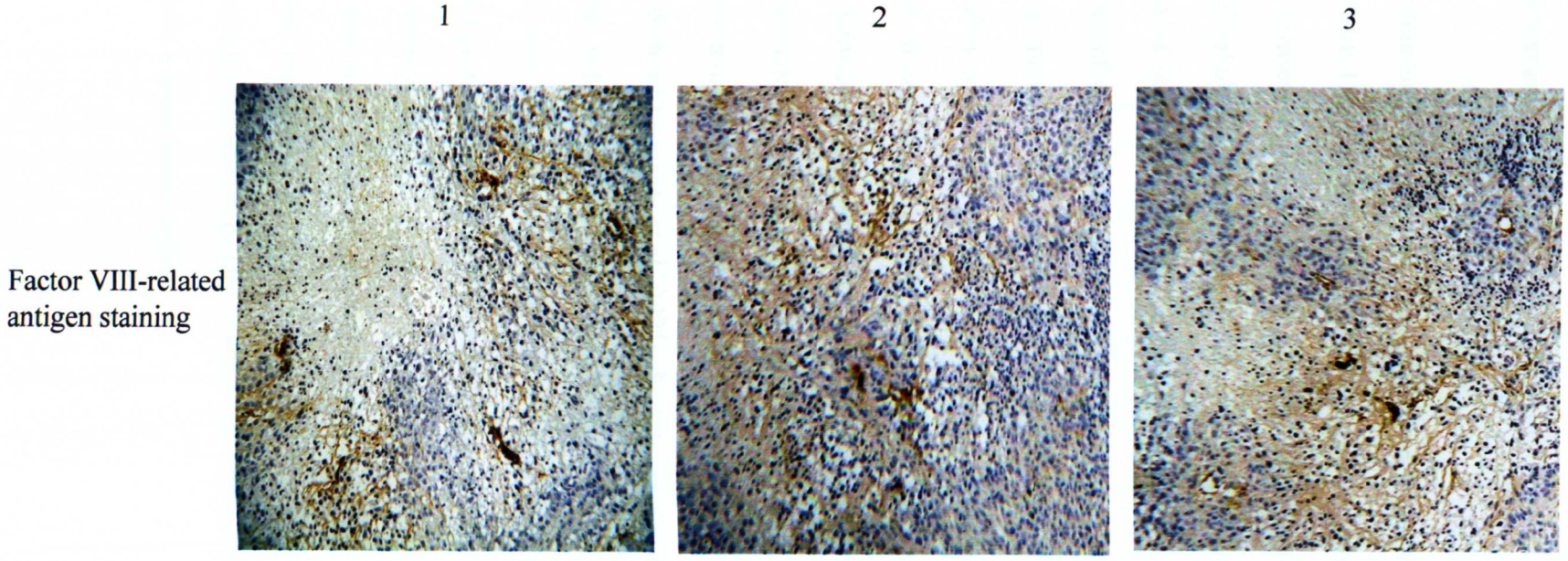

Figure 3.6c. Immunocytochemistry for detection of factor VIII-related antigen expressed in nude mice tumours. **1,** this sample is derived from mice inoculated s.c. with control transfectant cells, PC3M-pSV. **2,** this sample is derived from transfectant cells, PC3M-CFABP-1 cells, and (**3**) is from mice inoculated with PC3M-CFABP-3 cells.
Original magnification x50

3.6.2 Discussion

Primary tumours obtained from mice inoculated with control and antisense PC3M-C-FABP-1 and PC3M-C-FABP-3 transfectant cells were dissected and subjected to immunohistochemical staining to assess their levels of C-FABP, VEGF and Factor VIII-related antigen expression. The results show a differential expression of C-FABP, VEGF and Factor VIII-related antigen for detection of microvessel density in the three groups. The largest tumours had the greater expression of C-FABP (Figure3.6a) and VEGF (Figure 3.6b), and upon analysis, a higher number of microvessel density formation (Figure 3.6c). This relationship has been observed in other studies which reported that VEGF expression was significantly higher in prostate cancer cells than in non tumour adjacent cells, and resulted in a significant increase in micro vessel density (Ding *et al.*, 2005a). Another study reported that suppression of all known isoforms of VEGF with siRNA plasmid constructs demonstrated a significant reduction of VEGF expression in human prostate cancer cell line PC-3, resulting in a loss of tumour growth and neo-vascularisation (Wannenes *et al.*, 2005). Results reported within this Thesis revealed that VEGF expression and microvessel density are regulated in part by C-FABP expression. Furthermore, C-FABP over expression in benign non metastatic rat mammary cell lines were observed to induce a significant number of metastasis in Wister-Firth rats (Jing *et al.*, 2001). Masood *et al*, (2001) reported that VEGF not only supplied an independent network of blood vessels for growth and development of primary tumours, but also aided in metastasis. Consequently, differential expression of VEGF and Factor VIII-related antigen in tumours derived from antisense transfectants is regulated by C-FABP expression, and actual physiological demand of tumours for a stable blood supply.

A 2.5-fold reduction in VEGF expression was observed in antisense transfectant cells relative to control transfectant cells in mRNA. Immunohistochemistry of VEGF expression in tumour tissues observed differential expression of VEGF activity between antisense transfectant 1 and 3 cells. However, this relationship did not extend to the mRNA level. The findings suggest that the level of C-FABP expression was not directly proportional to the level of VEGF. Instead, a threshold effect was observed by which reduced levels of C-FABP exceed an optimum level at which maximal down regulation of VEGF expression occurs, and further reduction of C-FABP does not result in continued reduction of VEGF expression. At this point, the regulatory role of C-FABP on VEGF expression reaches saturation point and is unable to further reduce VEGF expression.

Suppression of C-FABP reduces VEGF expression and microvessel density. These findings suggest that over expression of C-FABP, as now reported in prostatic tissues, governs tumour growth and metastasis through up-regulation of VEGF expression. Additionally, VEGF promotes prostate cancer progression through angiogenesis, and can also promote tumourigenicity by acting as an autocrine growth factor (Masood *et al.*, 2001). Increased VEGF expression increases neovascularisation within tumours, enabling the process of malignant progression.

3.7 siRNA RESULTS SECTION

3.7.1 Measurement of protein levels of C-FABP expressed in siRNA transfectant cell clones

In the second group of experiments, C-FABP gene silencing was performed by siRNA to generate several single cell cloned transfectants with reduced C-FABP expression. A Western blot was used to measure C-FABP expression in siRNA transfectants relative to parental PC3M cells, and quantified using scanning densitometry analysis (Figure 3.7). A significant reduction (Student t-test <0.05) in C-FABP expression was observed in siRNA transfectants. Compared to parental PC3M cells, PC3M-2 transfectant cells had a 29% reduction, whereas PC3M-3, 5, and PC3M-6 siRNA transfectant cells showed a 99.9% reduction, 44% and a 31% reduction in normal C-FABP expression. As a result of these findings, PC3M-2 and PC3M-3 were used in future assays.

3.7.2 Measurement of mRNA levels of C-FABP in parental and siRNA transfectant cell clones

Northern hybridisation was performed to assess C-FABP expression levels in parental and siRNA transfectant cell lines (Figure 3.8). All cells lines positively expressed C-FABP activity as assessed by scanning densitometry analysis. Additionally, siRNA transfectant cells demonstrated reduced C-FABP expression relative to parental PC3M cells. A 1.1 fold reduction, 9.5 fold reduction, and a 1.5 fold reduction was observed in PC3M-2, 3 and 6 siRNA transfectant cells respectively compared to PC3M levels of C-FABP expression. If the level of C-FABP in

PC3M is set at 1, the relative C-FABP expressions in siRNA PC3M2, 3 and 6 transfectants were 0.88, 0.105 and 0.65 respectively.

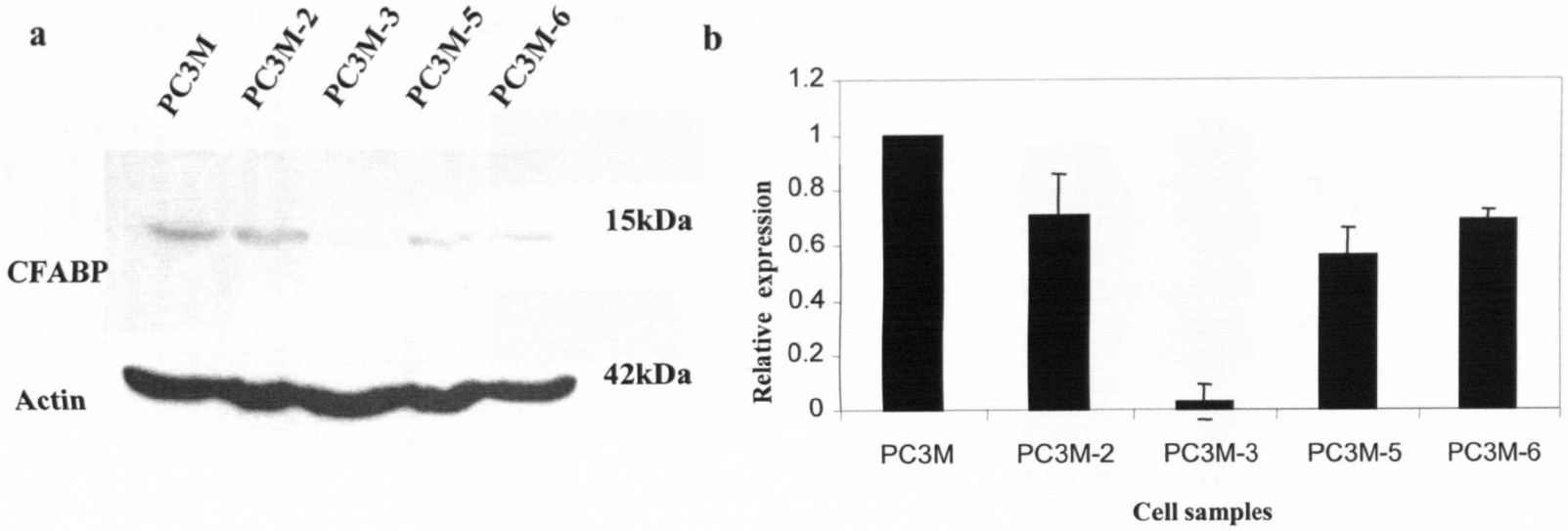

Figure 3.7.1. Measurement of protein levels of C-FABP expressed in parental PC3M and in different RNAi transfectant cell clones. **1a,** detection of C-FABP in control cells and in siRNA transfectant cell clones 1-4. Protein samples were extracted from each cell line and subjected to SDS-PAGE in 10% (w/v) polyarylamide gels, transferred by Western blotting and incubated with rabbit anti-C-FABP serum and then horseradish peroxidase-conjugated swine anti-rabbit immunoglobulin. The bound peroxidase was detected by ECL Western blot reagent kit using a light emitting non-radioactive method. The membrane was exposed to Kodak XAR-5 film for 1 minute. **1b,** Relative levels of C-FABP expressed in different cell lines. The level of C-FABP in control cells was set at 1.0, and the C-FABP levels in the siRNA transfectant clones were calculated by relating to that in the control. The possible loading errors were corrected by relating to amount of actin, and the results were shown as the mean (± s.e.) of three separate measurements.

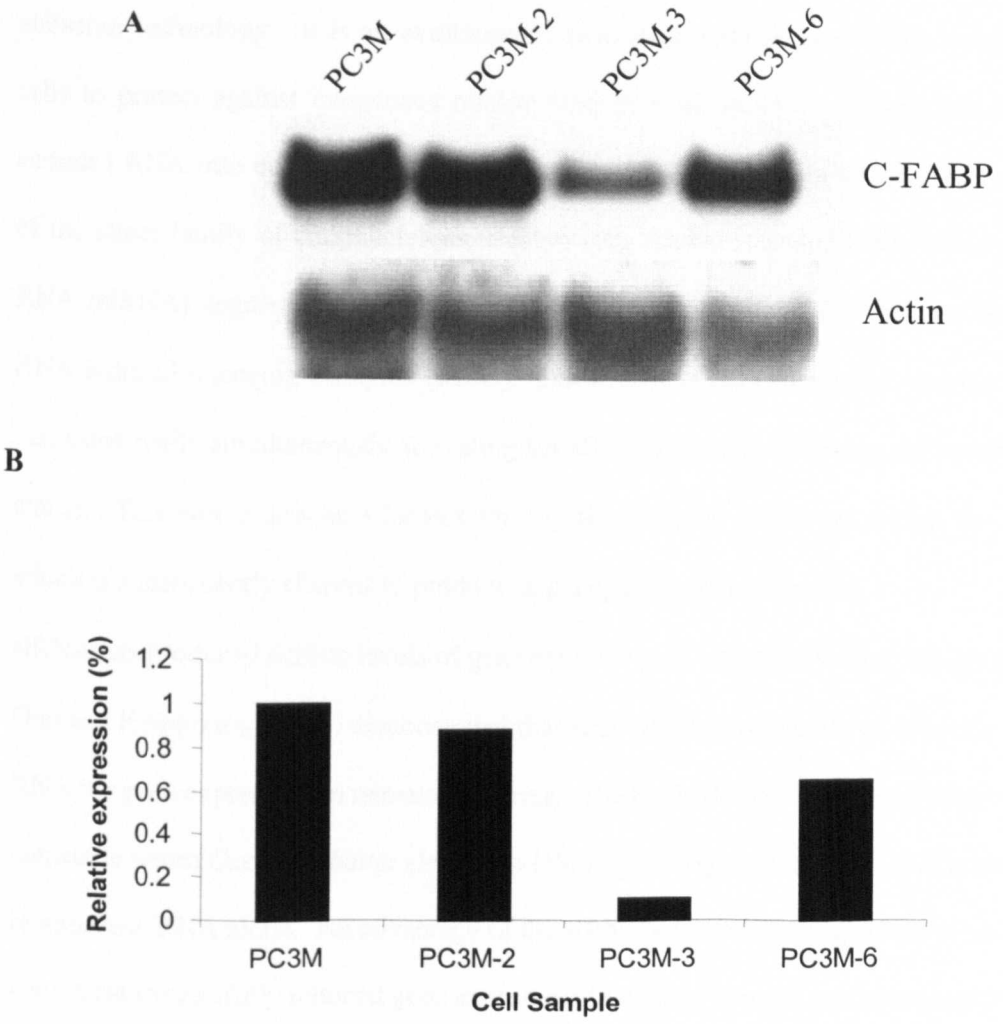

Figure 3.7.2 Measurement of mRNA levels of C-FABP expressed in parental PC3M cells and RNAi transfectant cell clones..

A. Auto radiography of Northern hybridisation for CFABP mRNA in parental PC3M and RNAi transfectant PC3M cell lines. Total RNA samples from each cell line (15μg) is electrophoresed under denaturing conditions, transferred to a nylon membrane and hybridised with [^{32}P]dCTP-labelled CFABP cDNA probe, washed and exposed to Kodak film and left to develop for 48hr. Radioactively labelled actin probe was also hybridised to membrane, washed and left exposed to Kodak film for 24hr.

B. Quantitative analysis of C-FABP and actin bands. Band intensity is measured by scanning densitometry in order to assess the relative level of C-FABP expression

3.7.3 Discussion of RNA Interference Technology

siRNA acts along similar principles of homologous sequence recognition and cleavage as antisense technology. It is an evolutionary conserved defence mechanism used by eukaryotic cells to protect against exogenous nucleic acid or viral attacks. Introduction of long double stranded RNA into eukaryotic cells initiates the siRNA pathway in which RNase III, a member of the Dicer family of endonucleases, cleaves long double stranded RNA into small interfering RNA (siRNA) segments approximately 21 – 23bp in length. siRNA are incorporated into an RNA Induced Silencing Complex (RISC). The double strand is unwound, and the sense strand is discarded while simultaneously activating the RISC complex containing the remaining antisense strand. This strand acts as a locator for any homologous sequences within the transcriptome, which is subsequently cleaved to produce target-specific gene silencing.

siRNA has produced similar levels of gene expression in a relatively short life span. A study by Guo and Kemphues, (1995) demonstrated that sense RNA was equally as effective as antisense RNA for gene expression in nematode worms. The methodology was successfully used in nematode worm *Caenorhabditis elegans* to inhibit gene expression by 10-fold relative to sense or antisense RNA alone. An advantage of the siRNA system is its versatility since silencing constructs successfully reduced gene expression in worms through gonad inoculation and feeding. Furthermore, exposure of parental animals to a few molecules of dsRNA produced systemic silencing in parental and F_1 progeny (Hannon, 2002). In this study, siRNA successfully suppressed C-FABP activity by 95% in an siRNA transfectant clone cell line. The wide use of siRNA as a form of studying gene function in a variety of cell models and diseases highlights the intellectual confidence and effectiveness of this protocol.

Antisense oligonucleotides and siRNA are both popular methods for inhibiting gene expression. They share many similarities in terms of their specificity and the degree of gene silencing that they achieve, however, siRNA is more favourable as it poses less limitations or requires less modifications for successful experimentation. It is more robust and is not affected by indiscriminate nuclease degradation. Furthermore, the growing use of lipid-based methods of transfection has increased efficiency of siRNA transportation into cells.

3.8 *IN VITRO* ASSAYS FOR siRNA TRANSFECTANT CELLS

3.8.1 Proliferation assay of siRNA transfectant cells

A proliferation assay was performed in parental PC3M and siRNA transfectant cell lines to determine whether suppressed C-FABP activity reinstated androgen sensitivity in androgen independent cells. To test this hypothesis, the proliferation rate of parental PC3M cells and siRNA transfectant cells was measured under two conditions: in the androgen positive condition, the cells were cultured in media supplemented with androgens, conversely in androgen negative condition, androgen supplementation was withheld (Figure 3.10.1).

A statistically significant difference in the proliferation rate of transfectant cells relative to parental PC3M cells was observed in androgen positive condition (Students T-Test $P<0.05$). In the second androgen negative condition, reduced growth rate of all transfectant cells relative to PC3M cells was observed, however, no statistically significant difference was observed in the proliferation rate of PC3M-3 and PC3M-6 siRNA transfectant cells relative to PC3M. Similarly, comparison of the rate of proliferation of the same cells between the two conditions did not produce any significant differences (Student t-test $P>0.05$) (Figure 3.8.1).

3.8.2 Soft agar colony formation assay of siRNA transfectant cells

A soft agar assay was performed to study effects of reduced C-FABP expression on tumourigenesis in siRNA transfectant cells in androgen positive and negative conditions (Figure 3.8.2). Colony formation was observed to occur at least four days earlier in parental PC3M and

PC3M-2 cell lines than in PC3M-3 and LNCaP cells. Also, parental PC3M and PC3M-2 cells had a greater number and size of colonies compared to PC3M-3 and LNCaP cells at the end of the 6 week experiment. No significant difference was identified (Students t-test $P>0.05$) in number of colonies formed between PC3M (110.6±15.64) and PC3M-2 transfectant (91±17.05) in androgen positive conditions. However, comparison of the number of colonies formed by PC3M-3 transfectant cells (47±11.53) and LNCaP cells (56±6.93) to that of PC3M showed a significant difference in the number of observed colonies (Students t-test <0.05). Parental PC3M cells generated a greater number of colonies (81.3±13) in androgen negative conditions; followed by, PC3M-2 (53±3.5), PC3M-3 (49.6±3.3) and LNCaP (36.3±2.9). A statistically significant difference (Students t-test $P<0.05$) in number of colonies formed was observed between PC3M and siRNA transfectant cell lines and LNCaP. In addition, a significant difference (Students t-test $P<0.05$) in number of colonies formed is also observed between the androgen positive and androgen negative conditions.

Table 3.8.2 – Number of colonies formed in androgen positive and negative conditions

Cell line	Mean number of colonies in androgen +ve	Mean number of colonies in androgen -ve	T-test paired for 2 sample means
PC3M	110.6±15.64	81.3±13	**P> 0.05**
PC3M-2	91±17.05	53±3.5	**P> 0.05**
PC3M-3	47±11.53	49.6±3.3	**P> 0.05**
LNCaP	56±6.93	36.3±2.9	**P<0.05**

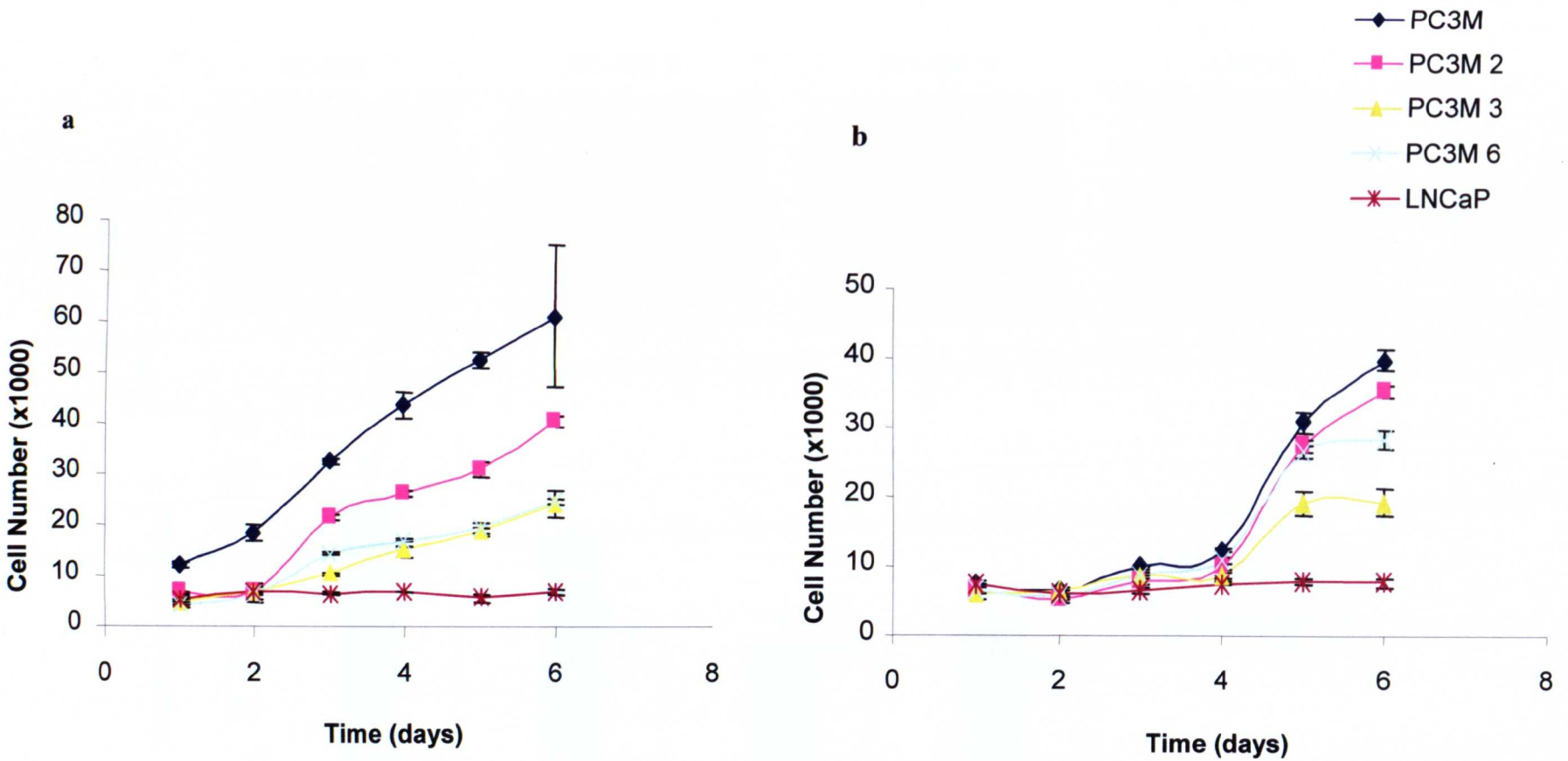

Figure 3.8.1. Proliferation rate of different cell lines. Proliferation assay was performed to determine the effects of the suppressed C-FABP expression on androgen sensitivity in the parental, RNAi transfectant PC3M 2, 3, 4 and the androgen responsive prostate cancer cell line LNCaP in androgen supplemented (**a**) and androgen deprived (**b**) conditions. Each cell line was cultured in triplicate at a density of 10^{x3}/well in 24 well plates. Cells were cultured in a humidified environment at 5% CO_2 at 37°C for 6 days, with 3-(4, 5-Dimethylthiazol-yl)-2,5-diphenyltetrazolium (MTT) colorimetric measurements taken every day. Results shown were the mean cell numbers (± SE) of 3 separate measurements.

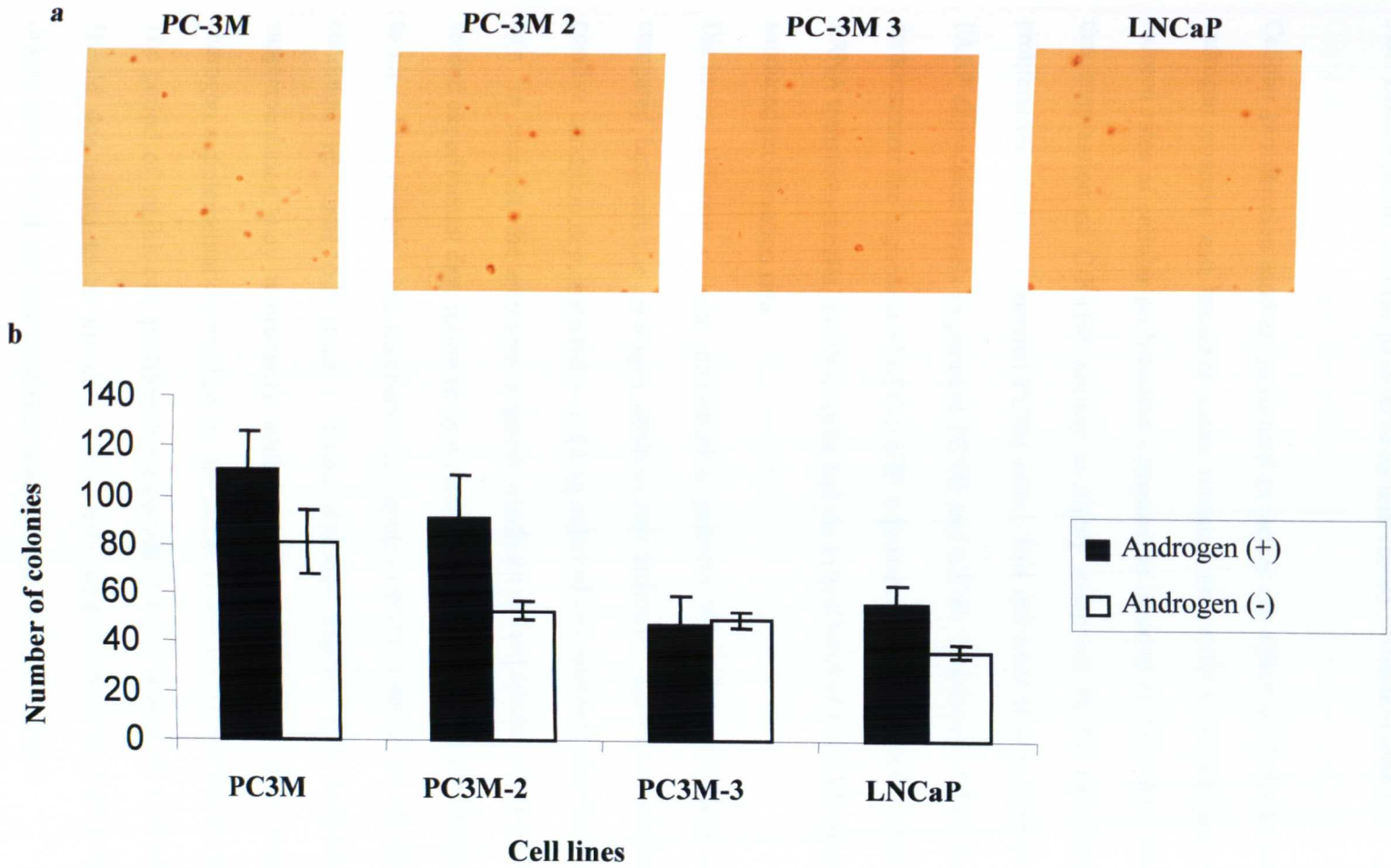

Figure 3.8.2. Effect of suppressed C-FABP expression and androgen deprivation on colony formation of the parental PC3M cells, RNAi transfectant PC3M-2, PC3M-2 and the LNCaP cell line.
a, qualitative analysis of colony formation. Photographs were taken under a light microscope after the cells were allowed to grow for 6 weeks on the soft agar. **b,** different numbers of the nodules growing on the soft agar assays produced by the parental PC3M cells, RNAi transfectant PC3M-2, 3 and the LNCaP cells in androgen positive (+) and negative (-) conditions. The numbers of nodules were shown by the mean (± SE) of three separate experiments.

3.8.3 Discussion of cellular proliferation and colony formation assays

Cellular proliferation studies performed to assess the effect of C-FABP suppression in both androgen positive and negative cases revealed that siRNA transfectant cells demonstrated reduced rates of cellular proliferation compared to parental PC3M cells. These results suggest that suppression of C-FABP activity in highly malignant PC3M cells reduced their rate of proliferation relative to parental PC3M cells. This inference is supported by comparison of C-FABP expression levels in parental PC3M and siRNA transfectant cells. Parental PC3M cells demonstrated the highest level of C-FABP expression and the greatest proliferation rate. Of the siRNA transfectant cells, PC3M-3 cells had the lowest level of C-FABP expression, resulting in a reduced proliferation rate.

Distinctly different cellular proliferation patterns were observed when cell numbers were compared between the androgen positive and androgen negative conditions. The androgen positive condition demonstrated a doubling effect of cell numbers after the second experimental day. In contrast, the androgen negative condition demonstrated a period of regression at the second experimental day, followed by a period of increased cellular proliferation from day's four to six. Furthermore, cell numbers were approximately matched in all cells in the negative condition up until day four. These findings suggest that suppression of androgen supplementation may temporarily inhibit cellular proliferation. It is possible that lack of androgen supplementation resulted in the failure of the androgen receptor signalling pathway. The period of inhibit cell proliferation observed (days 1-4) may be attributed to a lag phase. Should this prove to be the case, this result suggests that the highly malignant androgen independent PC3M cell line may have residual sensitivity to androgens.

It is not clear why suppressing C-FABP expression reduces cellular proliferation, especially as Owada *et al*, (2002) reported compelling evidence demonstrating a compensatory effect of heart-fatty acid binding protein tacking in the event of inhibited C-FABP expression. It may be due to a signalling pathway that is unknown or undiscovered and that is regulated by C-FABP expression. However, it is clear, that C-FABP suppression and androgen depletion have no combined synergistic effect on cellular proliferation than suppressed C-FABP activity alone.

Colony formation was assessed in parental PC3M cells and siRNA transfectant cells in androgen positive and androgen negative conditions. The results demonstrated that suppression of C-FABP activity reduced total number of colonies formed in both androgen positive and negative conditions. A significant difference was observed in the number of colonies formed between parental PC3M and siRNA transfectant PC3M-3 cells in androgen positive and negative conditions. However, no significant difference was observed when the number of colonies formed by PC3M-3 transfectant cells was compared in the androgen positive and negative conditions.

The soft agar colony formation assay was conducted in order to determine tumourigenic potential *in vitro*. This assay was performed in an androgen positive and negative condition to determine whether siRNA transfectant cells with suppressed C-FABP expression would produce different numbers of colonies in the androgen positive conditions relative to the negative conditions, thereby indicating whether C-FABP suppression and androgen deprivation exhibit a synergistic effect on tumourigenicity. Analysis of the number of colonies formed in each cell line in both conditions show that this relationship did not exist. As a matter of fact, the only differences observed in the number of colonies formed in all cell lines was directly related to the level of C-FABP expressed within each cell. In the siRNA transfectant PC3M-3 cell lines, a 31-

fold reduction of intrinsic C-FABP expression relative to parental PC3M cells resulted in a similar colony number count to that of LNCaP cells. This result is more significant when we considered that the PC3M-3 derivative cell line, PC3M, is highly malignant, whereas LNCaP are weakly malignant cell lines (Jing *et al.*, 2000a).

In vitro analysis of antisense and siRNA transfectant cells suggested that suppression of C-FABP reduced invasion, proliferation and tumour formation in transfectant cells relative to control cells. A comparison of scores between androgen positive and androgen negative groups suggest that androgen depletion had no additional effect on cell proliferation or colony formation than suppressed C-FABP activity, suggesting that C-FABP over-expression may not be involved in the switch in androgen sensitivity, since reducing C-FABP activity does not restore androgen sensitivity in highly malignant androgen insensitive cells *in vitro*.

3.9 siRNA TRANSFECTANT CELL TUMOURIGENICITY *IN VIVO*

To assess the effect of reduced C-FABP on tumourigenesis and to determine if reduced C-FABP expression in siRNA transfectant cells can instigate androgen sensitivity in highly malignant androgen insensitive cell lines, parental PC3M cells and PC3M-3 siRNA transfectant cell lines were inoculated into 4 groups of male ICRF immuno-compromised nude mice. In the first two groups, parental PC3M and transfectant PC3M-3 cell lines were inoculated into the shoulder fat pad subcutaneously, at a density of $2x10^6$ cells/200μl in the first two groups. In groups C and D, the recipient mice were castrated and then inoculated orthotopically with parental PC3M and transfectant PC3M-3 into the prostate at a density of $1x10^6$ cells/20μl PBS (Table 3.9.1).

Table 3.9.1 Nomenclature of Animal groups

Cell line inoculated	Number of mice	Surgical Procedure	Site of inoculation	Cell density	Nomenclature
PC3M	4	None	Shoulder region sc.	$2x10^6$ cells/200µl pbs	Group A
PC3M-3	4	None	Shoulder region sc.	$2x10^6$ cells/200µl pbs	Group B
PC3M	4	Castration	Prostate	$1x10^6$ cells/20µl pbs[a]	Group C
PC3M-3	3[b]	Castration	Prostate	$1x10^6$ cells/20µl pbs[a]	Group D

Table 3.11.1. Groups A and B represent the androgen positive *in vivo group* inoculated s.c. into the shoulder region of immuno-compromised CD/1 nude mice. The androgen negative castrated animals are represented in Groups C and D.
[a] differences in number of cells loaded is a result of loss of cell pellets in experimental preparation resulting in the numbers of cells inoculated into Groups C and D to being adjusted to $1x10^6$ cells/20µl .
[b] during post operative recovery, an animal suffered complications and was subsequently excluded from the study.

The results of the subcutaneous injection of parental PC3M and siRNA mediated PC3M3 cells into the shoulder fat pad of mice is detailed in Table 3.11.2. Group A mice inoculated with parental PC3M cells show a 100% tumour incidence rate within four days of inoculation, and maintained a steady growth rate over the duration of the experiment. Group B, inoculated with siRNA transfectant PC3M3 cells demonstrated 25% tumour incidence within four days of inoculation. This increased to 75% tumour incidence at the second week of experimentation, however, from week 3, regression in tumour incidence to 0% was observed and continued thus until week 6 where 75% of mice demonstrated quantifiable tumour growth (Figure 3.9).

Table 3.9.2 Incidence of tumours produced by parental and siRNA transfectant cells inoculated into nude mice

Mouse group	Cell line inoculated	Site of inoculation	Number of mice	Percentage of tumour incidence at autopsy	Median latent period in days (range)
Group A	PC3M	Shoulder region sc	4	4/4 (100%)	4 days
Group B	PC3M-3	Shoulder region sc	4	3/4 (75%)	9 (4 -14) days
Group C	PC3M	Prostate	4	4/4 (100%)	N/A
Group D	PC3M-3	Prostate	3	0/3 (0%)	N/A

An assessment of the median latent period of tumour incidence could not be performed on groups C and D as they were inoculated orthotopically into the prostate, hence, tumour presence could only be confirmed at autopsy. At autopsy, group C mice presented a 100% tumour incidence rate, whereas group D failed to produce any tumours.

Comparison of mean tumour volume for groups A ($1471\pm997mm^3$) and B ($175\pm225mm^3$) showed a statistically significant (Student t-test $P<0.05$) difference between parental PC3M cells and siRNA transfectant PC3M-3 cells lines. This represented an 8.5 fold reduction in mean tumour volume between groups A and B. A statistically significant (Students T-Test $P<0.05$) difference was also observed for mean tumour mass between groups C (2 ± 0.4g) and D (0) (Table 3.9.3).

Table 3.9.3 Mean tumour size and tumour growth rate produced by parental and siRNA transfectant cells inoculated into nude mice

Mouse group	Cell line inoculated	Site of inoculation	Number of mice	Number of weeks to autopsy	Tumour size
Group A	PC3M	Shoulder region	4	5	$1471mm^3 \pm 997mm^3$
Group B	PC3M3	Shoulder region	4	10	$176mm^3 \pm 225mm^3$
Group C	PC3M	Prostate	4	6.3	2g
Group D	PC3M3	Prostate	3	7	0g

Additionally, tumour growth rate was greatly reduced in siRNA transfected cell lines in group B relative to parental PC3M cell lines in group A. Group A mice were culled at 5weeks, whereas group B mice were culled at 10 weeks, and still produced quantifiably smaller tumours relative to group A.

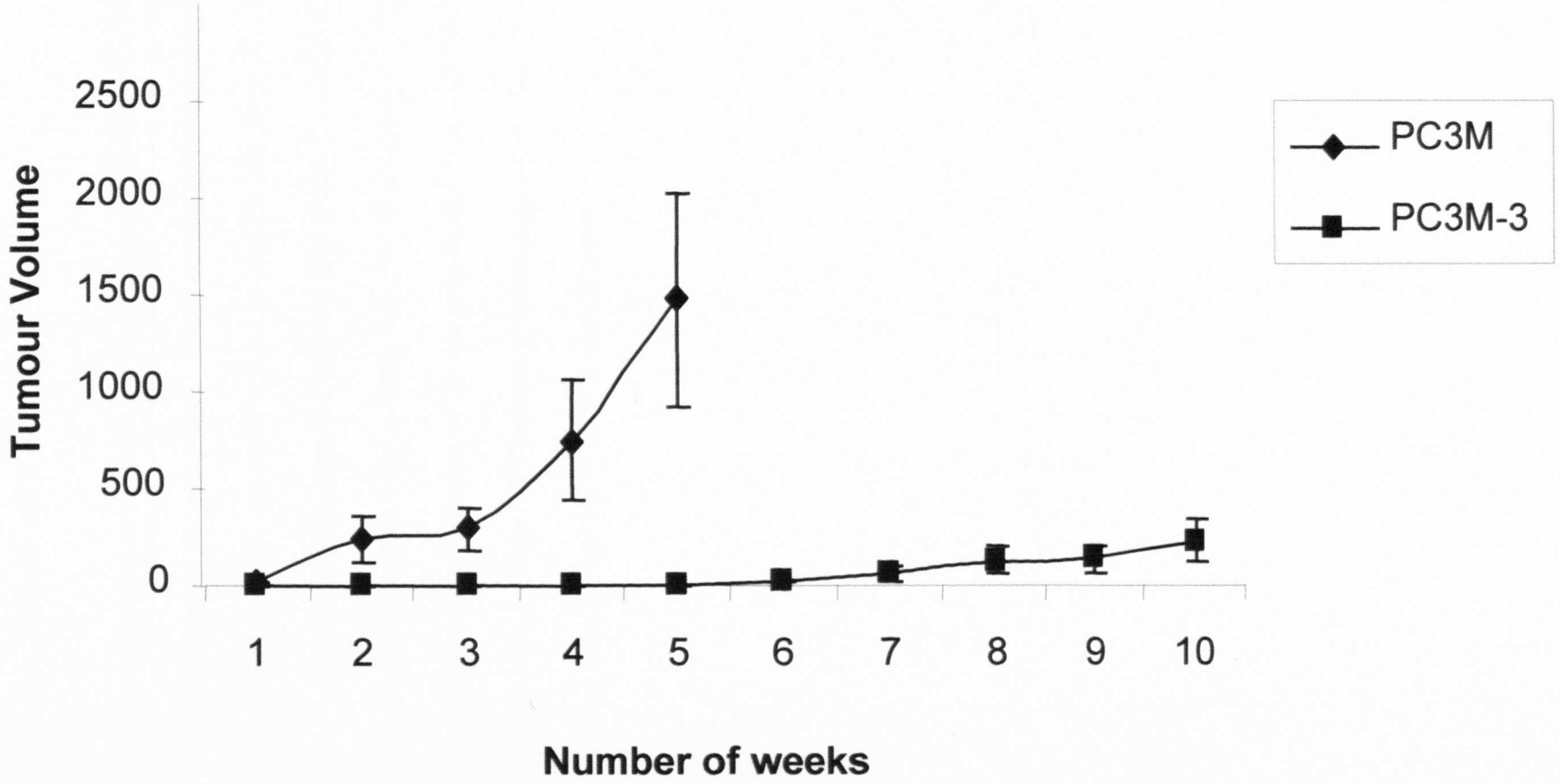

Figure 3.9 Tumour volumes produced by the parental PC3M cells and the RNAi transfectant PC3M-3 cells.
The parental PC3M cells and RNAi transfectant PC3M-3 cells were inoculated subcutaneously into two groups (4 each) of male immuno-compromised CD/1 nude mice by injecting to the shoulder regions. The tumour sizes were measured weekly for 5 weeks after the inoculation and tumour volumes were calculated using the formulae V = L x H x W x 0.5237 (Janik et al, 1975). The results shown were the mean tumour volumes (± SE) of four animals.

3.10 HISTOLOGICAL ANALYSIS OF METASTASIS

At autopsy, primary tumours (where available) were dissected together with lungs liver and heart of each mouse in the second round of *in vivo* studies. These tissues were fixed in 10% (v/v) aqueous formaldehyde and haematoxylin and eosin stained to identify the presence of tumour cells within these organs. Analysis of tissue samples revealed that group C mice produced 4/4 (100%) secondary micro-metastatic tumour cells in lungs and liver tissue (Figure 3.10). These figures demonstrated the malignant dissemination of tumour cells through vessels (Figure 3.10a), across membranes (Figure 3.10b), and into fully established micro-metastases (Figure 3.10c). Secondary tumour cells were not detected in any other groups of mice.

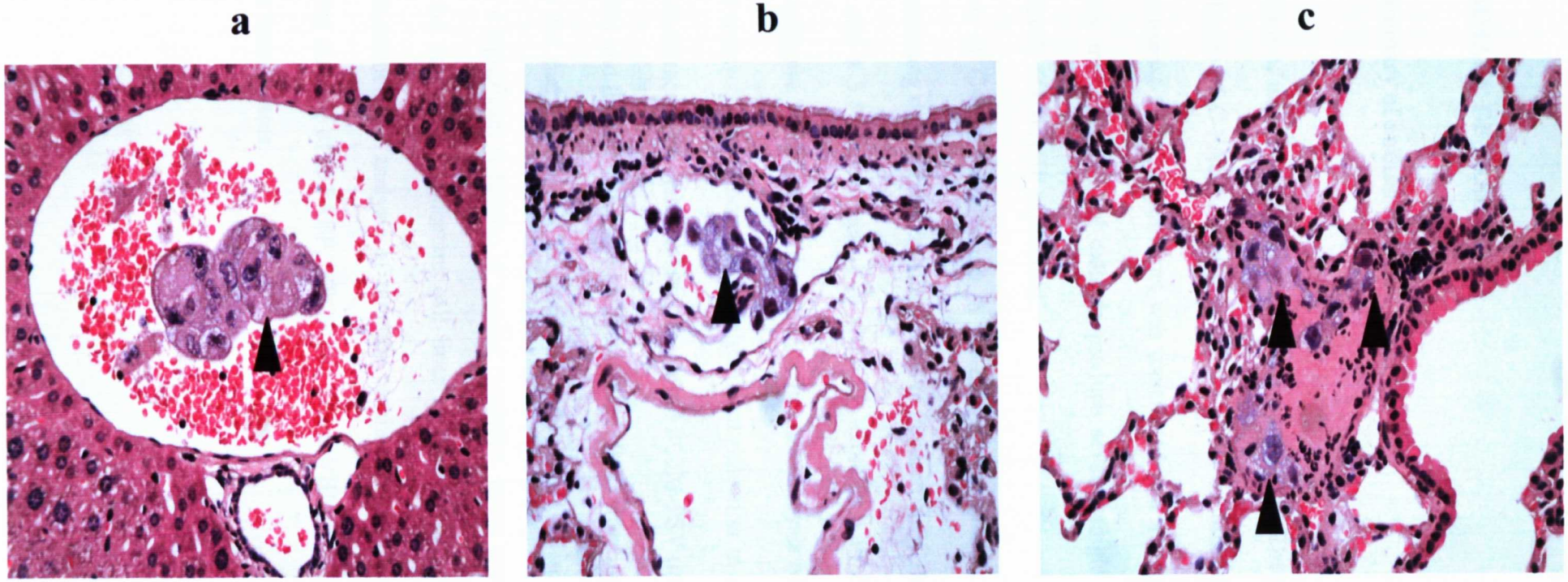

Figure 3.10. Histological examination of the malignant dissemination of the tumour cells. **a,** representative slide showing the presence of a cluster of tumour cells (originated from the control cells) in a vessel in the Liver. **b,** a cluster of tumour cells across the membranes of the blood vessel and invaded into the lung tissue. **c,** a fully established micro metastasis in lung tissue. Magnification – **a** x400, **b and c** x120

3.11 SUMMARY OF RESULTS

3.11.1 Summary of antisense section of results

Two sections of experiments were performed in this study. The first section assessed the role of reduced levels of C-FABP expression and its effect on tumourigenicity. For this purpose, a reverse antisense C-FABP construct was transfected into an expression vector, and introduced into highly malignant PC3M cells to produce several single cell cloned transfectants with reduced levels of C-FABP expression.

The levels of C-FABP expression in the cloned transfectants was quantified using Western blotting scanning densitometry analysis relative to parental PC3M cells. The results confirmed a 6.9 fold and a 3.8 fold reduction in C-FABP expression in PC3M-C-FABP3 and PC3M-C-FABP1 antisense transfectants respectively. *In vitro* analysis of the invasive potential of these antisense transfectants demonstrated a significant reduction in the percentage of cells invading through an extracellular matrix relative to control PC3M-PSV transfectant cells.

The control and the two antisense transfectant cell lines were inoculated subcutaneously into the shoulder fat pad of male ICRF immunocompromised mice. Analysis of tumourigenicity revealed a significant reduction in tumour incidence, mean tumour volume and tumour growth rate in the antisense transfectant cell lines relative to parental PC3M cells. Furthermore, immunohistochemical analysis of tumours obtained from mice at autopsy showed significant differential staining of C-FABP, VEGF and factor VIII related antigen in control, and the two antisense transfectants.

The results of immunohistochemical staining were consistent with Northern blot analysis of the control and two antisense transfectants which demonstrated significantly reduced levels of VEGF expression relative to the control transfectant group.

3.11.2 Summary of the siRNA round of results

The second round of experiments assessed whether suppressing C-FABP expression in the highly malignant androgen independent cell line PC3M would initiate androgen sensitivity. For this purpose, C-FABP expression was inhibited using siRNA and subjected to a series of *in vitro* and *in vivo* tests.

Western blot and scanning densitometry analysis showed that siRNA successfully reduced the levels of C-FABP expression in highly malignant PC3M cells by >90% in PC3M-3 transfectants. Similarly, a significant difference was observed at the RNA level between the siRNA transfectant cell lines relative to the parental PC3M cell.

The proliferation rate of the transfectant relative to parental PC3M cells in an androgen positive and androgen negative condition was assessed. In both conditions, a significant difference was observed between the siRNA transfectant and the parental PC3M cells. However, no significant difference was noted between the androgen positive and androgen negative condition.

In vitro analysis of tumourigenicity as assessed by soft agar assay showed a significant difference between the number of colonies formed in the siRNA PC3M- transfectant and the parental PC3M cells both androgen positive and androgen negative conditions. Furthermore, a statistically significant difference was observed between the numbers of colonies formed in the androgen negative condition relative to the androgen positive condition.

To assess tumourigenicity *in vivo*, two groups of mice were inoculated subcutaneously and orthotopically with the highly malignant parental PC3M cells, into the prostate, representing groups A and C respectively. Similarly, siRNA transfectant PC3M-3 cells were inoculated subcutaneously and orthotopically into the prostate, representing groups B and D respectively. A week prior to orthortopic inoculation, the animals in groups C and D were castrated to create an androgen negative environment, whereas groups A and B represented the androgen positive group.

Analysis of these results showed that group B animals produced statistically significant reductions in tumour incidence, and mean tumour volume when compared to group A animals. This is in-keeping with their levels of C-FABP expression. Similarly, group D animals demonstrated reduced tumour incidences, and mean tumour volume when compared to group C animals.

When the tumour incidence values for groups B and D were compared, the androgen positive group B animals produced significantly higher levels of tumour incidence than the androgen negative castrated group D animals. Immunocytochemical analysis of the heart, lungs and liver of all mice in all groups showed 100% metastases observed in group C animals, and no presence of metastases in any other animals.

CHAPTER FOUR: GENERAL DISCUSSION

Prostate cancer is now the most commonly occurring form of non-tobacco related cancer in men in the developing world. In the UK and Ireland, prostate cancer accounted for 1 in 6 diagnosed cancers, and represented 1 in 9 cancer deaths in men during the 1990s.

The molecular pathology of prostate cancer is poorly understood. This, in part, is due to the heterogeneity of the disease. Approximately 10% of all prostate cancers are a result of familial autosomal dominance inheritance (Smith *et al*, 1996), leaving approximately 90% as *de novo* sporadic mutations. To date, three different chromosomal loci have been identified by linkage analysis; however, not all pedigrees have shown successful linkage to these loci. Sporadic prostate cancer onset has been attributed to a variety of factors ranging from lack of selenium supplementation (Etminan *et al.*, 2005) to vitamin D (Stewart *et al.*, 2005) and high dairy fat intake (Hughes-Fulford *et al.*, 2005).

Epidemiological studies have established a link between omega 6 fatty acids and prostate cancer incidence (Aktas and Halperin, 2004; Larsson *et al.*, 2004). Aktas and Halperin, (2004) reviewed a series of studies investigating the relatively low incidence of prostate cancer with nutritional intake. They reported that Eskimo populations in Alaska and some of the Japanese population in Northern Japan that consumed diets made up almost entirely of fish had low incidences of prostate cancer. However, increasing high dairy fat diets associated with western countries, including the consumption of diary fatty acids, increased relative risk and incidence of prostate cancer amongst these populations. Augustsson *et al*, (2003) reported that eating fish more than three times a week was associated with reduced risk of prostate cancer. Furthermore, each

additional daily intake of 0.5g of marine fatty acid was associated with a 24% decreased risk of metastatic cancer.

Polyunsaturated fatty acids have been reported to influence and regulate a number of cellular functions such as synthesis of prostaglandins, immune response, and phospholipid membrane maintenance. Since down-regulation of gene expression by fatty acids requires a prerequisite 18 or more number of carbon fatty-acid molecule and at least 2 double bonds (Pegorier *et al.*, 2004), up-regulation of gene expression by fatty acid is independent to the number of carbon bonds within the molecule. Regulation of gene expression by fatty acids is dependent on an abundance and activity of at least four transcription factor families: peroxisome proliferators activated receptor (PPAR), liver-X receptor (LXR), hepatic nuclear factor 4 (HNF-4α), and sterol regulatory element binding protein (SREBP) (Pegorier *et al.*, 2004). Of these, fatty acids have been shown to be natural potent ligands for PPAR, and have been shown to bind to all three isoforms of PPAR. Furthermore, the recent discovery that fatty acids act as hormones and are able to regulate metabolism of transcription factors, and the discovery of the up-regulation of all three isoforms of PPAR in prostate cancer (Collett *et al.*, 2000) suggests that fatty acids, particularly, eicosanoids, derivates of arachidonic acid (Figure 4.1.1), may have an up-regulatory role in PPAR activity, hence an increased level of PPARα expression in tumour cells (Desvergne and Wahli, 1999).

Fatty acids also act as ligands to a family of intracellular lipid binding proteins known as fatty acid binding proteins. Immunocytochemical staining for the expression of C-FABP identified the presence of the protein in the cell cytoplasm, and within the nucleus (Adamson *et al.*, 2003). Given that FABP act as intracellular long chain fatty acid transporters, these results suggest that fatty acids are transported by fatty acid binding proteins around the cell cytoplasm for energy

metabolism, and within the cell nucleus for regulation of nuclear hormone transcription factors such as PPAR. The exact molecular mechanism that governs up-regulation of C-FABP is not fully understood, however, it is feasible to suggest that up-regulation of C-FABP expression may be a result of increased fatty acid signalling. This produces a negative feedback mechanism that results in up regulation of C-FABP for increased intracellular trafficking of fatty acids. Given that C-FABP was up-regulated in breast and prostate cell line models (Jing *et al.*, 2000a), and in squamous carcinoma of the bladder and skin (Ostergaard *et al.*, 1997), this Thesis investigated the role of C-FABP on tumourigenicity of prostate cancer. In this study, C-FABP expression was found to be differentially expressed in normal, benign prostatic hyperplasia and prostatic carcinoma. Furthermore, the suppression of C-FABP expression in highly malignant PC3M prostate cancer cell lines reduced the cells invasive potential *in vitro* and reduced tumour incidence and tumour volume *in vivo*. In addition, C-FABP expression was shown to regulate VEGF expression and micro-vessel density formation in tumours. These results clearly suggest the importance of C-FABP expression in the malignant progression of prostate cancer. However, greater clarification is required in order to determine whether C-FABP protein up-regulation is sufficient to activate a signalling pathway that leads to increased tumourigenicity in prostate cancer, or whether it is the long chain fatty acid ligand being carried by the C-FABP proteins which causes these abnormal changes in normal cell signalling. There is growing evidence that fatty acid binding protein ligands such as prostaglandin, an omega-6 fatty acid derivative, are able to up-regulate VEGF expression via activation of the epidermal growth factor receptor signalling pathway (Ding *et al.*, 2005b). There has also been recent evidence showing up-regulation of VEGF and cyclooxygenase 2 (COX-2) – the enzyme responsible for converting arachidonic acid to prostaglandins, in prostate cancer cells (Grau *et al.*, 2004). This

suggests a possible pathway by which increased fatty acid signalling increases C-FABP expression and ligand binding to fatty acids. It is feasible that omega-6 fatty acid signalling may increase the conversion of arachidonic acid into prostaglandin 2 by COX-2. Evidence has been provided showing that COX-2 up-regulation is linked to increased angiogenesis (Tsujii *et al.*, 1998). It is this author's contention that these processes are possibly linked in a general unifying theory. In fact, fatty acid synthase (FAS) has been demonstrated as being minimally expressed in normal human tissues, but over expressed in some human cancers (Baron *et al.*, 2004). Several studies have reported up-regulation of FAS mRNA and protein expression in prostate carcinoma relative to normal prostate tissue (Epstein *et al.*, 1995; Swinnen *et al.*, 2002; Swinnen *et al.*, 2000), and the highest levels of FAS were reported to be expressed in androgen independent bone metastases (Rossi *et al.*, 2003). FAS over-expression is an important factor in prostate cancer. FAS inhibitors have been reported to be involved in apoptosis. However, FAS over-expression has been reported to influence cellular proliferation by promoting synthesis of membrane phospsolipids necessary for DNA replication (Rossi *et al.*, 2003). Exploration of the mechanism of action of FAS in cell survival, proliferation and apoptosis may prove to be a productive endeavour.

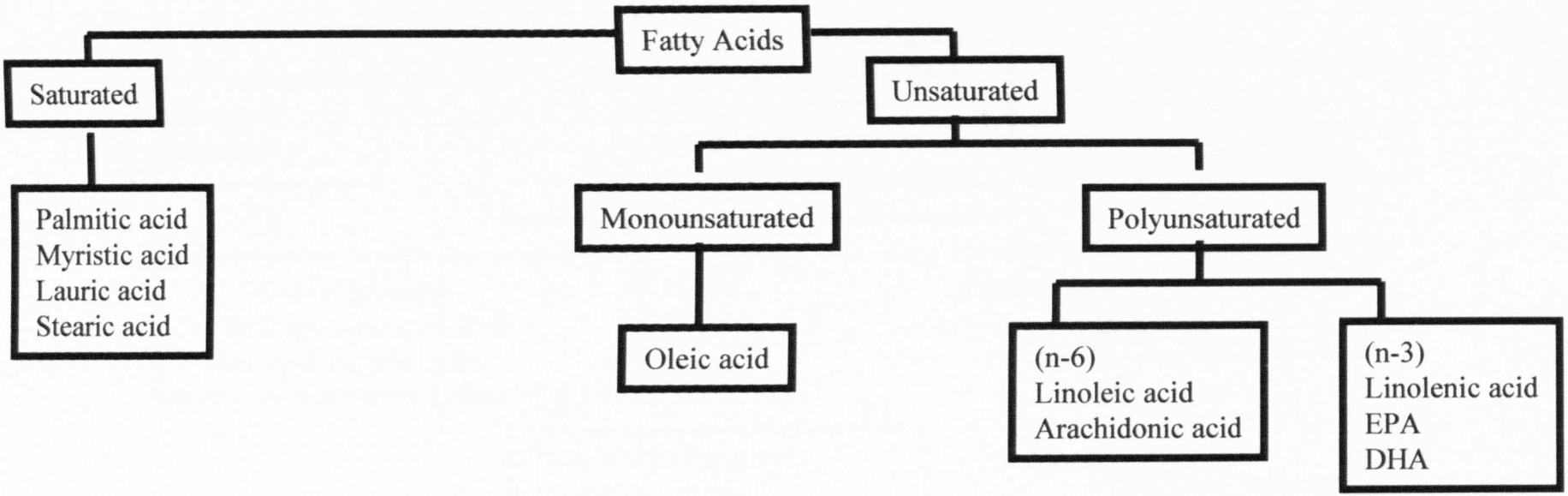

Figure 4.1.1 Family of Fatty Acids. Polyunsaturated fatty acids are made from two groups of fatty acids, Omega 6 (n-6) and Omega 3 (n-3) fatty acids. Omega 6 fatty acids are commonly obtained from sun flower oils, corn and soybeans, whereas Omega-3 fatty acids such as Eicosapentanoic acid and docosahexaenoic acid are chiefly found in marine fatty acids

Figure 4.1.2 Fatty acid, testosterone and prostate cancer

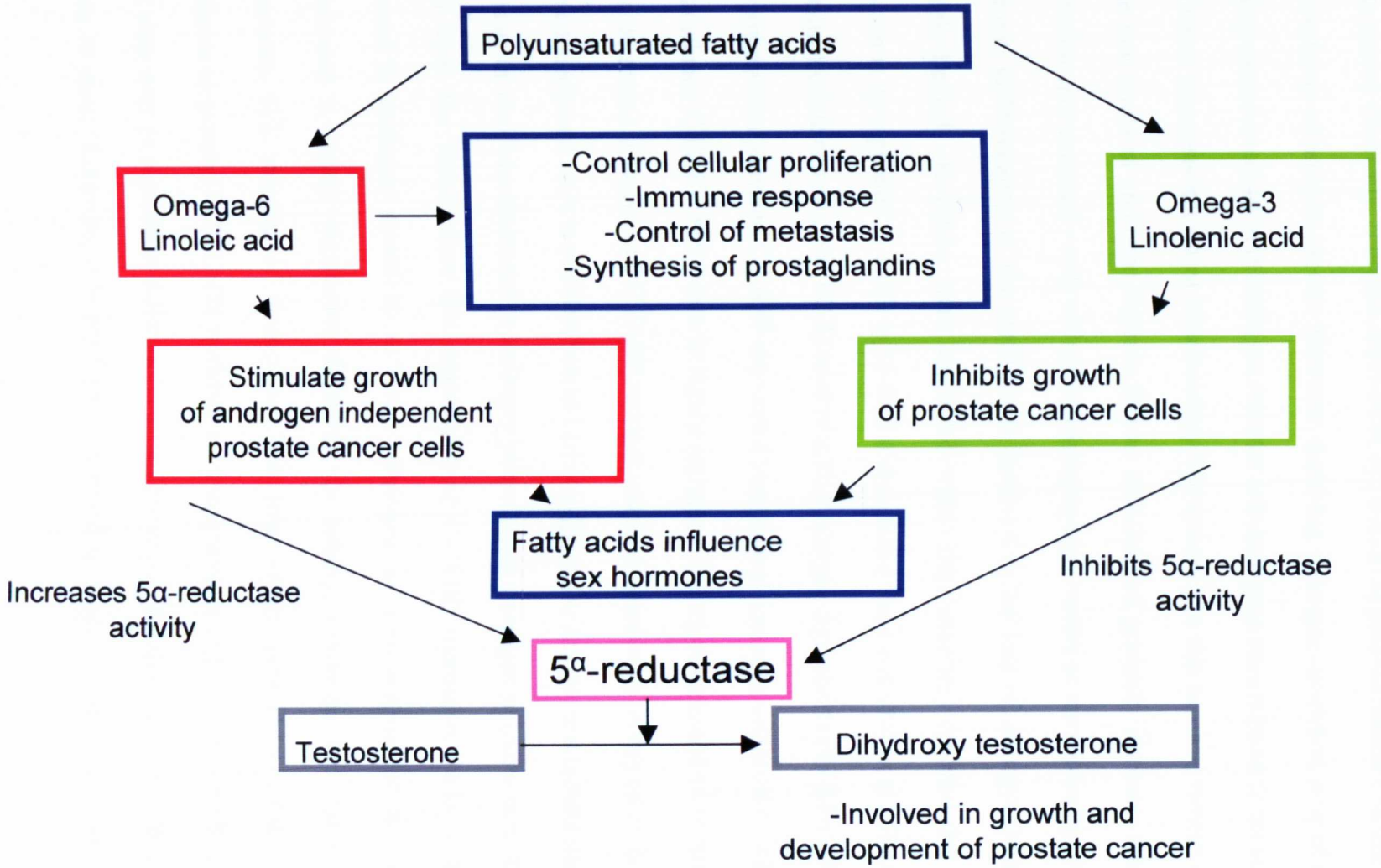

Loss of sensitivity to androgens marks a significant milestone in the malignant progression of prostate cancer. Clinically, androgen deprivation by physical or pharmaceutical castration is used in the treatment of prostate cancer. However, depriving androgen dependent cells of androgen signalling causes a reduction in androgen receptor activated gene transcription factor regulation, and initiates a process known as compensatory hyperplasia. In this process, tumour cells that tolerate low levels of androgen become able to stabilise and gradually increase, their rate of proliferation until eventually cells with greater independence evolve as the remaining progeny.

At present, understanding of the mechanisms involved in the loss of androgen sensitivity is extremely limited. However, work conducted within this laboratory reported that C-FABP expression is up-regulated as much as 15-fold at the protein level and 17-fold at mRNA level in metastatic prostate cancer cells (PC-3) relative to the androgen dependent cells (LNCaP). To test the hypothesis that elevated C-FABP expression may induce androgen insensitivity, siRNA was used to silence C-FABP expression in highly malignant androgen independent prostate cancer cells to determine if suppressed C-FABP restored androgen sensitivity. Analysis of the response of these transfectant cells in proliferation and colony formation *in vitro* and tumourigenicity and metastasis in *vivo* was measured in androgen positive and androgen negative conditions. The results from this Thesis show that suppression of C-FABP expression made no significant difference to androgen sensitivity *in vitro.* However, *in* vivo analysis of tumourigenicity demonstrated a highly significant difference in tumour incidence and tumour volume. Furthermore, H/E staining of lungs, heart and liver of all mice showed that orthortopic inoculation of parental PC3M cells produced secondary tumour cells in lungs and liver tissue. It is not clear why no significant difference was noticed in proliferation rate and colony formation of cells *in vitro.* Likewise, it is not fully understood why such a significant level of tumour

reduction was observed in siRNA transfectant cells relative to control groups. A recent study (Habib *et al.*, 2003) demonstrated that loss of 5alpha-reductase mRNA expression in bone and lymph node metastasis may be associated, in part, with the progression of these tumours to androgen insensitivity. Interestingly, fatty acids have been shown to be involved in the regulation of 5α-reductase (Meyer and Gillatt, 2002), an enzyme that converts testosterone into dihydroxytestosterone (DHT) (Figure 4.1.2). This suggests a direct relationship between ingestion of omega 6 fatty acids to onset of prostate cancer, metastasis and loss of androgen sensitivity. Evidently, cancer pathways are rarely that simplistic. Understanding of the tumour progression pathway is vital in expanding current treatment regimes.

In conclusion, it is evident that the level of C-FABP expression is an important regulatory factor in prostatic tumourigenesis incidence; progression and metastasis of prostate cancer. The C-FABP signalling pathway involves regulation of potent angiogenic factors particularly, VEGF, that support tumour development by neo-vascularisation and micro-vessel density formation. The investigation to explore the relationship between elevated C-FABP expression and loss of androgen sensitivity suggests that suppression of C-FABP expression does not restore androgen sensitivity in highly malignant androgen insensitive cell lines (PC3M) *in vitro*. Comparison of tumour incidence rates between group B mice and group C mice, representing the androgen positive and androgen negative group respectively, suggest that a combination of C-FABP protein inhibition and androgen suppression by castration may produce an additive effect to reduce tumour incidence values. Consequently, *in vivo* tumourigenicity assays indicate a possible synergistic relationship between C-FABP suppression and androgen depletion. Further

investigation is needed to establish whether the combination of these two factors may be a valid two-hit mode for the therapeutic management of prostate cancer.

REFERENCES

1. Abate-Shen, C., and Shen, M. M. (2000). Molecular genetics of prostate cancer. Genes Dev *14*, 2410-2434.
2. Abumrad, N., Coburn, C., and Ibrahimi, A. (1999). Membrane proteins implicated in long-chain fatty acid uptake by mammalian cells: CD36, FATP and FABPm. Biochim Biophys Acta *1441*, 4-13.
3. Achenbach, T. V., Brunner, B., and Heermeier, K. (2003). Oligonucleotide-based knockdown technologies: antisense versus RNA interference. Chembiochem *4*, 928-935.
4. Adamson, J., Morgan, E. A., Beesley, C., Mei, Y., Foster, C. S., Fujii, H., Rudland, P. S., Smith, P. H., and Ke, Y. (2003). High-level expression of cutaneous fatty acid-binding protein in prostatic carcinomas and its effect on tumorigenicity. Oncogene *22*, 2739-2749.
5. Aktas, H., and Halperin, J. A. (2004). Translational regulation of gene expression by omega-3 fatty acids. J Nutr *134*, 2487S-2491S.
6. Aronson, W. J., Glaspy, J. A., Reddy, S. T., Reese, D., Heber, D., and Bagga, D. (2001). Modulation of omega-3/omega-6 polyunsaturated ratios with dietary fish oils in men with prostate cancer. Urology *58*, 283-288.
7. Augustsson, K., Michaud, D. S., Rimm, E. B., Leitzmann, M. F., Stampfer, M. J., Willett, W. C., and Giovannucci, E. (2003). A prospective study of intake of fish and marine fatty acids and prostate cancer. Cancer Epidemiol Biomarkers Prev *12*, 64-67.
8. Bagga, D., Capone, S., Wang, H. J., Heber, D., Lill, M., Chap, L., and Glaspy, J. A. (1997). Dietary modulation of omega-3/omega-6 polyunsaturated fatty acid ratios in patients with breast cancer. J Natl Cancer Inst *89*, 1123-1131.

9. Banaszak, L., Winter, N., Xu, Z., Bernlohr, D. A., Cowan, S., and Jones, T. A. (1994). Lipid-binding proteins: a family of fatty acid and retinoid transport proteins. Adv Protein Chem *45*, 89-151.

10. Baron, A., Migita, T., Tang, D., and Loda, M. (2004). Fatty acid synthase: a metabolic oncogene in prostate cancer? J Cell Biochem *91*, 47-53.

11. Benedict, W. F., Xu, H. J., Hu, S. X., and Takahashi, R. (1990). Role of the retinoblastoma gene in the initiation and progression of human cancer. J Clin Invest *85*, 988-993.

12. Berchem, G. J., Bosseler, M., Sugars, L. Y., Voeller, H. J., Zeitlin, S., and Gelmann, E. P. (1995). Androgens induce resistance to bcl-2-mediated apoptosis in LNCaP prostate cancer cells. Cancer Res *55*, 735-738.

13. Bhatia-Gaur, R., Donjacour, A. A., Sciavolino, P. J., Kim, M., Desai, N., Young, P., Norton, C. R., Gridley, T., Cardiff, R. D., Cunha, G. R., *et al.* (1999). Roles for Nkx3.1 in prostate development and cancer. Genes Dev *13*, 966-977.

14. Binas, B., Danneberg, H., McWhir, J., Mullins, L., and Clark, A. J. (1999). Requirement for the heart-type fatty acid binding protein in cardiac fatty acid utilization. Faseb J *13*, 805-812.

15. Bookstein, R., Shew, J. Y., Chen, P. L., Scully, P., and Lee, W. H. (1990). Suppression of tumorigenicity of human prostate carcinoma cells by replacing a mutated RB gene. Science *247*, 712-715.

16. Borchers, T., Unterberg, C., Rudel, H., Robenek, H., and Spener, F. (1989). Subcellular distribution of cardiac fatty acid-binding protein in bovine heart muscle and quantitation with an enzyme-linked immunosorbent assay. Biochim Biophys Acta *1002*, 54-61.

17. Bostwick, D. G., and Brawer, M. K. (1987). Prostatic intra-epithelial neoplasia and early invasion in prostate cancer. Cancer *59*, 788-794.

18. Bratt, O. (2002). Hereditary prostate cancer: clinical aspects. J Urol *168*, 906-913.

19. Brouard, M. C., Saurat, J. H., Ghanem, G., and Siegenthaler, G. (2002). Urinary excretion of epidermal-type fatty acid-binding protein and S100A7 protein in patients with cutaneous melanoma. Melanoma Res *12*, 627-631.

20. Brummelkamp, T. R., Bernards, R., and Agami, R. (2002). A system for stable expression of short interfering RNAs in mammalian cells. Science *296*, 550-553.

21. Burnette, W. N. (1981). "Western blotting": electrophoretic transfer of proteins from sodium dodecyl sulfate--polyacrylamide gels to unmodified nitrocellulose and radiographic detection with antibody and radioiodinated protein A. Anal Biochem *112*, 195-203.

22. Caplen, N. J., Parrish, S., Imani, F., Fire, A., and Morgan, R. A. (2001). Specific inhibition of gene expression by small double-stranded RNAs in invertebrate and vertebrate systems. Proc Natl Acad Sci U S A *98*, 9742-9747.

23. Carpten, J., Nupponen, N., Isaacs, S., Sood, R., Robbins, C., Xu, J., Faruque, M., Moses, T., Ewing, C., Gillanders, E., *et al.* (2002). Germline mutations in the ribonuclease L gene in families showing linkage with HPC1. Nat Genet *30*, 181-184.

24. Carter, B. S., Beaty, T. H., Steinberg, G. D., Childs, B., and Walsh, P. C. (1992a). Mendelian inheritance of familial prostate cancer. Proc Natl Acad Sci U S A *89*, 3367-3371.

25. Carter, B. S., Bova, G. S., Beaty, T. H., Steinberg, G. D., Childs, B., Isaacs, W. B., and Walsh, P. C. (1993). Hereditary prostate cancer: epidemiologic and clinical features. J Urol *150*, 797-802.

26. Carter, H. B., Morrell, C. H., Pearson, J. D., Brant, L. J., Plato, C. C., Metter, E. J., Chan, D. W., Fozard, J. L., and Walsh, P. C. (1992b). Estimation of prostatic growth using serial prostate-specific antigen measurements in men with and without prostate disease. Cancer Res *52*, 3323-3328.

27. Carter, H. B., Pearson, J. D., Metter, E. J., Brant, L. J., Chan, D. W., Andres, R., Fozard, J. L., and Walsh, P. C. (1992c). Longitudinal evaluation of prostate-specific antigen levels in men with and without prostate disease. Jama *267*, 2215-2220.

28. Celis, A., Rasmussen, H. H., Celis, P., Basse, B., Lauridsen, J. B., Ratz, G., Hein, B., Ostergaard, M., Wolf, H., Orntoft, T., and Celis, J. E. (1999). Short-term culturing of low-grade superficial bladder transitional cell carcinomas leads to changes in the expression levels of several proteins involved in key cellular activities. Electrophoresis *20*, 355-361.

29. Chen, C. D., Welsbie, D. S., Tran, C., Baek, S. H., Chen, R., Vessella, R., Rosenfeld, M. G., and Sawyers, C. L. (2004). Molecular determinants of resistance to antiandrogen therapy. Nat Med *10*, 33-39.

30. Chen, H., Ke, Y., Oates, A. J., Barraclough, R., and Rudland, P. S. (1997). Isolation of and effector for metastasis-inducing DNAs from a human metastatic carcinoma cell line. Oncogene *14*, 1581-1588.

31. Chen, H. J., Treweeke, A. T., Ke, Y. Q., West, D. C., and Toh, C. H. (2000). Angiogenically active vascular endothelial growth factor is over-expressed in malignant human and rat prostate carcinoma cells. Br J Cancer *82*, 1694-1701.

32. Cher, M. L., Bova, G. S., Moore, D. H., Small, E. J., Carroll, P. R., Pin, S. S., Epstein, J. I., Isaacs, W. B., and Jensen, R. H. (1996). Genetic alterations in untreated metastases and androgen-independent prostate cancer detected by comparative genomic hybridization and allelotyping. Cancer Res *56*, 3091-3102.

33. Chevalier, S., Defoy, I., Lacoste, J., Hamel, L., Guy, L., Begin, L. R., and Aprikian, A. G. (2002). Vascular endothelial growth factor and signaling in the prostate: more than angiogenesis. Mol Cell Endocrinol *189*, 169-179.

34. Chien, J., Wong, E., Nikes, E., Noble, M. J., Pantazis, C. G., and Shah, G. V. (1999). Constitutive activation of stimulatory guanine nucleotide binding protein (G(S)alphaQL)-mediated signaling increases invasiveness and tumorigenicity of PC-3M prostate cancer cells. Oncogene *18*, 3376-3382.

35. Cifone, M. A., and Fidler, I. J. (1981). Increasing metastatic potential is associated with increasing genetic instability of clones isolated from murine neoplasms. Proc Natl Acad Sci U S A *78*, 6949-6952.

36. Clarke, S. D. (2000). Polyunsaturated fatty acid regulation of gene transcription: a mechanism to improve energy balance and insulin resistance. Br J Nutr *83 Suppl 1*, S59-66.

37. Cohen, S. N., Chang, A. C., and Hsu, L. (1972). Nonchromosomal antibiotic resistance in bacteria: genetic transformation of Escherichia coli by R-factor DNA. Proc Natl Acad Sci U S A *69*, 2110-2114.

38. Collett, G. P., Betts, A. M., Johnson, M. I., Pulimood, A. B., Cook, S., Neal, D. E., and Robson, C. N. (2000). Peroxisome proliferator-activated receptor alpha is an androgen-responsive gene in human prostate and is highly expressed in prostatic adenocarcinoma. Clin Cancer Res *6*, 3241-3248.

39. Colosimo, A., Goncz, K. K., Holmes, A. R., Kunzelmann, K., Novelli, G., Malone, R. W., Bennett, M. J., and Gruenert, D. C. (2000). Transfer and expression of foreign genes in mammalian cells. Biotechniques *29*, 314-318, 320-312, 324 passim.

40. Cook, L. S., Goldoft, M., Schwartz, S. M., and Weiss, N. S. (1999). Incidence of adenocarcinoma of the prostate in Asian immigrants to the United States and their descendants. J Urol *161*, 152-155.

41. Cowen, D., Troncoso, P., Khoo, V. S., Zagars, G. K., von Eschenbach, A. C., Meistrich, M. L., and Pollack, A. (2002). Ki-67 staining is an independent correlate of biochemical failure in prostate cancer treated with radiotherapy. Clin Cancer Res *8*, 1148-1154.

42. Craft, N., Shostak, Y., Carey, M., and Sawyers, C. L. (1999). A mechanism for hormone-independent prostate cancer through modulation of androgen receptor signaling by the HER-2/neu tyrosine kinase. Nat Med *5*, 280-285.

43. Crawford, E. D. (2003). Epidemiology of prostate cancer. Urology *62*, 3-12.

44. Culig, Z., Hobisch, A., Bartsch, G., and Klocker, H. (2000). Androgen receptor--an update of mechanisms of action in prostate cancer. Urol Res *28*, 211-219.

45. Culig, Z., Hobisch, A., Cronauer, M. V., Radmayr, C., Trapman, J., Hittmair, A., Bartsch, G., and Klocker, H. (1994). Androgen receptor activation in prostatic tumor cell lines by insulin-like growth factor-I, keratinocyte growth factor, and epidermal growth factor. Cancer Res *54*, 5474-5478.

46. Culig, Z., Klocker, H., Bartsch, G., and Hobisch, A. (2002). Androgen receptors in prostate cancer. Endocr Relat Cancer *9*, 155-170.

47. Cvetkovic, D., Movsas, B., Dicker, A. P., Hanlon, A. L., Greenberg, R. E., Chapman, J. D., Hanks, G. E., and Tricoli, J. V. (2001). Increased hypoxia correlates with increased expression of the angiogenesis marker vascular endothelial growth factor in human prostate cancer. Urology *57*, 821-825.

48. Davies, B. R., Barraclough, R., and Rudland, P. S. (1994). Induction of metastatic ability in a stably diploid benign rat mammary epithelial cell line by transfection with DNA from human malignant breast carcinoma cell lines. Cancer Res *54*, 2785-2793.

49. Deshmukh, N., Scotson, J., Dodson, A. R., Smith, P. H., Ke, Y., and Foster, C. S. (1997). Differential expression of acidic and basic fibroblast growth factors in benign prostatic hyperplasia identified by immunohistochemistry. Br J Urol *80*, 869-874.

50. Desvergne, B., and Wahli, W. (1999). Peroxisome proliferator-activated receptors: nuclear control of metabolism. Endocr Rev *20*, 649-688.

51. Di Cristofano, A., Pesce, B., Cordon-Cardo, C., and Pandolfi, P. P. (1998). Pten is essential for embryonic development and tumour suppression. Nat Genet *19*, 348-355.

52. Ding, G. F., Li, J. C., Xu, Y. F., Sun, Y., and Tao, L. (2005a). [Correlation between the expression of VEGF-C mRNA, VEGFR-3, CD31 and tumor metastases in Chinese with prostate cancer]. Shi Yan Sheng Wu Xue Bao *38*, 257-264.

53. Ding, Y. B., Shi, R. H., Tong, J. D., Li, X. Y., Zhang, G. X., Xiao, W. M., Yang, J. G., Bao, Y., Wu, J., Yan, Z. G., and Wang, X. H. (2005b). PGE2 up-regulates vascular endothelial growth factor expression in MKN28 gastric cancer cells via epidermal growth factor receptor signaling system. Exp Oncol *27*, 108-113.

54. Dong, J. T. (2006). Prevalent mutations in prostate cancer. J Cell Biochem *97*, 433-447.

55. Ebner, R., and Derynck, R. (1991). Epidermal growth factor and transforming growth factor-alpha: differential intracellular routing and processing of ligand-receptor complexes. Cell Regul *2*, 599-612.

56. Edlund, M., Sung, S. Y., and Chung, L. W. (2004). Modulation of prostate cancer growth in bone microenvironments. J Cell Biochem *91*, 686-705.

57. Elbashir, S. M., Harborth, J., Lendeckel, W., Yalcin, A., Weber, K., and Tuschl, T. (2001). Duplexes of 21-nucleotide RNAs mediate RNA interference in cultured mammalian cells. Nature *411*, 494-498.

58. Epstein, J. I., Carmichael, M., and Partin, A. W. (1995). OA-519 (fatty acid synthase) as an independent predictor of pathologic state in adenocarcinoma of the prostate. Urology *45*, 81-86.

59. Etminan, M., Fitzgerald, J. M., Gleave, M., and Chambers, K. (2005). Intake of Selenium in the Prevention of Prostate Cancer: a Systematic Review and Meta-analysis*. Cancer Causes Control *16*, 1125-1131.

60. Fahimi, H. D., Voelkl, A., Vincent, S. H., and Muller-Eberhard, U. (1990). Localization of the heme-binding protein in the cytoplasm and of a heme-binding protein-like immunoreactive protein in the nucleus of rat liver parenchymal cells: immunocytochemical evidence of the subcellular distribution corroborated by radioimmunoassay and immunoblotting. Hepatology *11*, 859-865.

61. Feinberg, A. P., and Vogelstein, B. (1983). A technique for radiolabeling DNA restriction endonuclease fragments to high specific activity. Anal Biochem *132*, 6-13.

62. Feinberg, A. P., and Vogelstein, B. (1984). "A technique for radiolabeling DNA restriction endonuclease fragments to high specific activity". Addendum. Anal Biochem *137*, 266-267.

63. Feldman, B. J., and Feldman, D. (2001). The development of androgen-independent prostate cancer. Nat Rev Cancer *1*, 34-45.

64. Ferrara, N., Gerber, H. P., and LeCouter, J. (2003). The biology of VEGF and its receptors. Nat Med *9*, 669-676.

65. Ferrer, F. A., Miller, L. J., Andrawis, R. I., Kurtzman, S. H., Albertsen, P. C., Laudone, V. P., and Kreutzer, D. L. (1997). Vascular endothelial growth factor

(VEGF) expression in human prostate cancer: in situ and in vitro expression of VEGF by human prostate cancer cells. J Urol *157*, 2329-2333.

66. Fidler, I. J. (1970). Metastasis: guantitative analysis of distribution and fate of tumor embolilabeled with 125 I-5-iodo-2'-deoxyuridine. J Natl Cancer Inst *45*, 773-782.
67. Fire, A., Xu, S., Montgomery, M. K., Kostas, S. A., Driver, S. E., and Mello, C. C. (1998). Potent and specific genetic interference by double-stranded RNA in Caenorhabditis elegans. Nature *391*, 806-811.
68. Foster, C. S., Cornford, P., Forsyth, L., Djamgoz, M. B., and Ke, Y. (1999). The cellular and molecular basis of prostate cancer. BJU Int *83*, 171-194.
69. Foster, C. S., and Ke, Y. (1997). Stem cells in prostatic epithelia. Int J Exp Pathol *78*, 311-329.
70. Friend, D. S., Papahadjopoulos, D., and Debs, R. J. (1996). Endocytosis and intracellular processing accompanying transfection mediated by cationic liposomes. Biochim Biophys Acta *1278*, 41-50.
71. Frohnert, B. I., and Bernlohr, D. A. (2000). Regulation of fatty acid transporters in mammalian cells. Prog Lipid Res *39*, 83-107.
72. Gaddipati, J. P., McLeod, D. G., Heidenberg, H. B., Sesterhenn, I. A., Finger, M. J., Moul, J. W., and Srivastava, S. (1994). Frequent detection of codon 877 mutation in the androgen receptor gene in advanced prostate cancers. Cancer Res *54*, 2861-2864.
73. Gao, A. C., Lou, W., and Isaacs, J. T. (1998). Down-regulation of homeobox gene GBX2 expression inhibits human prostate cancer clonogenic ability and tumorigenicity. Cancer Res *58*, 1391-1394.
74. Gioeli, D. (2005). Signal transduction in prostate cancer progression. Clin Sci (Lond) *108*, 293-308.

75. Glatz, J. F., and Storch, J. (2001). Unravelling the significance of cellular fatty acid-binding proteins. Curr Opin Lipidol *12*, 267-274.

76. Glatz, J. F., and van der Vusse, G. J. (1996). Cellular fatty acid-binding proteins: their function and physiological significance. Prog Lipid Res *35*, 243-282.

77. Goldberg, D. A. (1980). Isolation and partial characterization of the Drosophila alcohol dehydrogenase gene. Proc Natl Acad Sci U S A *77*, 5794-5798.

78. Grau, R., Iniguez, M. A., and Fresno, M. (2004). Inhibition of activator protein 1 activation, vascular endothelial growth factor, and cyclooxygenase-2 expression by 15-deoxy-Delta12,14-prostaglandin J2 in colon carcinoma cells: evidence for a redox-sensitive peroxisome proliferator-activated receptor-gamma-independent mechanism. Cancer Res *64*, 5162-5171.

79. Green, D. W., Roh, H., Pippin, J., and Drebin, J. A. (2000). Antisense oligonucleotides: an evolving technology for the modulation of gene expression in human disease. J Am Coll Surg *191*, 93-105.

80. Gronberg, H., Isaacs, S. D., Smith, J. R., Carpten, J. D., Bova, G. S., Freije, D., Xu, J., Meyers, D. A., Collins, F. S., Trent, J. M., *et al.* (1997). Characteristics of prostate cancer in families potentially linked to the hereditary prostate cancer 1 (HPC1) locus. Jama *278*, 1251-1255.

81. Guo, S., and Kemphues, K. J. (1995). par-1, a gene required for establishing polarity in C. elegans embryos, encodes a putative Ser/Thr kinase that is asymmetrically distributed. Cell *81*, 611-620.

82. Gupta, S., Srivastava, M., Ahmad, N., Bostwick, D. G., and Mukhtar, H. (2000). Over-expression of cyclooxygenase-2 in human prostate adenocarcinoma. Prostate *42*, 73-78.

83. Habib, F. K., Ross, M., Bayne, C. W., Bollina, P., Grigor, K., and Chapman, K. (2003). The loss of 5alpha-reductase type I and type II mRNA expression in metastatic prostate cancer to bone and lymph node metastasis. Clin Cancer Res *9*, 1815-1819.

84. Haggman, M. J., Wojno, K. J., Pearsall, C. P., and Macoska, J. A. (1997). Allelic loss of 8p sequences in prostatic intraepithelial neoplasia and carcinoma. Urology *50*, 643-647.

85. Hamilton, J. A., and Kamp, F. (1999). How are free fatty acids transported in membranes? Is it by proteins or by free diffusion through the lipids? Diabetes *48*, 2255-2269.

86. Hanahan, D., and Folkman, J. (1996). Patterns and emerging mechanisms of the angiogenic switch during tumorigenesis. Cell *86*, 353-364.

87. Hannon, G. J. (2002). RNA interference. Nature *418*, 244-251.

88. Harper, M. E., Glynne-Jones, E., Goddard, L., Wilson, D. W., Matenhelia, S. S., Conn, I. G., Peeling, W. B., and Griffiths, K. (1992). Relationship of proliferating cell nuclear antigen (PCNA) in prostatic carcinomas to various clinical parameters. Prostate *20*, 243-253.

89. Harris, S. E., Harris, M. A., Mahy, P., Wozney, J., Feng, J. Q., and Mundy, G. R. (1994). Expression of bone morphogenetic protein messenger RNAs by normal rat and human prostate and prostate cancer cells. Prostate *24*, 204-211.

90. Haunerland, N. H., and Spener, F. (2004). Fatty acid-binding proteins--insights from genetic manipulations. Prog Lipid Res *43*, 328-349.

91. Hayes, S. A., Huang, X., Kambhampati, S., Platanias, L. C., and Bergan, R. C. (2003). p38 MAP kinase modulates Smad-dependent changes in human prostate cell adhesion. Oncogene *22*, 4841-4850.

92. He, W. W., Sciavolino, P. J., Wing, J., Augustus, M., Hudson, P., Meissner, P. S., Curtis, R. T., Shell, B. K., Bostwick, D. G., Tindall, D. J., *et al.* (1997). A novel human prostate-specific, androgen-regulated homeobox gene (NKX3.1) that maps to 8p21, a region frequently deleted in prostate cancer. Genomics *43*, 69-77.

93. Hobisch, A., Culig, Z., Radmayr, C., Bartsch, G., Klocker, H., and Hittmair, A. (1995). Distant metastases from prostatic carcinoma express androgen receptor protein. Cancer Res *55*, 3068-3072.

94. Hobisch, A., Culig, Z., Radmayr, C., Bartsch, G., Klocker, H., and Hittmair, A. (1996). Androgen receptor status of lymph node metastases from prostate cancer. Prostate *28*, 129-135.

95. Horoszewicz, J. S., Leong, S. S., Kawinski, E., Karr, J. P., Rosenthal, H., Chu, T. M., Mirand, E. A., and Murphy, G. P. (1983). LNCaP model of human prostatic carcinoma. Cancer Res *43*, 1809-1818.

96. Huang, X., Chen, S., Xu, L., Liu, Y., Deb, D. K., Platanias, L. C., and Bergan, R. C. (2005). Genistein inhibits p38 map kinase activation, matrix metalloproteinase type 2, and cell invasion in human prostate epithelial cells. Cancer Res *65*, 3470-3478.

97. Hughes-Fulford, M., Tjandrawinata, R. R., Li, C. F., and Sayyah, S. (2005). Arachidonic acid, an omega-6 fatty acid, induces cytoplasmic phospholipase A2 in prostate carcinoma cells. Carcinogenesis *26*, 1520-1526.

98. Huss, W. J., Hanrahan, C. F., Barrios, R. J., Simons, J. W., and Greenberg, N. M. (2001). Angiogenesis and prostate cancer: identification of a molecular progression switch. Cancer Res *61*, 2736-2743.

99. Ikeda, I., Miura, T., and Kondo, I. (1996). Pyridinium cross-links as urinary markers of bone metastases in patients with prostate cancer. Br J Urol *77*, 102-106.

100. Ittmann, M. M., and Wieczorek, R. (1996). Alterations of the retinoblastoma gene in clinically localized, stage B prostate adenocarcinomas. Hum Pathol *27*, 28-34.

101. Jamieson, S., Barraclough, R., and Rudland, P. S. (1990). Generation of metastatic variants by transfection of a nonmetastatic rat mammary epithelial cell line with DNA from a metastatic rat mammary cell line. Pathobiology *58*, 329-342.

102. Jarrard, D. F., Bova, G. S., Ewing, C. M., Pin, S. S., Nguyen, S. H., Baylin, S. B., Cairns, P., Sidransky, D., Herman, J. G., and Isaacs, W. B. (1997). Deletional, mutational, and methylation analyses of CDKN2 (p16/MTS1) in primary and metastatic prostate cancer. Genes Chromosomes Cancer *19*, 90-96.

103. Jing, C., Beesley, C., Foster, C. S., Chen, H., Rudland, P. S., West, D. C., Fujii, H., Smith, P. H., and Ke, Y. (2001). Human cutaneous fatty acid-binding protein induces metastasis by up-regulating the expression of vascular endothelial growth factor gene in rat Rama 37 model cells. Cancer Res *61*, 4357-4364.

104. Jing, C., Beesley, C., Foster, C. S., Rudland, P. S., Fujii, H., Ono, T., Chen, H., Smith, P. H., and Ke, Y. (2000a). Identification of the messenger RNA for human cutaneous fatty acid-binding protein as a metastasis inducer. Cancer Res *60*, 2390-2398.

105. Jing, C., Rudland, P. S., Foster, C. S., and Ke, Y. (2000b). Microquantity differential display: a strategy for a systematic analysis of differential gene expression with a small quantity of starting RNA. Anal Biochem *287*, 334-337.

106. K, G., and S, K., eds. (2003). Molecular Mechanism of Prostate Cancer Invasion and Metastasis (Academic Press).

107. Kaighn, M. E., Lechner, J. F., Narayan, K. S., and Jones, L. W. (1978). Prostate carcinoma: tissue culture cell lines. Natl Cancer Inst Monogr, 17-21.

108. Karan, D., Lin, M. F., Johansson, S. L., and Batra, S. K. (2003). Current status of the molecular genetics of human prostatic adenocarcinomas. Int J Cancer *103*, 285-293.

109. Ke, Y., Beesley, C., Smith, P., Barraclough, R., Rudland, P., and Foster, C. S. (1998). Generation of metastatic variants by transfection of a rat non-metastatic epithelial cell line with genomic DNA from rat prostatic carcinoma cells. Br J Cancer *77*, 287-296.

110. Ke, Y., Jing, C., Rudland, P. S., Smith, P. H., and Foster, C. S. (1999). Systematic comparison of gene expression through analysis of cDNA fragments within or near to the protein-coding region. Nucleic Acids Res *27*, 912-914.

111. Keller, E. T. (2002). The role of osteoclastic activity in prostate cancer skeletal metastases. Drugs Today (Barc) *38*, 91-102.

112. Keller, E. T., and Brown, J. (2004). Prostate cancer bone metastases promote both osteolytic and osteoblastic activity. J Cell Biochem *91*, 718-729.

113. Kleihues, P., Schauble, B., zur Hausen, A., Esteve, J., and Ohgaki, H. (1997). Tumors associated with p53 germline mutations: a synopsis of 91 families. Am J Pathol *150*, 1-13.

114. Kleinfeld, A. M. (2000). Lipid phase fatty acid flip-flop, is it fast enough for cellular transport? J Membr Biol *175*, 79-86.

115. Knudson, A. G., Jr. (1977). Genetics and etiology of human cancer. Adv Hum Genet *8*, 1-66.

116. Kozlowski, J. M., Fidler, I. J., Campbell, D., Xu, Z. L., Kaighn, M. E., and Hart, I. R. (1984). Metastatic behavior of human tumor cell lines grown in the nude mouse. Cancer Res *44*, 3522-3529.

117. Krajewski, S., Krajewska, M., Shabaik, A., Miyashita, T., Wang, H. G., and Reed, J. C. (1994a). Immunohistochemical determination of in vivo distribution of Bax, a dominant inhibitor of Bcl-2. Am J Pathol *145*, 1323-1336.

118. Krajewski, S., Krajewska, M., Shabaik, A., Wang, H. G., Irie, S., Fong, L., and Reed, J. C. (1994b). Immunohistochemical analysis of in vivo patterns of Bcl-X expression. Cancer Res *54*, 5501-5507.

119. Labrie, F., Belanger, A., Dupont, A., Luu-The, V., Simard, J., and Labrie, C. (1993). Science behind total androgen blockade: from gene to combination therapy. Clin Invest Med *16*, 475-492.

120. Labrie, F., Dupont, A., Belanger, A., St-Arnaud, R., Giguere, M., Lacourciere, Y., Emond, J., and Monfette, G. (1986). Treatment of prostate cancer with gonadotropin-releasing hormone agonists. Endocr Rev *7*, 67-74.

121. Larsson, S. C., Kumlin, M., Ingelman-Sundberg, M., and Wolk, A. (2004). Dietary long-chain n-3 fatty acids for the prevention of cancer: a review of potential mechanisms. Am J Clin Nutr *79*, 935-945.

122. Lenferink, A. E., Kramer, R. H., van Vugt, M. J., Konigswieser, M., Di Fiore, P. P., van Zoelen, E. J., and van de Poll, M. L. (1997). Superagonistic behaviour of epidermal growth factor/transforming growth factor-alpha chimaeras: correlation with receptor routing after ligand-induced internalization. Biochem J *327 (Pt 3)*, 859-865.

123. Li, C., Larsson, C., Futreal, A., Lancaster, J., Phelan, C., Aspenblad, U., Sundelin, B., Liu, Y., Ekman, P., Auer, G., and Bergerheim, U. S. (1998). Identification of two distinct deleted regions on chromosome 13 in prostate cancer. Oncogene *16*, 481-487.

124. Li, J., Yen, C., Liaw, D., Podsypanina, K., Bose, S., Wang, S. I., Puc, J., Miliaresis, C., Rodgers, L., McCombie, R., *et al.* (1997). PTEN, a putative protein tyrosine

phosphatase gene mutated in human brain, breast, and prostate cancer. Science *275*, 1943-1947.

125. Liu, A. Y., True, L. D., LaTray, L., Nelson, P. S., Ellis, W. J., Vessella, R. L., Lange, P. H., Hood, L., and van den Engh, G. (1997). Cell-cell interaction in prostate gene regulation and cytodifferentiation. Proc Natl Acad Sci U S A *94*, 10705-10710.

126. Lu, Q. L., Abel, P., Foster, C. S., and Lalani, E. N. (1996). bcl-2: role in epithelial differentiation and oncogenesis. Hum Pathol *27*, 102-110.

127. Luukko, K., Ylikorkala, A., Tiainen, M., and Makela, T. P. (1999). Expression of LKB1 and PTEN tumor suppressor genes during mouse embryonic development. Mech Dev *83*, 187-190.

128. Makridakis, N., Ross, R. K., Pike, M. C., Chang, L., Stanczyk, F. Z., Kolonel, L. N., Shi, C. Y., Yu, M. C., Henderson, B. E., and Reichardt, J. K. (1997). A prevalent missense substitution that modulates activity of prostatic steroid 5alpha-reductase. Cancer Res *57*, 1020-1022.

129. Marcelli, M., Ittmann, M., Mariani, S., Sutherland, R., Nigam, R., Murthy, L., Zhao, Y., DiConcini, D., Puxeddu, E., Esen, A., *et al.* (2000). Androgen receptor mutations in prostate cancer. Cancer Res *60*, 944-949.

130. Martin, G., Schoonjans, K., Lefebvre, A. M., Staels, B., and Auwerx, J. (1997). Coordinate regulation of the expression of the fatty acid transport protein and acyl-CoA synthetase genes by PPARalpha and PPARgamma activators. J Biol Chem *272*, 28210-28217.

131. Masood, R., Cai, J., Zheng, T., Smith, D. L., Hinton, D. R., and Gill, P. S. (2001). Vascular endothelial growth factor (VEGF) is an autocrine growth factor for VEGF receptor-positive human tumors. Blood *98*, 1904-1913.

132. Masouye, I., Saurat, J. H., and Siegenthaler, G. (1996). Epidermal fatty-acid-binding protein in psoriasis, basal and squamous cell carcinomas: an immunohistological study. Dermatology *192*, 208-213.

133. McDonnell, T. J., Troncoso, P., Brisbay, S. M., Logothetis, C., Chung, L. W., Hsieh, J. T., Tu, S. M., and Campbell, M. L. (1992). Expression of the protooncogene bcl-2 in the prostate and its association with emergence of androgen-independent prostate cancer. Cancer Res *52*, 6940-6944.

134. McLoughlin, J., Foster, C. S., Price, P., Williams, G., and Abel, P. D. (1993). Evaluation of Ki-67 monoclonal antibody as prognostic indicator for prostatic carcinoma. Br J Urol *72*, 92-97.

135. McNeal, J. E., and Bostwick, D. G. (1986). Intraductal dysplasia: a premalignant lesion of the prostate. Hum Pathol *17*, 64-71.

136. Meyer, J. P., and Gillatt, D. A. (2002). Can diet affect prostate cancer? BJU Int *89*, 250-254.

137. Montironi, R., Mazzucchelli, R., Algaba, F., and Lopez-Beltran, A. (2000). Morphological identification of the patterns of prostatic intraepithelial neoplasia and their importance. J Clin Pathol *53*, 655-665.

138. Mulligan, J. M., Mai, K. T., Parks, W., and Gerridzen, R. G. (1997). Proliferating cell nuclear antigen (PCNA) and MIB 1: Markers of locally advanced and biologically aggressive prostate cancer. Can J Urol *4*, 422-425.

139. Mydlo, J., and Godec, C. J. (2003). Prostate cancer: science and clinical practice (Amsterdam; London: Academic Press).

140. Neufeld, G., Cohen, T., Gengrinovitch, S., and Poltorak, Z. (1999). Vascular endothelial growth factor (VEGF) and its receptors. Faseb J *13*, 9-22.

141. Novakofski, J. (2004). Adipogenesis: usefulness of in vitro and in vivo experimental models. J Anim Sci *82*, 905-915.

142. Ostergaard, M., Rasmussen, H. H., Nielsen, H. V., Vorum, H., Orntoft, T. F., Wolf, H., and Celis, J. E. (1997). Proteome profiling of bladder squamous cell carcinomas: identification of markers that define their degree of differentiation. Cancer Res *57*, 4111-4117.

143. Owada, Y., Suzuki, I., Noda, T., and Kondo, H. (2002a). Analysis on the phenotype of E-FABP-gene knockout mice. Mol Cell Biochem *239*, 83-86.

144. Owada, Y., Takano, H., Yamanaka, H., Kobayashi, H., Sugitani, Y., Tomioka, Y., Suzuki, I., Suzuki, R., Terui, T., Mizugaki, M., *et al.* (2002b). Altered water barrier function in epidermal-type fatty acid binding protein-deficient mice. J Invest Dermatol *118*, 430-435.

145. Paget, S. (1889). The distribution of secondary growths in cancer of the breast. Lancet *1*, 571-573.

146. Pandian, S., Heys, S. D., Wahle, K. W. J., and McClinton, S. (2000). Dietary Fat and Prostate Cancer: A Review. The prostate journal *2*, 123 - 129.

147. Pegorier, J. P., Le May, C., and Girard, J. (2004). Control of gene expression by fatty acids. J Nutr *134*, 2444S-2449S.

148. Pilat, M. J., Kamradt, J. M., and Pienta, K. J. (1998). Hormone resistance in prostate cancer. Cancer Metastasis Rev *17*, 373-381.

149. Platt, N., and Gordon, S. (2001). Is the class A macrophage scavenger receptor (SR-A) multifunctional? - The mouse's tale. J Clin Invest *108*, 649-654.

150. Prehn, R. T. (1999). On the prevention and therapy of prostate cancer by androgen administration. Cancer Res *59*, 4161-4164.

151. Pugh, C. W., and Ratcliffe, P. J. (2003). Regulation of angiogenesis by hypoxia: role of the HIF system. Nat Med *9*, 677-684.

152. Qi, C., Zhu, Y., and Reddy, J. K. (2000). Peroxisome proliferator-activated receptors, coactivators, and downstream targets. Cell Biochem Biophys *32 Spring*, 187-204.

153. Reed, J. C. (1994). Bcl-2 and the regulation of programmed cell death. J Cell Biol *124*, 1-6.

154. Rennert, H., Zeigler-Johnson, C. M., Addya, K., Finley, M. J., Walker, A. H., Spangler, E., Leonard, D. G., Wein, A., Malkowicz, S. B., and Rebbeck, T. R. (2005). Association of susceptibility alleles in ELAC2/HPC2, RNASEL/HPC1, and MSR1 with prostate cancer severity in European American and African American men. Cancer Epidemiol Biomarkers Prev *14*, 949-957.

155. Roodman, G. D. (2004). Mechanisms of bone metastasis. N Engl J Med *350*, 1655-1664.

156. Rosen, E. D., and Spiegelman, B. M. (2001). Journal of Biological Chemistry *276*, 37741 37744.

157. Ross, A. C. (1993). Cellular metabolism and activation of retinoids: roles of cellular retinoid-binding proteins. Faseb J *7*, 317-327.

158. Rossi, S., Graner, E., Febbo, P., Weinstein, L., Bhattacharya, N., Onody, T., Bubley, G., Balk, S., and Loda, M. (2003). Fatty acid synthase expression defines distinct molecular signatures in prostate cancer. Mol Cancer Res *1*, 707-715.

159. Rubenstein, M., Slobodskoy, L., Mirochnik, Y., and Guinan, P. (2002). Backbone modification alters the efficacy of antisense oligonucleotides directed against mRNA encoding either TGF-alpha or EGFR in the treatment of prostate cancer cell lines. Methods Find Exp Clin Pharmacol *24*, 649-652.

160. Sakr, W. A., Grignon, D. J., and Haas, G. P. (1998). Pathology of premalignant lesions and carcinoma of the prostate in African-American men. Semin Urol Oncol *16*, 214-220.

161. Sakr, W. A., Haas, G. P., Cassin, B. F., Pontes, J. E., and Crissman, J. D. (1993). The frequency of carcinoma and intraepithelial neoplasia of the prostate in young male patients. J Urol *150*, 379-385.

162. Sakr, W. A., Macoska, J. A., Benson, P., Grignon, D. J., Wolman, S. R., Pontes, J. E., and Crissman, J. D. (1994). Allelic loss in locally metastatic, multisampled prostate cancer. Cancer Res *54*, 3273-3277.

163. Sato, Y. (2003). Molecular diagnosis of tumor angiogenesis and anti-angiogenic cancer therapy. Int J Clin Oncol *8*, 200-206.

164. Savinainen, K. J., Saramaki, O. R., Linja, M. J., Bratt, O., Tammela, T. L., Isola, J. J., and Visakorpi, T. (2002). Expression and gene copy number analysis of ERBB2 oncogene in prostate cancer. Am J Pathol *160*, 339-345.

165. Schaid, D. J. (2004). The complex genetic epidemiology of prostate cancer. Hum Mol Genet *13 Spec No 1*, R103-121.

166. Scher, H. I., Sarkis, A., Reuter, V., Cohen, D., Netto, G., Petrylak, D., Lianes, P., Fuks, Z., Mendelsohn, J., and Cordon-Cardo, C. (1995). Changing pattern of expression of the epidermal growth factor receptor and transforming growth factor alpha in the progression of prostatic neoplasms. Clin Cancer Res *1*, 545-550.

167. Schleicher, C. H., Cordoba, O. L., Santome, J. A., and Dell'Angelica, E. C. (1995). Molecular evolution of the multigene family of intracellular lipid-binding proteins. Biochem Mol Biol Int *36*, 1117-1125.

168. Seed, B. (1982). Diazotizable arylamine cellulose papers for the coupling and hybridization of nucleic acids. Nucleic Acids Res *10*, 1799-1810.

susceptibility locus for prostate cancer on chromosome 1 suggested by a genome-wide search. Science *274*, 1371-1374.

177. Smith, P., Rhodes, N. P., Shortland, A. P., Fraser, S. P., Djamgoz, M. B., Ke, Y., and Foster, C. S. (1998). Sodium channel protein expression enhances the invasiveness of rat and human prostate cancer cells. FEBS Lett *423*, 19-24.

178. Southern, E. M. (1975). Detection of specific sequences among DNA fragments separated by gel electrophoresis. J Mol Biol *98*, 503-517.

179. Stanbridge, E. J. (1990). Human tumor suppressor genes. Annu Rev Genet *24*, 615-657.

180. Stewart, L. V., Lyles, B., Lin, M. F., and Weigel, N. L. (2005). Vitamin D receptor agonists induce prostatic acid phosphatase to reduce cell growth and HER-2 signaling in LNCaP-derived human prostate cancer cells. J Steroid Biochem Mol Biol.

181. Sun, H., Lesche, R., Li, D. M., Liliental, J., Zhang, H., Gao, J., Gavrilova, N., Mueller, B., Liu, X., and Wu, H. (1999). PTEN modulates cell cycle progression and cell survival by regulating phosphatidylinositol 3,4,5,-trisphosphate and Akt/protein kinase B signaling pathway. Proc Natl Acad Sci U S A *96*, 6199-6204.

182. Sun, J., Hsu, F. C., Turner, A. R., Zheng, S. L., Chang, B. L., Liu, W., Isaacs, W. B., and Xu, J. (2006). Meta-analysis of association of rare mutations and common sequence variants in the MSR1 gene and prostate cancer risk. Prostate.

183. Suzuki, H., Freije, D., Nusskern, D. R., Okami, K., Cairns, P., Sidransky, D., Isaacs, W. B., and Bova, G. S. (1998). Interfocal heterogeneity of PTEN/MMAC1 gene alterations in multiple metastatic prostate cancer tissues. Cancer Res *58*, 204-209.

184. Swinnen, J. V., Roskams, T., Joniau, S., Van Poppel, H., Oyen, R., Baert, L., Heyns, W., and Verhoeven, G. (2002). Overexpression of fatty acid synthase is an

early and common event in the development of prostate cancer. Int J Cancer *98*, 19-22.

185. Swinnen, J. V., Vanderhoydonc, F., Elgamal, A. A., Eelen, M., Vercaeren, I., Joniau, S., Van Poppel, H., Baert, L., Goossens, K., Heyns, W., and Verhoeven, G. (2000). Selective activation of the fatty acid synthesis pathway in human prostate cancer. Int J Cancer *88*, 176-179.

186. Taftachi, R., Ayhan, A., Ekici, S., Ergen, A., and Ozen, H. (2005). Proliferating-cell nuclear antigen (PCNA) as an independent prognostic marker in patients after prostatectomy: a comparison of PCNA and Ki-67. BJU Int *95*, 650-654.

187. Takaku, H., Minagawa, A., Takagi, M., and Nashimoto, M. (2003). A candidate prostate cancer susceptibility gene encodes tRNA 3' processing endoribonuclease. Nucleic Acids Res *31*, 2272-2278.

188. Takeuchi, S., Arai, K., Saitoh, H., Yoshida, K., and Miura, M. (1996). Urinary pyridinoline and deoxypyridinoline as potential markers of bone metastasis in patients with prostate cancer. J Urol *156*, 1691-1695.

189. Taplin, M. E., Bubley, G. J., Shuster, T. D., Frantz, M. E., Spooner, A. E., Ogata, G. K., Keer, H. N., and Balk, S. P. (1995). Mutation of the androgen-receptor gene in metastatic androgen-independent prostate cancer. N Engl J Med *332*, 1393-1398.

190. Tavtigian, S. V., Simard, J., Teng, D. H., Abtin, V., Baumgard, M., Beck, A., Camp, N. J., Carillo, A. R., Chen, Y., Dayananth, P., *et al.* (2001). A candidate prostate cancer susceptibility gene at chromosome 17p. Nat Genet *27*, 172-180.

191. Thomas, P. S. (1980). Hybridization of denatured RNA and small DNA fragments transferred to nitrocellulose. Proc Natl Acad Sci U S A *77*, 5201-5205.

192. Tovar Sepulveda, V. A., and Falzon, M. (2002). Parathyroid hormone-related protein enhances PC-3 prostate cancer cell growth via both autocrine/paracrine and intracrine pathways. Regul Pept *105*, 109-120.

193. Towbin, H., Staehelin, T., and Gordon, J. (1979). Electrophoretic transfer of proteins from polyacrylamide gels to nitrocellulose sheets: procedure and some applications. Proc Natl Acad Sci U S A *76*, 4350-4354.

194. Tsujii, M., Kawano, S., Tsuji, S., Sawaoka, H., Hori, M., and DuBois, R. N. (1998). Cyclooxygenase regulates angiogenesis induced by colon cancer cells. Cell *93*, 705-716.

195. van Bilsen, M., van der Vusse, G. J., Gilde, A. J., Lindhout, M., and van der Lee, K. A. (2002). Peroxisome proliferator-activated receptors: lipid binding proteins controling gene expression. Mol Cell Biochem *239*, 131-138.

196. Veldscholte, J., Berrevoets, C. A., Ris-Stalpers, C., Kuiper, G. G., Jenster, G., Trapman, J., Brinkmann, A. O., and Mulder, E. (1992). The androgen receptor in LNCaP cells contains a mutation in the ligand binding domain which affects steroid binding characteristics and response to antiandrogens. J Steroid Biochem Mol Biol *41*, 665-669.

197. Vesalainen, S. L., Lipponen, P. K., Talja, M. T., Alhava, E. M., and Syrjanen, K. J. (1994). Proliferating cell nuclear antigen and p53 expression as prognostic factors in T1-2M0 prostatic adenocarcinoma. Int J Cancer *58*, 303-308.

198. Visakorpi, T. (1992). Proliferative activity determined by DNA flow cytometry and proliferating cell nuclear antigen (PCNA) immunohistochemistry as a prognostic factor in prostatic carcinoma. J Pathol *168*, 7-13.

169. Segawa, Y., Yoshimura, R., Hase, T., Nakatani, T., Wada, S., Kawahito, Y., Kishimoto, T., and Sano, H. (2002). Expression of peroxisome proliferator-activated receptor (PPAR) in human prostate cancer. Prostate *51*, 108-116.

170. Shi, Y., and Massague, J. (2003). Mechanisms of TGF-beta signaling from cell membrane to the nucleus. Cell *113*, 685-700.

171. Shimizu, H., Ross, R. K., Bernstein, L., Yatani, R., Henderson, B. E., and Mack, T. M. (1991). Cancers of the prostate and breast among Japanese and white immigrants in Los Angeles County. Br J Cancer *63*, 963-966.

172. Shweiki, D., Itin, A., Soffer, D., and Keshet, E. (1992). Vascular endothelial growth factor induced by hypoxia may mediate hypoxia-initiated angiogenesis. Nature *359*, 843-845.

173. Signoretti, S., Montironi, R., Manola, J., Altimari, A., Tam, C., Bubley, G., Balk, S., Thomas, G., Kaplan, I., Hlatky, L., *et al.* (2000). Her-2-neu expression and progression toward androgen independence in human prostate cancer. J Natl Cancer Inst *92*, 1918-1925.

174. Sinha, P., Hutter, G., Kottgen, E., Dietel, M., Schadendorf, D., and Lage, H. (1999). Increased expression of epidermal fatty acid binding protein, cofilin, and 14-3-3-sigma (stratifin) detected by two-dimensional gel electrophoresis, mass spectrometry and microsequencing of drug-resistant human adenocarcinoma of the pancreas. Electrophoresis *20*, 2952-2960.

175. Small, E. J., and Srinivas, S. (1995). The antiandrogen withdrawal syndrome. Experience in a large cohort of unselected patients with advanced prostate cancer. Cancer *76*, 1428-1434.

176. Smith, J. R., Freije, D., Carpten, J. D., Gronberg, H., Xu, J., Isaacs, S. D., Brownstein, M. J., Bova, G. S., Guo, H., Bujnovszky, P., *et al.* (1996). Major

199. Vlietstra, R. J., van Alewijk, D. C., Hermans, K. G., van Steenbrugge, G. J., and Trapman, J. (1998). Frequent inactivation of PTEN in prostate cancer cell lines and xenografts. Cancer Res *58*, 2720-2723.

200. Voeller, H. J., Augustus, M., Madike, V., Bova, G. S., Carter, K. C., and Gelmann, E. P. (1997). Coding region of NKX3.1, a prostate-specific homeobox gene on 8p21, is not mutated in human prostate cancers. Cancer Res *57*, 4455-4459.

201. Wagner, R. W., Matteucci, M. D., Grant, D., Huang, T., and Froehler, B. C. (1996). Potent and selective inhibition of gene expression by an antisense heptanucleotide. Nat Biotechnol *14*, 840-844.

202. Waltenberger, J., Claesson-Welsh, L., Siegbahn, A., Shibuya, M., and Heldin, C. H. (1994). Different signal transduction properties of KDR and Flt1, two receptors for vascular endothelial growth factor. J Biol Chem *269*, 26988-26995.

203. Wannenes, F., Ciafre, S. A., Niola, F., Frajese, G., and Farace, M. G. (2005). Vector-based RNA interference against vascular endothelial growth factor-A significantly limits vascularization and growth of prostate cancer in vivo. Cancer Gene Ther.

204. Webber, M. M., Bello, D., and Quader, S. (1997). Immortalized and tumorigenic adult human prostatic epithelial cell lines: characteristics and applications Part 2. Tumorigenic cell lines. Prostate *30*, 58-64.

205. White, B. A., and Bancroft, F. C. (1982). Cytoplasmic dot hybridization. Simple analysis of relative mRNA levels in multiple small cell or tissue samples. J Biol Chem *257*, 8569-8572.

206. Xu, J., Zheng, S. L., Carpten, J. D., Nupponen, N. N., Robbins, C. M., Mestre, J., Moses, T. Y., Faith, D. A., Kelly, B. D., Isaacs, S. D., *et al.* (2001). Evaluation of

linkage and association of HPC2/ELAC2 in patients with familial or sporadic prostate cancer. Am J Hum Genet *68*, 901-911.

207. Zamecnik, P. C., and Stephenson, M. L. (1978). Inhibition of Rous sarcoma virus replication and cell transformation by a specific oligodeoxynucleotide. Proc Natl Acad Sci U S A *75*, 280-284.

208. Zegarra-Moro, O. L., Schmidt, L. J., Huang, H., and Tindall, D. J. (2002). Disruption of androgen receptor function inhibits proliferation of androgen-refractory prostate cancer cells. Cancer Res *62*, 1008-1013.

209. Zetter, B. R. (1998). Angiogenesis and tumor metastasis. Annu Rev Med *49*, 407-424.

210. Zhu, N., and Wang, Z. (1999). Calreticulin expression is associated with androgen regulation of the sensitivity to calcium ionophore-induced apoptosis in LNCaP prostate cancer cells. Cancer Res *59*, 1896-1902.

211. Zimmerman, A. W., and Veerkamp, J. H. (2002). New insights into the structure and function of fatty acid-binding proteins. Cell Mol Life Sci *59*, 1096-1116.

APPENDIX 1 - MATERIALS AND REAGENTS

APPENDIX 1.1 IMMUNOHISTOCHEMICAL STAINING

Amersham International, Amersham, UK

Donkey anti-rabbit immunoglobulin conjugated to biotin

Dako Ltd, UK

Rabbit anti-Factor VIII-related antigen serum

DakoCytomation

EnVision+ System-HRP (DAB)

Feather Industries, Tokyo, Japan

Microtome blades

Grant Instruments, Cambridge, England

Water Bath

Hydrogen peroxide/methanol

30% H_2O_2

400ml methanol

Iwaki Glass Corp., Niigata, Japan

Primary Anti-C-FABP sera

Leitz, Luton, England

Leitz 1512 microtome

Santa Cruz Biotechnology Inc, Santa Cruz, , USA

Primary anti-VEGF

Scott's Tap Water

17.5g $NaHCO_3$

100g $MgSO_4$

0.5g Thymol

5 litres of tap water

Shandon Southern, Cheshire UK

Sequenze staining clips

Sigma Aldrich Ltd, Poole Dorset UK

Bovine Serum Albumin

Surgipath Medical Ind., Inc

Richmond United States

Eosin

Gills Haematoxylin

Precleaned ground edged 90° twin frosted microscopic slides (26 x 76 1,0 mm)

Tris buffered saline

0.05M Tris

0.14M NaCl

Tris-EDTA

10mM Tris Base

1mM EDTA Solution

0.05% Tween 20, pH 9.0

APPENDIX 1.2 CELL CULTURE MATERIALS AND REAGENTS

Androgen positive medium

RPMI Medium 1640 500ml

Penicillin/ Streptomycin 100 IU

Hydrocortisone 50ng/ml

Testosterone 50ng/ml

4% Stripped Foetal Calf serum

L-Glutamine 0.292µg/ml

Androgen negative medium

RPMI Medium 1640 500ml

Penicillin/ Streptomycin 100 IU

4% Stripped Foetal Calf serum

L-Glutamine 0.292µg/ml

Becton Dickinson, Madrid, Spain

Needles and Syringes

Bibby Sterilin, Staffordshire, UK

Tissue culture pipettes 5ml – 25ml

Cryo-Medium

Routine cell culture medium 92.5%

DMSO 7.5%

Gibco ™ Invitrogen Corporation, Paisley, Scotland, UK

L-glutamine (200mM)

Penicillin/streptomycin 100IU

Geneticin G-418 Sulphate

PBS Tablets

Trypsin, 2.5%

Grant Instruments, Cambridge, UK

Water bath

Heraeus Instruments, Germany

Centrifuge

Lab Systems Multiskan MS, Finland

Multiskan reader

Membrane filtration products, USA

Cellulose dialysing membrane

Nalgene, USA

Cryo-box

Nunc, Denmark

Cryogenic tubes

Tissue Culture plates and flasks

Sarstedt, Germany

1.5ml eppendorf tubes

Scientific Laboratory Supplies, Nottingham, UK

Haemocytometer

Selective Medium

RPMI Medium 1640 500ml

Penicillin/ Streptomycin 100 IU

Hydrocortisone 50ng/ml

Testosterone 50ng/ml

10% Foetal Calf serum

L-Glutamine 0.292μg/ml

Geneticin 0.5mg/ml

Sigma Aldrich Ltd, Poole Dorset UK

RPMI 1640 Medium (500ml)

Hydrocotisone Testosterone

Foetal calf Serum

Dimethyl Sulphoxide

0.22μm Millipore filters

MTT (3-[4,5 – Dimethylthiazol – 2 – yl]) – 2,5 – diphenyl tetrazolium bromide

Extracellular matrix gel from Engelbreth Holm-Swarm Mouse Sarcoma

ThermoForma, Mariette, Ohio, USA

Stericycle CO_2 incubator

Trypsin/EDTA

Versene 0.53mM

Trypsin 2.5%

APPENDIX 1.3 – CLONING AND TRANSFECTION MATERIALS AND REAGENTS

Boehringer Mannheim

HindIII

EcoRI

XbaI

Buffer B

Glaxo Wellcome

pSV-Neo expression vector

HEPES Buffered Saline

0.025M HEPES

0.14M NaCl

0.75mM Sodium hydrogen phosphate

0.125M calcium chloride

Adjust to pH7.1

Invitrogen Ltd, Paisley, UK

pBluescript Vector

Sequencing primers

New Brunswick Scientific Edison, New Jersey, USA

Incubator shaker

Promega, USA

pGEMTeasy

Wizard® SV Gel and PCR Clean-Up System

Qiagen, West Sussex, UK

Qiaprep ® Miniprep kit

Gibco, Paisley, UK

PBS tablets

LB-Agar (pH7.0) -500mls

1% Tryptone

0.5% Yeast Extract

1% NaCl

1% Agar

LB-Medium (pH7.0) – 1 Litre

1% Tryptone

0.5% Yeast Extract

1% NaCl

APPENDIX 1.4 WESTERN HYBRIDISATION MATERIALS AND REAGENTS

Amersham, Amersham, UK

ECL detection kit

Nitrocellulose Membrane

Bandelin Electronic, Germany

Bandelin Sonoplus Sonicator

Bio-rad Laboratories, USA

Protean III

Power Pac 3000

Cambrex Biosciences, Berkshire, England, UK

Protein Markers

Scientific Laboratory Supplies, Nottingham, UK

3MM Filter Paper

Destaining Solution

86.7% dH_2O

6.7% Acetic acid

6.7% methanol

Iwaki Glass Corp., Niigata, Japan

Primary Anti-C-FABP sera

Kinematica, Switzerland

Polytron Homogeniser

Kodak, Eastman Kodak company, Rochester, NY, USA

GBX developer

GBX Fixative

X-Omat AR film

Protein Transfer Buffer

20% Methanol

25mM Tris

0.192M Glycine

0.1% SDS

Routine cell culture medium

RPMI Medium 1640 500ml

Penicillin 100μg/ml

Streptomycin 0.25μg/ml

Hydrocortisone 50ng/ml

Testosterone 50ng/ml

10% Stripped Foetal Calf serum

L-Glutamine 0.292μg/ml

Sample Running Buffer

0.192M Glycine

50mM Tris

0.1% Sodium dodecyl sulphate (SDS)

Severn Biotech Ltd, UK

Coomassie Blue

Commasie blue 2.5g

45% Methanol

10% Acetic acid

45% dH_2O

Sigma Aldrich Ltd, Poole Dorset

Sodium dodecyl sulphate (SDS) (Lauryl sulphate)

10% Ponceau S Solution (90mls H_2O, 10mls Ponceau S Solution)

Tween20

Actin primary mouse monoclonal antibody

Secondary anti-mouse conjugated HRP

Secondary anti-rabbit conjugated HRP

Tris-buffered saline (pH7.6)

0.05M Tris –base

0.14M NaCl

Washing Buffer (pH7.6)

0.05M Tris –base

0.14M NaCl

0.05% Tween20

Flowgen, Nottingham UK

5% Protoblock

5g Reagent A

10mls Reagent B

90mls H_2O

APPENDIX 1.5 SOUTHERN BLOT MATERIALS AND REAGENTS

Biogene Ltd; Bedfordshire, UK

Agarose

Boehringer-Mannheim, Germany

DNA Marker III

DNA Loading Buffer

0.25% Bromophenol blue

0.25% Xylene cyanol

30% Glycerol

In distilled water

Flowgen

Low melting point agarose

Kodak, Eastman Kodak company, Rochester, NY, USA

GBX developer

GBX Fixative

X-Omat AR film

Mini-Instruments, Essex, England

Series 900 mini-monitor G-M tube

Qiagen™ Midi-prep plasmid extraction buffers

Buffer P1 – Resuspension Buffer

50mM Tris.Cl (pH8.0)

10mM EDTA

100μg/ml RNase A

Buffer P2 – Lysis Buffer

200mM NaOH

1% SDS (w/v)

Buffer P3 – Neutralising Buffer

3.0M K-acetate (pH5.5)

Buffer QBT – Equilibration Buffer

750mM NaCl

50mM MOPS (pH7.0)

15% Isopropanol

0.15% Triton ® X – 100

Buffer QC – Wash Buffer

1.0M NaCl

50mM MOPS (pH7.0)

15% isopropanol

Buffer QF – Elution Buffer

1.25M NaCl

50mM Tris.Cl (pH8.5)

15% Isopropanol

Roche

Random Primed Labelling Kit

Sigma Aldrich Ltd, Poole Dorset

Ethidium Bromide

Sodium Hydroxide

Ethanol

Dextran Sulphate

Salmon Sperm DNA

Sodium Chloride

Sodiem Citrate

20x SSC

3M NaCl

0.3M Sodium citrate

SSPE

3M NaCl

0.2M $NaH_2PO_4.H_2O$

TBE Buffer (50x)

0.045M Trizma basse

0.045M Boric acid

0.001M EDTA

Techne, Cambridge UK

Hybridisation tubes

Techne Hybridiser HB-1D

U.V. Upland, California, USA

302nm U.V. Transilluminator

Wizard® SV Gel and PCR Clean-Up System Buffers - Promega

Membrane Binding Solution

4.5M Guanidine isothiocyante

0.5M K-acetate (pH5.0)

Membrane Wash Solution

10mM K-acetate (pH5.0)

80% ethanol

16.7μM EDTA (pH8.0)

APPENDIX 1.6 IN VIVO ASSAY MATERIALS AND REAGENTS

Charles Rivers Laboratories

CD/1 Nude mice

Harlan sera-lab, Leicestershire, England.

Male ICRF immuno-compromised nude mice

APPENDIX 1.7 NORTHERN HYBRIDISATION MATERIALS AND REAGENTS

Amersham, Amersham, UK

[α^{-32}P]dCTP

Qiagen, West Sussex, UK

RNeasy ™ Midi prep kit

Roche

Random Primed Labelling Kit

Sigma Aldrich Ltd, Dorset, UK

Diethyl pyrocarbonate (DEPC)

3-(N-morpholino) propanesulphonic acid (MOPS, pH 7.0)

Formamide

Salmon Sperm DNA

Dextran Sulphate

Sodium Hydroxide

Formamide

Formaldehyde

APPENDIX 1.8 siRNA MATERIALS AND REAGENTS

Ambion, Cambridgeshire, UK

pSilencer-U6 Vector

Annealing buffer

100mM K-acetate

30mM HEPES-KOH pH7 7.4

2mM Mg-acetate

Invitrogen Paisley, UK

Custom synthesis of silencing construct

New England Biolabs Inc., USA

T4 DNA ligase Buffer

T4 DNA Ligase

Qiagen ™ Plasmid Midi-prep buffers – Sussex, UK

Buffer P1

50mM Tris.Clm pH8.0

10mM EDTA

100µg/ml RNase A

Buffer P2

200mM NaOH, 1% SDS (w/v)

Buffer P3 neutralising buffer

3.0M potassium acetate pH 5.5

Equilibration buffer QBT

750mM NaCl

50mM MOPS, pH 7.0

15% isopropanol (v/v)

0.15 Trition ® X-100 (v/v)

Wash buffer QC

1.0 NaCl

2.0 50mM MOPS, pH 7.0

3.0 15% isopropanol (v/v)

Elution buffer QF

1.25 M NaCl

50mM Tris.Cl, pH 8.5

15% isopropanol (v/v)

RF1 buffer

100mMKCl

50mM MgCl2.4H20

30mM K-acetate

10mM CaCl2 15% w/v glycerol, pH to 6.8, autoclave

RF2 buffer

10mM MOPS

10mM KCl

75mM CaCl2.2H2O

15% glycerol, pH to 6.8 with NaOH, autoclave

SOC buffer

2% bactotryptone

0.5% Yeast extract

10mM NaCl, 1M $MgCl_2$

1M $MgSO_4$

250mM KCl

1M glucose

2M $MgCl_2$

APPENDIX 2

Summary of incidence of metastasis in mice

Mouse Number	Cell line inoculated	Primary tumour volume	Metastasis		
			Heart	Lungs	Liver
1	PC3M	621.3mm^3	N	N	N
2	PC3M	1749mm^3	N	N	N
3	PC3M	753mm^3	N	N	N
4	PC3M	2761mm^3	N	N	N
5	PC3M3	502mm^3	N	N	N
6	PC3M3	0	N	N	N
7	PC3M3	110mm^3	N	N	N
8	PC3M3	75.3mm^3	N	N	N
10	PC3M	2.12g	N	Y	Y
11	PC3M	2.52g	N	N	Y
12	PC3M	1.62g	N	Y	N
13	PC3M	1.85g	N	Y	N
15	PC3M3	0	N	N	N
16	PC3M3	0	N	N	N
17	PC3M3	0	N	N	N

Following inoculation, final tumour volumes were obtained at autopsy in mm^3 or in grammes. Dissections of primary tumours (where available), heart lungs and liver were removed, processed and cut into sections. These sections were stained with haematoxylin and eosin to identify secondary sites of tumour